PREVENTION OF REBAR CORROSION BY NATURAL ANTIOXIDANTS DERIVED FROM GREEN TEA

Ivan Pradipta

Bachelor in Food Science and Technology (Honours)

A thesis submitted for the Degree in Doctor of Philosophy

School of Engineering

Monash University

June 2019

COPYRIGHT NOTICES

ABSTRACT

Corrosion inhibitors for reinforced concrete are an easy-to-use and cost-effective approach to prevent or reduce the corrosion of steel reinforcing bar (rebar). Nonetheless, the most common corrosion inhibitors today are the inorganic corrosion inhibitors. These inorganic-based inhibitors exhibit potential health and environmental hazards. Thus, a substitution of the inorganic corrosion inhibitors with the less-toxic and more environmentally-friendly ('green') organic corrosion inhibitors is encouraged. Unfortunately, there are only limited studies on the corrosion inhibition efficiency of green corrosion inhibitors under alkaline conditions, such as those found in concrete. Thus, this study aims to enrich the limited studies, by proposing an investigation on corrosion inhibition efficiency (IE) of natural antioxidants (extracted from green tea) at the alkaline concrete pH.

Natural antioxidants are rich in polar atoms and electron-rich bonds. These functional groups favor the adsorption of antioxidant molecules on rebar surface, to form a protective layer as mixed-type corrosion inhibitors. The formation of protective layer increases rebar resistance to potential/current which may induce rebar corrosion (i.e. polarization resistance), and inhibits the electrochemical reactions of rebar corrosion simultaneously: anodic reaction of iron oxidation and cathodic reaction of oxygen reduction. Green tea is one of the richest sources of natural antioxidants, having a ten to thirty-fold higher antioxidant activity than berries, which are established rich sources of natural antioxidants. Therefore, as a proof of concept, green tea was selected as the source of natural antioxidants for this research. It is postulated that given this very high antioxidant activity, green tea has a higher chance of inhibiting rebar corrosion.

Corrosion inhibition efficiency of green tea was initially investigated in simulated concrete pore solution (SCPS). Green tea was added as aqueous extracts of 1% and 2% green tea (by cement weight) to replace water. In SCPS, the green tea extracts inhibited rebar corrosion: addition of the extracts reduced rebar corrosion rate and delayed the sudden increase of corrosion rate (which correlates to corrosion initiation). The green tea extracts showed the highest IE after 1 day (±92% inhibition). They acted as mixed-type corrosion inhibitors which increased rebar polarization

resistance, and induced changes to the rate of iron oxidation and oxygen reduction without significantly changing the open circuit potential. Open circuit potential is the rebar potential in absence of influence from external potential/current. Overall, the extract of 2% green tea showed a higher IE than the extract of 1% green tea. Therefore, the extract of 2% green tea was selected for further studies.

After the corrosion tests in SCPS, IE of the green tea extract (GT) was investigated in mortar, and compared with the IE of a commercial calcium nitrite corrosion inhibitor (CI). At equal volume, GT exhibited a significantly higher IE than CI (75-80% vs. 14-24%). The higher recorded IE was not related to an improved physical protection of mortar, as GT-based mortar displayed a comparable compressive strength to CI-based mortar. Instead, the higher IE of GT was due to a significant increase in polarization resistance (which suggested the formation of a protective layer) and a significant reduction in iron oxidation rate. On the other hand, the changes in oxygen reduction rate and open circuit potential were not significant. Thus, similar to its mechanisms of action in SCPS, GT behaved as a mixed-type corrosion inhibitor in mortar.

Formation of protective layer on rebar surface, as suggested by the increase in polarization resistance, was validated by visual inspections and microscopic examinations (optical microscope and scanning electron microscope). Elemental analyses with energy-dispersive X-ray spectroscopy (EDX), as well as further analyses with X-ray diffraction (XRD) and Fourier transform infrared spectroscopy (FTIR) indicated an enrichment of the layer with calcium carbonate polymorphs (calcite, aragonite, and vaterite). This layer exhibited an anti-corrosion activity, as its presence reduced rebar weight loss. Corrosion reduction due to this layer was further supported by a similar chloride permeability between control and GT-based concrete, and a similar corrosion rate of steel reinforced control mortar and steel reinforced mortar incorporating the residual solid of GT. These similarities eliminated the possible reduction in corrosion rate due to an improved physical protection of mortar/concrete against corrosion.

Overall, the potential of natural antioxidants as green corrosion inhibitors has been positively demonstrated by GT through this research study. GT reduced rebar corrosion rate by inducing formation of a protective layer enriched with calcium carbonate (calcite, aragonite, and

vaterite) and increasing rebar polarization resistance. Amongst the GT chemical constituents, catechin or (-)-epicatechin, (-)-epicatechin gallate, (-)-epigallocatechin gallate were likely responsible for the anti-corrosion activity of GT as a mixed-type corrosion inhibitor. The increase in polarization resistance and decrease in corrosion rate were affected by the magnitude of GT's antioxidant activity. Nonetheless, in this study GT showed a higher IE than CI, particularly at the higher range of volume. Therefore, the IE of more cost-effective sources of natural antioxidants as green corrosion inhibitors in concrete warrant investigations in future studies.

RESEARCH OUTCOME

Published journal article

Pradipta, I. et al. (2019). *Natural organic antioxidants from green tea form a protective layer to inhibit corrosion of steel reinforcing bars embedded in mortar*. Construction and Building Materials 221: pp. 351-362.

Submitted journal article under peer-review*

Pradipta, I. et al. (2019). *Natural organic antioxidants from green tea inhibit corrosion of steel reinforcing bars embedded in mortar*. Manuscript submitted for publication.

* Reviewers' comments have been received and addressed

Published conference proceeding

Pradipta, I. et al. (2018). *Corrosion inhibition of green tea extract on steel reinforcing bar embedded in mortar*. in *IOP Conference Series: Materials Science and Engineering*. IOP Publishing.

Received Best Presentation Awards in participated conferences

1. Pradipta, I. et al. *Green tea extract inhibits corrosion of steel reinforcing bars embedded in mortar*. Oral session presented at *2018 3rd International Conference on Building Materials and Construction.* 23rd to 25th February 2018, Nha Trang, Vietnam.
2. Pradipta, I. et al. *Inhibition on corrosion of steel reinforcing bar embedded in mortar by green tea*. Oral session presented at *The 14th International Conference on Concrete Engineering and Technology 2018.* 7th to 10th August 2018, Kuala Lumpur, Malaysia.

DECLARATIONS

This thesis contains no material which has been accepted for the award of any other degree or diploma at any university or equivalent institution and that, to the best of my knowledge and belief, this thesis contains no material previously published or written by another person, except where due reference is made in the text of this thesis.

Signature: 

Print name: IVAN PRADIPTA

Date: 31st May 2019

ACKNOWLEDGEMENTS

First and foremost, I would like to sincerely thank my principal supervisor, Dr. Daniel Kong and associate supervisor Dr. Joash Tan Ban Lee. Throughout my candidature, my supervisors have provided me with valuable supports. They have guided me with their vast experiences and knowledge, and helped me grow both personally and professionally. Particularly, I would like to acknowledge their supports in improving my problem-solving skills, independent thinking, academic writing, and academic presentation. It is thanks to them that I was awarded as one of the 'Best Presenters' in the two conferences that I participated. In addition to my supervisors, I would like to thank the panel members of my milestone reviews, especially to Dr. Suvash Chandra Paul, Dr. Ahmad Mousa, and Dr. Kong Sih Ying, who provided important recommendations which improved the quality of my research.

I would like to convey my sincere appreciation to Mrs. JC Chua, Mr. Remy Rafie, and Mrs. Lim Ming Nee from Metrohm Malaysia for providing technical assistances on conducting electrochemical measurements. My genuine gratitude goes to Mr. Mohd. Hafizan, Mr. Muhammad Afiq Fadhly, and Mr. Amir Syafiq Samsudin from Civil Engineering laboratories for the continuous supports throughout the years. I also extend my deepest gratitude to Mr. Afiq bin Anuar for the invaluable assistances on performing electron microscopy and X-ray diffraction analyses. I am indebted to Mr. Raja Hasnan too, for the inestimable supports and guidance on the setup of accelerated corrosion. Additionally, I would like to gratefully thank Mrs. Nurziana Sharmilla Nawawi and Dr. Syafiq Asnawi Zainal Abidin for the substantial assistances on liquid chromatography-mass spectrometry and liquid chromatography-tandem mass spectrometry analyses.

This project will not be possible without financial supports. Hence, I would like to gratefully acknowledge the research funding from School of Engineering, and Graduate Research Merit Scholarship from Monash University Malaysia. I would also like to thank Ms. Lim Pooi Mee and administrative team from the School of Engineering for assisting me with the financial requisitions and reimbursements throughout my candidature.

I am grateful to my colleagues and friends, especially to Mr. Andreas Aditya Hermawan, Mr. Loi Shi Jun, Mr. Cheng Hong Sheng, Ms. Janet Tan Jia Yin, Mr. Chris Teo Yong Kiat, Ms. Fatin Kamaruddin, Ms. Nooryasmin Anwar, and Ms. Chai Jun Ching. I would like to thank the mentioned people for the unforgettable discussions, brainstorming sessions, and other moments spent together.

Last but not least, I would like to thank my beloved parents, Mr. Rudy Susanto and Mrs. Yuliana Permatasari Nugroho. I cannot thank them enough for their compassion and continuous supports throughout my journey. I dedicate this thesis to both of them.

SUPERVISORY TEAM

Principal supervisor

Dr. Daniel Kong
School of Engineering
Monash University Malaysia
Jalan Lagoon Selatan
47500 Bandar Sunway
Selangor Malaysia

Associate supervisor

Dr. Joash Tan Ban Lee
School of Science
Monash University Malaysia
Jalan Lagoon Selatan
47500 Bandar Sunway
Selangor Malaysia

TABLE OF CONTENTS

LIST OF FIGURES

LIST OF TABLES

CHAPTER 1: INTRODUCTION

1.1 Overview and significance of this study

Corrosion of steel reinforcing bar (rebar) in reinforced concrete structures is a detrimental issue with significant socio-economic impacts [1-5]. Rebar corrosion occurs due to the reduction in concrete pH (concrete carbonation) and/or chloride attack [6-9]. Comparatively, the chloride-induced corrosion is more severe, exhibiting a higher corrosion propagation rate and shorter propagation time than the concrete-carbonation-induced corrosion [6].

The significant impacts of rebar corrosion have encouraged the development of various corrosion protection methods [10, 11]. Among the available methods, electrochemical protection with cathodic protection (CP) and substitution of carbon steel rebar with stainless steel rebar (SS) are the most effective. However, the high costs of CP and SS deter a wide commercialization of these methods [5, 12-14]. Therefore, a more cost-effective corrosion protection method is required.

Corrosion inhibitors are one of the simplest and most cost-effective alternatives to CP and SS [3, 15]. Nonetheless, the most effective corrosion inhibitors today are the inorganic corrosion inhibitors, in particular calcium nitrite corrosion inhibitor (CI) [16-19]. CI has been used in reinforced concrete since 1970's and is an anodic corrosion inhibitor with high solubility in water, producing calcium and nitrite ions [20]. The nitrite ion is the active constituent of CI as an anodic corrosion inhibitor (i.e. oxidizer). The nitrite ion oxidizes Fe^{2+} ion (produced by oxidation of metallic iron during anodic reaction of rebar corrosion) to Fe^{3+} ion, and promotes formation of a passive film to inhibit rebar corrosion [18-21]. However, being an anodic corrosion inhibitor, inadequate CI dosage has a risk of enhanced rebar corrosion, as illustrated theoretically by Hansson et al. [22] and experimentally by Reou and Ann [23]. Moreover, due to the consumption of nitrite during oxidation of Fe^{2+} to Fe^{3+}, long-term corrosion protection by CI is a concern [24-26]. The nitrite consumption is particularly accelerated when

oxygen is present in concrete, which oxidizes the calcium nitrite to calcium nitrate [24-26]. Therefore, it is recommended to use CI in concrete with low water/binder ratio (or other methods to reduce concrete permeability such as the use of supplementary cementitious materials) and sufficient cover depth, to prevent nitrite leaching and reduce oxygen ingress [24, 27, 28]. Nevertheless, protection efficiency of the concrete with low water/binder ratio and sufficient cover depth has increased, which confounds the improved efficiency upon CI incorporation [29]. Furthermore, there have been debates on the efficiency of CI against corrosion, especially in presence of cracks [29, 30]. In general, it is reported that CI increases chloride threshold concentration and prolongs time-to-corrosion (indicating that CI is able to delay corrosion initiation or reduce initial corrosion) [20, 27]. Nonetheless, there are studies reporting that CI is ineffective once corrosion initiates [28, 31-35]. In addition, some studies reported that CI increases chloride transport into concrete, which offsets the beneficial increase in chloride threshold concentration [23, 25].

In order to address the enhanced corrosion risk of CI and concerns on potential health and environment hazards of inorganic corrosion inhibitors, commercial organic corrosion inhibitors were introduced in 1980's [20, 35, 36]. The organic-based inhibitors are mixed-type corrosion inhibitors, which form a protective layer on rebar surface to reduce iron oxidation and oxygen reduction (i.e. anodic and cathodic reactions of rebar corrosion) simultaneously [27, 35, 37]. Nonetheless, the efficiency of these organic inhibitors is conflicting [20]. This may be partly due to the lack of information on the exact active constituents of the inhibitors, concentration of the active constituents, and the required inhibitor dosages relative to the concentration of aggressive species [20, 21, 27, 34]. Thus, research has been investigating on the efficiency of less toxic and more environmentally-friendly ('green') alternatives to existing commercial inorganic and organic corrosion inhibitors. Unfortunately, there are only limited studies on the efficiency of green corrosion inhibitors under alkaline environment, such as that observed in concrete application. Hence, this project aims to contribute towards the limited studies on the efficiency of green inhibitors at alkaline concrete pH, and promote further studies on this topic.

1.2 Objectives and scopes of this study

In this study, the authors have investigated the efficiency of natural antioxidants as green corrosion inhibitors in alkaline pH of concrete. Studies have shown that polar atoms and electron-rich bonds favor anti-corrosion activity, by promoting the adsorption of inhibitor molecules on rebar surface as mixed-type corrosion inhibitors [8, 38]. Natural antioxidants are organic compounds which are abundant in nature, and exhibit multiple polar atoms and electron-rich bonds in the antioxidant structures [39]. Therefore, the antioxidants are potential mixed-type corrosion inhibitors and green alternatives to inorganic corrosion inhibitors. Green tea is one of the richest sources of natural antioxidants [40-43]. It records ten to thirty-fold higher antioxidant activity than berries, which are the other rich sources of natural antioxidants [44]. This extremely high antioxidant activity should favor green tea to inhibit rebar corrosion. Therefore, green tea was selected as the source of natural antioxidants in this study.

Corrosion inhibitors are incorporated into concrete as admixed corrosion inhibitors to prevent corrosion initiation or migrating corrosion inhibitors to remediate ongoing corrosion [32, 45]. Given the severity and short propagation time of chloride-induced corrosion, the main objective of this study is to investigate the efficiency of natural antioxidants as admixed corrosion inhibitors to prevent chloride-induced rebar corrosion. This objective is achieved by choosing green tea as the source of natural antioxidants. There are three areas of focus in this study: 1) efficiency of green tea against the chloride-induced corrosion, 2) relationship between antioxidant activity and corrosion inhibition efficiency of green tea, and 3) plausible corrosion-inhibiting mechanisms of green tea.

This study initially determined the physical form (dry admixture or aqueous extract) to administer green tea as an admixed corrosion inhibitor and investigated the corrosion inhibition efficiency of green tea in simulated concrete pore solution. Upon completion of the corrosion tests in solution, corrosion inhibition efficiency of green tea in mortar was investigated, and compared with CI. Finally, the plausible corrosion-inhibiting mechanisms of green tea were studied.

1.3 Organization of thesis

This thesis is organized into six chapters. Chapter 1 provides an overview and elaborates the significance of this study. Chapter 2 describes rebar corrosion, existing corrosion protection methods for rebar, corrosion inhibitors as a corrosion protection method of rebar, selection of natural antioxidants as potential green corrosion inhibitors, and determination of green tea as a suitable source of natural antioxidants. Chapter 3 investigates the corrosion inhibition efficiency of green tea in simulated concrete pore solution. In Chapter 4, corrosion inhibition efficiency of green tea was further studied in mortar, and compared with the efficiency of CI. Chapter 5 illustrates the corrosion-inhibiting mechanisms of green tea. Finally, Chapter 6 provides the overall conclusions and recommendations for future studies.

CHAPTER 2: LITERATURE REVIEW

2.1 Overview of reinforced concrete structure

Reinforced concrete (RC) is the most popular construction material today [8, 46, 47]. It consists of concrete as the main building block and steel reinforcing bars (rebars) as the supporting elements. The steel rebars are embedded in concrete to improve the inherently low tensile strength and for crack control in concrete [48-53]. Amongst the various types of steel rebar, carbon steel rebar is the most commonly used commercially [54]. This rebar type is lower in cost due to the low cost of iron which is the major element of the rebar (± 97%) [55].

2.2 Durability and deterioration of RC structures

In the past, strength was the sole concern of engineers and construction industry involving RC structures [48, 49, 56, 57]. However, recent experiences with legacy structures have indicated that solely focusing on strength and neglecting durability properties adversely affect structural safety and serviceability [56, 58, 59]. Corrosion of steel rebar is one of the most substantial durability issues of RC structures [1-5]. The corrosion reduces the cross-sectional area and supporting capacity of steel rebar, and produces corrosion products which expands the volume of corroding rebar surface by two to nine-fold [11, 60, 61]. The volume expansion reduces the bond strength between the corroding rebar and surrounding concrete cover, and generates pressure on the concrete which ultimately results in concrete cracking, spalling, or delamination [5, 10, 48, 61, 62]. These structural damages naturally raise safety concerns [3, 32, 54, 59, 63, 64], and repairs of the damaged structures incur significant direct and indirect costs. The direct costs involve financial costs of more than US$100 billion per annum worldwide [6, 57, 61, 65, 66]. On the other hand, the indirect costs involve the disruptions on socio-economic activities during repair (such as due to traffic delays) which lead to reduced productivity [54]. According to Perez-Quiroz et al. [54], the indirect costs potentially amount to ten-times as high as the direct costs.

2.2.1 Passive steel rebar embedded in concrete

Steel rebar embedded in concrete is protected from corrosion by the alkaline pH of concrete (pH 12-14) [12, 58, 67, 68]. The alkaline pH is contributed by calcium hydroxide (also known as Portlandite), which is generated during cement hydration [6]. During cement hydration, the two major minerals of cement, tricalcium silicate ($3CaO.SiO_2$) and dicalcium silicate ($2CaO.SiO_2$), react with water according to Equations 1 and 2 [50, 69] respectively.

$$2(3CaO.SiO_2) + 6\ H_2O \rightarrow 3CaO.2SiO_2.3H_2O + 3\ Ca(OH)_2 \quad (1)$$

$$2(2CaO.SiO_2) + 4\ H_2O \rightarrow 3CaO.2SiO_2.3H_2O + Ca(OH)_2 \quad (2)$$

As shown in Equations 1 and 2, hydrolysis of tricalcium and dicalcium silicate during cement hydration produce Portlandite and calcium silicate hydrate ($CaO.SiO_2.H_2O$ or CSH in short) [50]. The Portlandite is responsible for the alkaline pH of concrete. On the other hand, the CSH is the major constituent of concrete matrix, which binds other concrete components such as the aggregates [50].

Alkaline pH of concrete protects steel rebar from corrosion by altering the electrochemical states of the metal elements in the rebar. For example, the concrete alkalinity promotes the formation of water-insoluble iron (III) oxides: Fe_2O_3 and Fe_3O_4 on carbon steel rebar [5, 6, 70]. Formations of the iron oxides are illustrated in Figure 1, at pH 12-14 and potential range defined by the two dotted lines, which represents the stable potential range of water to accept electrons from iron oxidation [71, 72]). The Fe_2O_3 and Fe_3O_4 form a protective layer on rebar surface to restrict ion movement between rebar and surrounding concrete, and reduces rebar corrosion rate [5, 6]. This electrochemical state of a rebar with a reduced corrosion rate is known as the passive state [73].

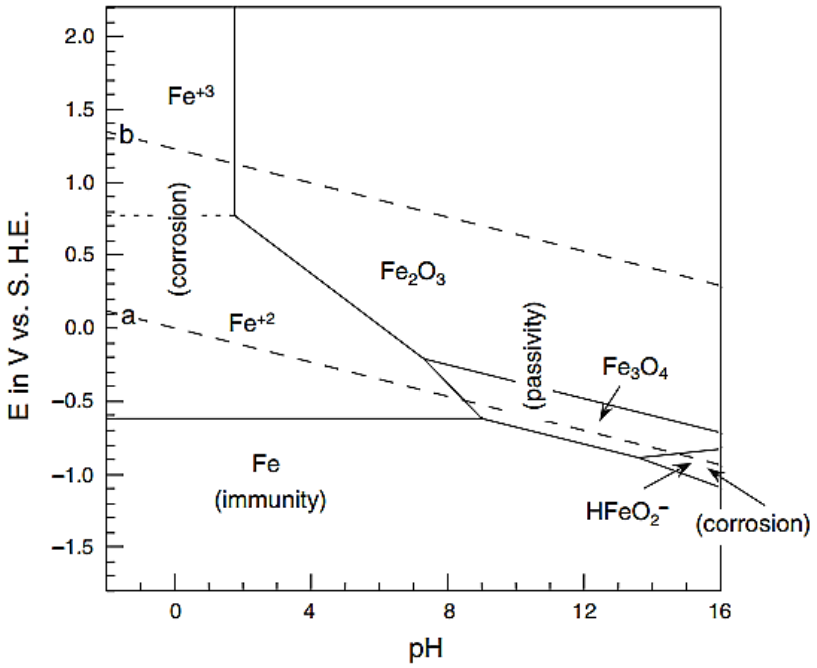

Figure 1: Pourbaix (potential vs. pH) diagram of iron-water system at 25°C and dissolved iron ion activity of 10^{-6} mol/L (Adapted from McCafferty [71]).

2.2.2 Corrosion of steel rebar

Corrosion of steel rebar is a natural process which occurs due to the tendency of metals to attain lower and thermodynamically-more favorable energy states with higher stability [5, 56, 70]. The lower energy states are attained when metals are in oxidized states, particularly the naturally-occurring, oxidized-mineralized states [5, 74]. Corrosion of steel rebar consists of two half-cell reactions shown in Equations 3 and 4 [75]:

i. Anodic reaction (oxidation/dissolution of iron):

$$Fe \rightarrow Fe^{2+} + 2e^{-} \quad (3)$$

ii. Cathodic reaction (oxygen reduction):

$$2\,H_2O + O_2 + 4e^{-} \rightarrow 4\,OH^{-} \quad (4)$$

The half-cell anodic and cathodic reactions are illustrated in Figure 2, where the pore water in concrete acts as an electrolyte which promotes the flow of current and electrons [5].

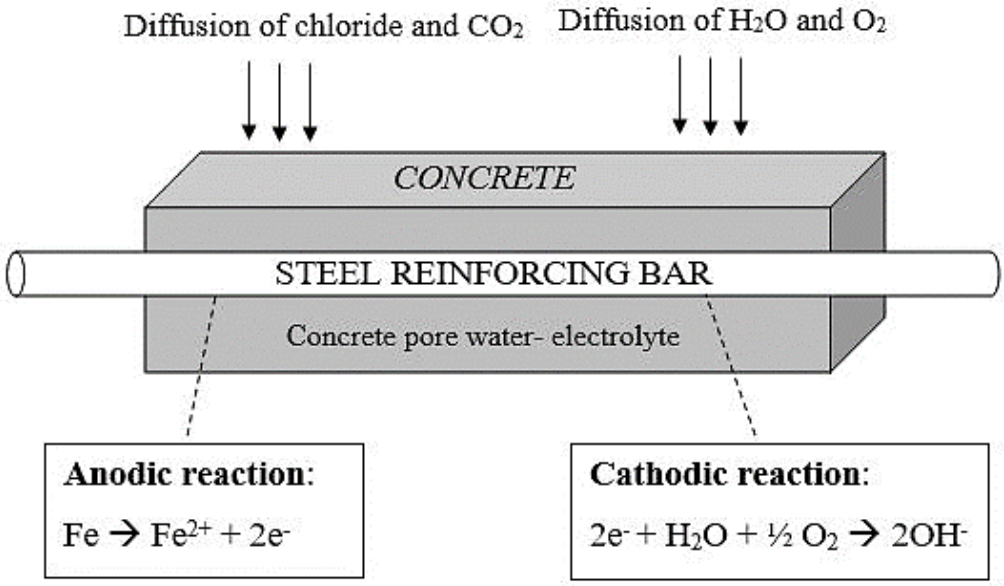

Figure 2: Half-cell anodic and cathodic corrosion reactions of steel reinforcing bar embedded in concrete (Adapted and modified from Hansson et al. [22]).

Rebar corrosion occurs due to the penetration of corrosion-inducing (i.e. aggressive) species into concrete. There are two commonly known aggressive species which induce rebar corrosion, namely carbon dioxide and chloride. Corrosion of steel rebar due to the carbon dioxide and chloride are discussed in Section 2.2.2.1 and 2.2.2.2.

2.2.2.1 Steel rebar corrosion due to carbon dioxide ingress

Atmospheric carbon dioxide penetrates into concrete [5, 56, 62] and reacts with Portlandite producing calcium carbonate [5]. The consumption of Portlandite substantially reduces concrete alkalinity to approximately pH 9.0 (i.e. concrete carbonation) [5, 9, 58, 76]. This pH reduction disturbs the formation of a new passive layer and the stability of a formed passive layer [5, 6, 74, 76]. The disruption on the formation of new passive layer is due to the reduced availability of hydroxyl ions

(OH^-) with decreasing pH levels, which are required to react with Fe^{2+} species to form Fe^{3+} species (Equations 5 and 6) [76]. On the other hand, the disruption on the stability of formed passive layer is due to the reduction in amount of OH^-, which shifts the reaction equilibriums in Equations 5 and 6 to the left (reactants) since the formation of passive layer is a reversible process [6, 74, 76].

$$3\ Fe(OH)_2 + 2\ OH^- \rightleftharpoons Fe_3O_4 + 4\ H_2O + 2e^- \quad (5)$$

$$3\ FeO + 2\ OH^- \rightleftharpoons Fe_3O_4 + H_2O + 2e^- \quad (6)$$

Rebar corrosion due to concrete carbonation is a *general* corrosion, in which each pair of anodic and cathodic sites are located adjacent to each other on the same rebar surface (Figure 3) [65, 77, 78]. Therefore, a spatial separation between anodic and cathodic sites is absent (i.e. microcell corrosion), allowing the corrosion to occur across the entire rebar surface (i.e. uniform corrosion) [78, 79].

2.2.2.2 Steel rebar corrosion due to chloride ingress

Chloride-induced corrosion occurs due to the ingress of chloride from a natural saline environment (marine environment or soil and groundwater with significant amount of chloride) [6, 48, 54, 80] or the application of deicing salts in temperate countries [4, 6, 54, 80]. The mechanism by which chloride induces the corrosion of passive rebar remains unclear. However, Szklarska-Smialowska [81] suggested that chloride ions generate a very high local current which disrupts the passive film.

Chloride-induced corrosion is initiated when chloride concentration at the rebar surface reaches its chloride threshold concentration. The reported threshold concentration varies greatly, ranging from 0.2-1.0% by weight of cement, and is affected by several factors [5, 20, 82, 83]. For instance, the type of concrete binder (cement alone or combination of cement and other cementitious materials) and tricalcium aluminate content of cement determine the chloride binding capacity of the concrete [5, 6, 58]. On the other hand, concrete porosity determines the ease of chloride penetration, while the initial pH of concrete (i.e. $[OH^-]$ /$[Cl^-]$ ratio) determines the

amount of hydroxyl ion available to prevent chloride-induced corrosion [5, 11]. Hydroxyl ion has a pH-increasing effect which promotes rebar passivation against the corrosion-inducing activity of chloride [83].

Chloride-induced corrosion is a *localized* corrosion [78]. It induces a significant anodic activity at affected area (i.e. anodic site, Figure 3) but keeping the unaffected area passive, being a cathodic site [5, 54, 71, 82, 84]. This creates a spatial separation between the anodic and cathodic sites (Figure 3, macrocell corrosion) [65]. The *localized* attack of chloride forms a smaller anodic site known as pit, which increases the anodic reaction rate significantly to balance the reaction rate of the larger cathodic site [54, 74]. Moreover, corrosion propagation at the pit produces hydronium ion (H^+, Equation 7) which combines with the regenerated chloride (i.e. autocatalysis process [56]) and forms hydrochloric acid.

$$FeCl_2 + 2\ H_2O \rightarrow Fe(OH)_2 + 2\ H^+ + 2\ Cl^- \quad (7)$$

The formation of hydrochloric acid reduces the pH at pit to approximately 3.0 [11, 85] and shifts the electrochemical state of the rebar into a corroding state, leading to an enhanced rebar corrosion [5]. Therefore, due to pit formation, chloride-induced corrosion exhibits a faster propagation (i.e. higher severity) than carbonation-induced corrosion [6].

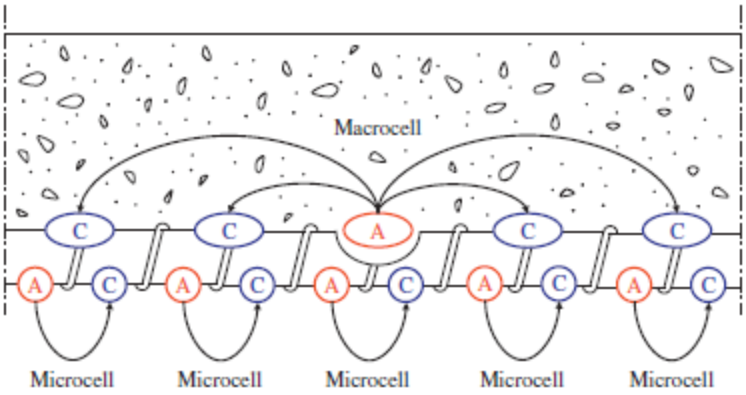

Figure 3: Microcell and macrocell corrosion of steel reinforcing bar (Adapted from Cheung and Cao [77]). Abbreviations: A= anodic site and C= cathodic site.

2.3 Overview on corrosion protection methods of steel rebar

Various corrosion protection methods are currently available to combat the detrimental impacts of rebar corrosion [10, 11]. The most fundamental approach to protect rebar from corrosion is to reduce the penetration of aggressive species into concrete, by increasing the protection quality of the concrete [6]. This can be achieved by adopting an adequate depth of concrete cover with satisfactory strength and acceptable porosity [11, 49, 67]. Nonetheless, additional corrosion protection methods are necessary for RC structure which is exposed to aggressive environment (i.e. high concentration of chloride and/or carbon dioxide), particularly when the structure has an expected long service life and long repair time [10]. The additional corrosion protection methods are either applied on concrete to further reduce the penetration of aggressive species or applied on steel rebar to directly improve the corrosion resistance of the rebar. Examples of the corrosion protection methods are summarized in Tables 1 and 2. In those tables, the main functions, major benefits, and limitations of the methods are described. Table 1 discusses the *methods which are applied to the concrete matrix* such as fiber reinforced concrete, supplementary cementitious materials, and concrete sealers. On the other hand, Table 2 discusses the *methods which are applied to the steel rebar* such as cathodic protection, electrochemical realkalization, electrochemical chloride extraction, galvanized steel rebar, stainless steel rebar, and rebar organic coating.

Table 1: Corrosion protection methods for concrete matrix

Method	Functions	Competitive benefits	Limitations
Fiber reinforced concrete	Improves tensile strength of concrete [86, 87] Improves concrete resistance to crack initiation and propagation [86, 87]	Can be used to repair a damaged reinforced concrete structure [88]	Reduction in workability of fresh concrete [86]
Supplementary cementitious material (SCM)	Pozzolanic activity and fine particles of SCM (finer than cement) create a denser and more uniform concrete matrix, which improves concrete durability [58, 89, 90] SCM binds chloride and increases chloride threshold concentration [91]	Sustainable construction [1]: - Replaces cement [89, 92, 93] - Utilization of SCM derived from industrial by-product reduces environmental pollution [92, 94] - Reduces cost of concrete [92]	The amount of SCM with high pozzolanic activity is limited and therefore the price is high [89] Percentage of cement replacement with SCM must be optimized to prevent negative impacts on the properties of fresh and hardened concrete [5, 58]
Concrete sealers	Reduce water ingress into concrete [95]	Simple and cost-effective [5, 96]	Efficiency depends on surface imperfections and pretreatments, cyclic wetting-drying, skill of operator, and application rate [95]

	Increase concrete resistivity [5]	Particularly useful to prevent re-migration of ions after electrochemical repair [58]	Over time, environmental factors such as UV radiation, rainfall, humidity, and chloride exposure may reduce efficiency [96-98]
		Can be applied on new or repaired reinforced concrete structure [97]	Different thermal expansion coefficient between sealing layer and concrete may cause incompatibility and delamination of the layer [48, 99]

Table 2: Corrosion protection methods for steel reinforcing bar

Method	Functions	Competitive benefits	Limitations
Cathodic protection (CP)	Applying a cathodic potential (i.e. cathodic polarization) to bring rebar potential to potential range with targeted corrosion rate [100] The applied current suppresses anodic reaction while allowing cathodic reaction to produce hydroxyl ions The hydroxyl ions strengthen the existing passive film or re-passivate the rebar [5, 75].	Effective long-term protection (10-20 years without major replacement of CP components) given a routine maintenance and monitoring [14, 101] Can be used to prevent rebar corrosion (i.e. cathodic prevention) or repair ongoing corrosion (i.e. cathodic protection) [5, 11, 67, 102] Impressed current cathodic protection (ICCP) system is used to protect and repair a large structure (due to the ability to adjust current output) [5, 14] Sacrificial anode cathodic protection (SACP) system is used for a small and targeted (patch) repair [5, 14] Repair of a damaged structure using CP is more cost and time-effective than conventional repair because only damaged	For ICCP system: - Complex instrumentation leads to high initial investment [14, 104] - Regular monitoring is necessary, adding costs for electricity and specialist [14, 100, 104] - Electrical components of ICCP are prone to environmental damages [14] - Applied current density must be optimized [75, 100, 104-106] - Under-protection (i.e. too low current density) does not adequately protect steel rebar - Overprotection (i.e. too high current density) may lead to hydrogen damage (hydrogen embrittlement) and reduction in concrete-rebar bond strength For SACP system: - Duration of corrosion protection depends on the lifespan of the anode [5, 14, 100]

		concrete is removed; contaminated but undamaged concrete is kept in place [5, 11, 62, 100, 102, 103] Repair with CP prevents the onset of corrosion at adjacent area to removed-damaged area (i.e. incipient anode phenomenon) [5, 77] Longer life cycle of CP-repaired structure (more than 10 years, time until minor repair of CP system is about 15 years) than conventionally repaired structure [11, 101] Service life of a structure repaired with SACP system is approximately 10 years [5, 14] Service life of a structure repaired with ICCP system is approximately 25 years [14]	- Maximum applied current density is limited by the maximum current density of the anode, which may lead to failure in arresting active corrosion [5, 14, 100, 104]
Electrochemical realkalization (ER)	Applying current between rebar and external anode	Long-term corrosion protection for carbonated concrete (at least ten years) [100]	Requires 50 to 500-times higher electrical charge than the electrical charge of CP for 6 to 18 days (ER is applied temporarily

	immersed in alkaline solution Allows production of hydroxyl ions at rebar vicinity and migration of alkali ions into concrete Reinstates alkalinity of carbonated concrete [58, 62, 100]		compared to CP which is installed permanently) [58, 100] Higher initial cost than CP May require repeated treatments in the long-term Risk of hydrogen embrittlement in prestressed structures (due to the high current density) [100] Risk of alkali-aggregate activation and loss of steel-concrete bond in normal structures due to the sudden increase in hydroxyl ions and alkali ions [100] Lower efficiency when applied on concrete added with mineral admixtures [5]
Electrochemical chloride extraction (ECE)	Applying current between rebar and external anode immersed in alkaline solution, to remove	Suitable for heavily chloride-contaminated and corroded structure	Requires 50 to 500-times higher electrical charge than the electrical charge of CP for 6-8 weeks [100]

	chloride ion from rebar surface [58, 100] The produced hydroxyl ions provide alkalinity to concrete surrounding the rebar and restore rebar passivity [58, 100]		Higher initial cost than CP (due to temporary application of ECE compared to the permanent application of CP) May require repeated treatments in the long-term [100] Risk of hydrogen embrittlement in prestressed structures [100] Risk of alkali-aggregate activation and loss of steel-concrete bond in normal structures [100] Lower efficiency when applied on concrete added with mineral admixtures [5]
Galvanized steel rebar	Provides sacrificial protection to steel rebar [5, 107, 108] Corrosion products of zinc form physical barrier against the penetration of	Cost-effective [112] Improves rebar resistance to concrete carbonation-induced corrosion, due to the wider pH range over which zinc remains passive [5, 71, 113, 114]	The higher corrosion resistance of galvanized steel only lasts as long as the galvanic layer remains [110, 114, 115]

	aggressive species [108-111]		
Stainless steel rebar	Improves corrosion resistance of carbon steel rebar by alloying the rebar with more corrosion-resistant metal elements than iron such as chromium, nickel, and molybdenum [55, 85, 116]. The elements produce a more stable passive film [5]	Excellent corrosion resistance [13] Higher initial cost is projected to be paid-off in the long-term due to the lower maintenance and repair costs [54, 55] Excellent alternative to cathodic protection for a long-term corrosion protection [13, 117]	Higher cost (6 to 10-times) than carbon steel rebar [5, 12, 13] Improvement on corrosion resistance depends on the type of stainless steel rebar (better type has a higher cost) [5, 13]
Organic coating of rebar	Physical barrier against aggressive species [5]	Relatively lower cost [5] Simple [58]	High susceptibility to abrasion and mechanical damages [5] High risk to pitting corrosion, leading to inefficient long-term corrosion protection [5]

2.4 Corrosion inhibitors as a corrosion protection method of steel rebar

As established in Section 2.3, cathodic protection (CP) and stainless steel rebar (SS) are currently the two most effective corrosion protection methods for rebar. However, high cost impedes a wide commercialization of these methods. Corrosion inhibitor approach is the more attractive alternative to CP and SS [3, 15]. The inhibitors are cost-effective [3, 45, 118] and practical to use on-site due to easy handling and simple applications [16, 66, 119, 120]. Corrosion inhibitors are incorporated during mixing of fresh concrete to delay corrosion initiation (i.e. admixed corrosion inhibitors) or applied on the surface of hardened concrete to reduce ongoing corrosion (i.e. migrating corrosion inhibitors) [32, 45]. Corrosion inhibitors are differentiated from another type of corrosion prevention methods namely concrete pore blockers. The pore blockers inhibit rebar corrosion by preventing the penetration and thus reducing the concentration of aggressive species in concrete [5, 18, 45]. In comparison, the corrosion-inhibiting mechanisms of corrosion inhibitors are elaborated in the next section.

2.4.1 Corrosion-inhibiting mechanisms of corrosion inhibitors

Corrosion inhibitors do not significantly change the concentration of aggressive species. Instead, corrosion inhibitors work by directly reducing the rate of: 1) half-cell anodic reaction (i.e. anodic corrosion inhibitors), or 2) half-cell cathodic reaction (i.e. cathodic corrosion inhibitors), or 3) both anodic and cathodic reactions (i.e. mixed-type corrosion inhibitors) [18]. The corrosion-inhibiting mechanisms of anodic and cathodic corrosion inhibitors are illustrated in Figure 4.

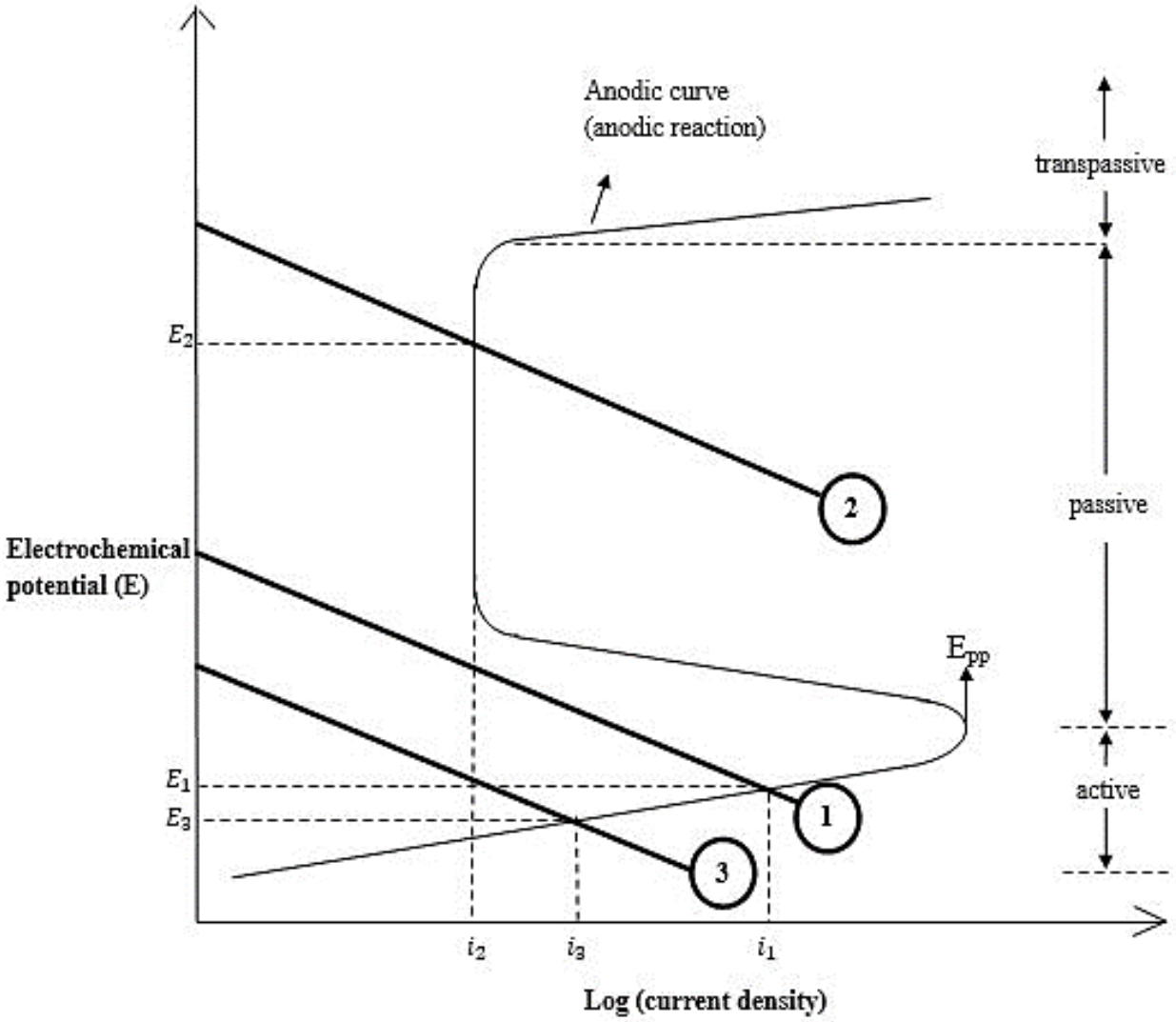

Figure 4: Effect of anodic and cathodic corrosion inhibitors on corrosion potential and corrosion current density (i.e. corrosion rate) of steel reinforcing bar (Adapted and modified from Hansson et al. [22]).

Figure 4 depicts the half-cell anodic and cathodic reactions of steel rebar corrosion (illustrated in Equations 3 and 4), in presence and absence of anodic and cathodic corrosion inhibitors. The half-cell anodic reaction is represented by the anodic curve while the half-cell cathodic reaction is represented by the diagonal lines numbered 1-3 (cathodic curves). The intersection points of the anodic and cathodic curves denote the electrochemical states of the rebar, which are represented by the

electrochemical potential and current density [22, 121]. The potential is known as corrosion potential (E_{corr}) and the current is known as corrosion current density (i_{corr}) [10, 22, 122].

As shown in Figure 4, in absence of a corrosion inhibitor, the anodic and cathodic curves intersect at E_{corr} of E_1 and i_{corr} of i_1. An anodic corrosion inhibitor forms a protective layer on the rebar surface, which shifts the rebar potential to a passive potential range and increases E_{corr} to E_2 whilst reducing i_{corr} to i_2 [5, 123, 124]. On the other hand, a cathodic corrosion inhibitor reduces the rate of oxygen reduction, shifting down the cathodic curve and reduces the E_{corr} and i_{corr} to E_3 and i_3 [5, 8, 22, 124]. Since i_{corr} is proportionally correlated with corrosion rate, the decrease in i_{corr} from i_1 to i_2 and i_3 demonstrates the corrosion inhibition by the anodic and cathodic corrosion inhibitors [22, 48, 125]. In addition, the shift in E_{corr} from E_1 to E_2 in presence of anodic corrosion inhibitor shifts rebar electrochemical state from an active corrosion state to a passive state with reduced corrosion rate [126, 127]. On the other hand, the reduction in E_{corr} from E_1 to E_3 in presence of a cathodic corrosion inhibitor reduces the driving force for rebar corrosion [102]. The driving force is the difference between E_{corr} and equilibrium potential of iron (E_{eq}) (Figure 5, E_R) when a steel rebar is in active corrosion state [102]. The equilibrium potential (E_{eq}) or reversible potential (E_R) of iron indicates the redox potential of iron ($E_{Fe/Fe^{2+}}$), at which the rate of iron oxidation and reduction are equal when iron is the only redox species in the system [74, 128]. Since both E_3 and E_1 indicate active corrosion states of rebar (Figure 4), the lower E_3 than E_1 reduces the driving force for rebar corrosion [102].

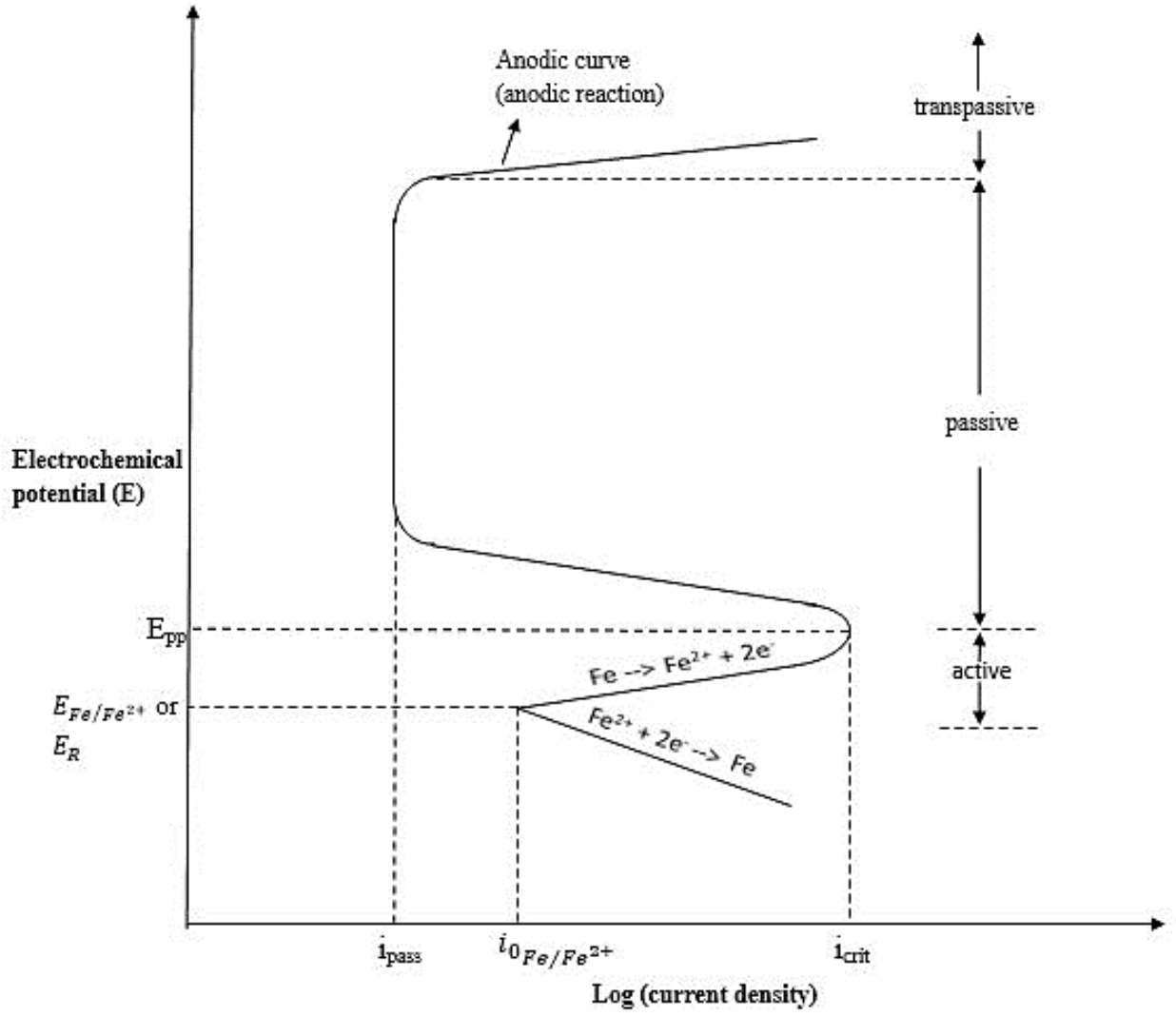

Figure 5: Typical potential vs. current density curve (Evans diagram) illustrating active/passive transition of iron (Adapted and modified from Schmuki and Graham [74] and Robert [129]).

In comparison to the corrosion inhibition mechanisms of anodic and cathodic corrosion inhibitors, a mixed-type corrosion inhibitor reduces corrosion rate (i_{corr}) without significantly changing the E_{corr} (Figure 6) [3, 5, 64, 119, 130, 131]. This is due to the adsorption of inhibitor molecules on rebar surface, which blocks the anodic and cathodic sites, and reduces the rate of anodic and cathodic reactions simultaneously [3, 5, 10, 19, 64]. The adsorption of mixed-type corrosion inhibitor is promoted by electron-rich bonds and polar atoms (such as sulfur, oxygen, nitrogen, and phosphorus)

in inhibitor structures as the adsorption centers [3, 64]. The simultaneous inhibition of anodic and cathodic reactions leads to a more effective corrosion inhibition by mixed-type corrosion inhibitor than anodic and cathodic corrosion inhibitors [45]. Effects of the three types of corrosion inhibitor on corrosion rate, E_{corr} , and i_{corr} are summarized in Table 3.

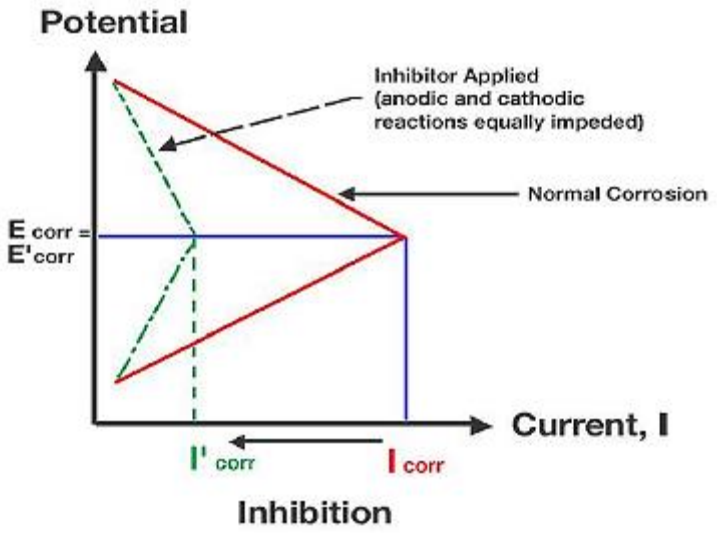

Figure 6: Inhibition on half-cell anodic and cathodic corrosion reactions of steel reinforcing bar by a mixed-type corrosion inhibitor (Adapted from Tanner [45]).

Table 3: Effect of anodic, cathodic, and mixed-type corrosion inhibitors on corrosion potential (E_{corr}), corrosion current density (i_{corr}), and corrosion rate of steel reinforcing bar

Corrosion inhibitor	E_{corr}	i_{corr}	Corrosion rate
Anodic	↑	↓	↓
Cathodic	↓	↓	↓
Mixed-type	No significant change	↓	↓

2.4.2 Present-day corrosion inhibitors

Today, inorganic and organic corrosion inhibitors are available in the market. The inorganic inhibitors, in particular calcium nitrite corrosion inhibitor (CI), are considered more effective than the organic inhibitor counterparts [20, 27]. CI has been used in reinforced concrete since 1970 and is presently regarded as the most effective corrosion inhibitor [16-19]. It is an anodic corrosion inhibitor which is added into fresh concrete as an admixed corrosion inhibitor [18, 31, 32]. CI prevents rebar corrosion by promoting formation of passive film on rebar surface, as illustrated in Equations 8 and 9 [18-21].

$$2\ Fe^{2+} + 2\ OH^- + 2\ NO_2^- \rightarrow 2\ NO + Fe_2O_3 + H_2O \quad (8)$$

$$Fe^{2+} + OH^- + NO_2^- \rightarrow NO + \gamma\text{-}FeOOH \quad (9)$$

Nonetheless, being an anodic corrosion inhibitor, inadequate CI dosage causes a risk of enhanced corrosion, as illustrated in Figure 7 [18, 19, 23, 31].

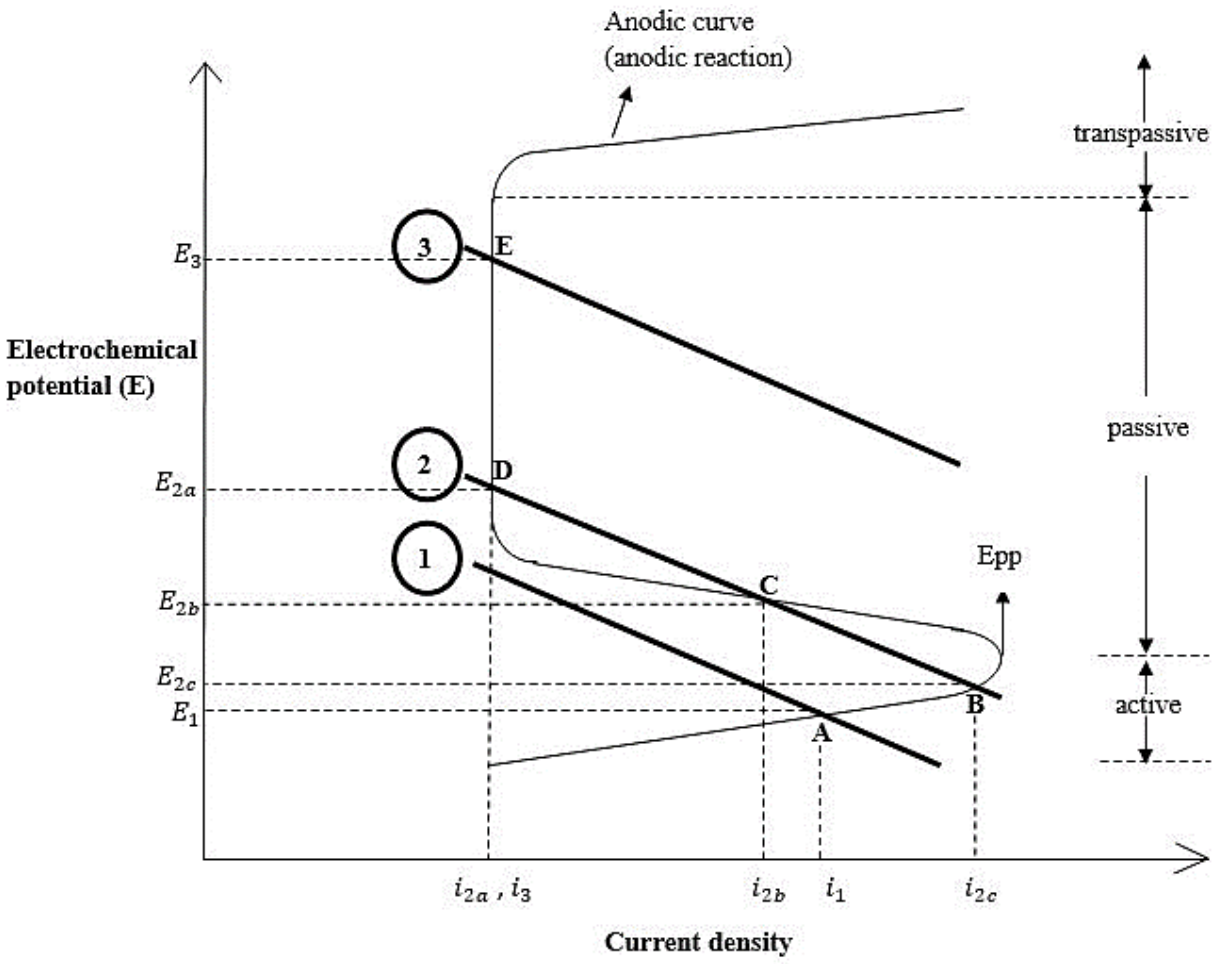

Figure 7: Effect of anodic corrosion inhibitor dosage on corrosion potential and corrosion current density (i.e. corrosion rate) of steel reinforcing bar (Adapted and modified from Hansson et al. [22]).

In absence of an anodic corrosion inhibitor (Figure 7), the E_{corr} and i_{corr} at E_1 and i_1 represent an actively corroding rebar. Addition of anodic corrosion inhibitor in adequate dosage shifts the rebar potential to a passive potential range (point E), increasing E_{corr} to E_3 and reducing i_{corr} to i_3 [123]; indicating a rebar protection from corrosion. However, the effect of inadequate dosage of anodic corrosion inhibitor is uncertain. As suggested in Figure 7, when the dosage of anodic corrosion inhibitor is inadequate, electrochemical states of the rebar can be represented by three points: B, C, and D. At points C and D, the inhibitor effectively protects the rebar, as demonstrated by higher E_{2a} and E_{2b} and lower i_{2a} and i_{2b} than E_1 and i_1. However, at

point B, the inhibitor fails to increase rebar potential above the primary passive potential (E_{pp}), which is the threshold potential at which the transition from an actively corroding to a passive rebar occurs [22]. Due to this failure, the rebar remains at an active corrosion state. Therefore, at point B, which indicates a rebar in active corrosion state, the increase in i_{corr} from i_1 to i_{2c} increases rebar corrosion rate. Hence, inadequate dosage of anodic corrosion inhibitor may enhance rebar corrosion, instead of promoting rebar passivation [22, 132].

In addition to the risk of enhanced corrosion, some studies [28-35] have reported unsatisfactory efficiency of CI, especially when cracks are present and corrosion has initiated. Unfortunately, the nitrite ion which is responsible for anti-corrosion of CI has been consumed during passive film formation (Equations 8 and 9), leading to concern on the efficiency of CI to protect rebar from corrosion in the long-term [24-26]. The nitrite is also consumed when oxygen is present in the concrete, due to the oxidation of the nitrite to nitrate; which may explain the unsatisfactory efficiency of CI in cracked concrete [24-26]. When cracks are present, some nitrite may also leach out from the concrete given the high solubility of calcium nitrite in water [20]. Thus, the use of CI in combination with methods to reduce concrete permeability (such as the use of low water/binder ratio, sufficient cover depth, and supplementary cementitious materials) are recommended [24, 27, 28, 133]. Nevertheless, corrosion protection efficiency of the concrete with reduced permeability has increased, which causes the improvement on corrosion inhibition efficiency upon CI incorporation less apparent [29]. Furthermore, some studies [23, 25, 134] have reported a higher chloride diffusion in concrete added with CI. The increased chloride diffusion is undesirable because it counteracts the beneficial effect of CI which increases chloride threshold concentration [23, 25, 134].

Commercial organic corrosion inhibitors (amines, alkanolamines, or emulsion of fatty acid esters) were marketed in 1980-1990's as the alternatives to potentially hazardous inorganic corrosion inhibitors [5, 16, 17, 20, 29, 35, 118, 135, 136]. The organic inhibitors are mixed-type corrosion inhibitors [27, 35, 37], thus preventing the

risk of enhanced corrosion which is associated with an anodic corrosion inhibitor [20, 35, 36]. Nonetheless, the efficiency of these organic inhibitors is arguable [20], which is plausibly due to the variations in chemical compositions of the organic inhibitors used in different studies, since the exact active constituents of the organic corrosion inhibitors are often not disclosed given proprietary reason. In addition, information on the concentration of the active constituents and the required inhibitor dosages relative to the concentration of aggressive species (i.e. chloride) are also lacking [20, 21, 27, 34].

The conflicting reports on the efficiency of existing inorganic and organic corrosion inhibitors have encouraged studies on the efficiency of non-toxic and environmentally-friendly ('green') alternatives to the existing corrosion inhibitors [15-17, 64, 137]. However, this remains an understudied field, with only limited studies on the corrosion inhibition efficiency (IE) of green corrosion inhibitors in alkaline pH of concrete, compared to similar studies in acidic medium [15, 130, 131, 138-146]. Experimental setups for the studies on green corrosion inhibitors in alkaline pH of concrete are presented in Table 4. On the other hand, the findings for the research studies presented in Table 4 are elaborated in Table 5. Given the scarcity of studies on green corrosion inhibitors under alkaline pH, this study on the IE of natural antioxidants (specifically from green tea) at alkaline concrete pH aims to fill this knowledge gap. The selection of natural antioxidants as green corrosion inhibitors is justified in the next section.

Table 4: Experimental setups for **s**tudies on non-toxic and environmentally-friendly ('green') corrosion inhibitors in alkaline pH of concrete

Reference	Corrosion inhibitor	Concentration	Media	Aggressive species	Setup
Feng et al. [8]	Imidazoline derivative: 1-[N, N'-bis (hydroxylethylether)-aminoethyl]-2-stearicimidazoline (HASI)	0.19-1.89 mM	Simulated concrete pore solution (SCPS)	5% (w/v) sodium chloride (NaCl)	Immersion
Asipita et al. [17]	*Bambusa arundinacea* leaf extract	2% (by cement weight)	Concrete	Water	Immersion
Bolzoni et al. [20]	Amines (dimethylethanolamine and triethylenetetramine) Amino acids (sodium aspartate, asparagine, sodium glutamate, and glutamine)	In solution: 1 M	SCPS	NaCl up to 1 M	Immersion
		In concrete: 1% (by cement weight)	Concrete	3.5% NaCl solution	Cyclic wetting-drying

	Carboxylic acids (sodium benzoate, sodium tartrate, EDTA)				
Jiang et al. [59]	Deoxyribonucleic acid (DNA)	0.0012, 0.0025, 0.0050, and 0.0100%	SCPS	0.01 and up to 0.10 M NaCl	Immersion
Okeniyi et al. [118]	*Anthocleista djalonensis* leaf extract	0.16-0.42% (by cement weight)	Concrete	3.5% NaCl solution	Immersion
Jiang et al. [120]	DNA	0.0025 and 0.0050% (by cement weight)	Mortar	3.5% NaCl solution	Cyclic wetting-drying (3 days of wetting and 3 days of drying)
Abdel-Gaber et al. [121]	*Solenostemma arghel* extract	250 ppm	Concrete	0.5 M NaCl solution	Immersion
Etteyeb and Novoa [147]	Extract of *Eucalyptus globulus* leaves (EG) Extract of *Punica granatum* trunk (PG)	EG: 1.09 g/L PG: 2.65 g/L OE: 0.79 g/L	0.1 M NaOH solution (pH 12.5)	0.5 M NaCl	Immersion

	Extract of *Olea europaea* secondary rods (OE)				
Asaad et al. [148]	Complex of silver nanoparticle and palm oil leaf extract (EG/AgNP)	5% (by cement weight)	Concrete	Natural seawater	Weekly cyclic wetting-drying
Shanmugapriya et al. [149]	Aqueous extract of turmeric	2% and up to 10% (v/v), with 2% increments	SCPS	Well water containing 660 ppm chloride	Immersion

Table 5: Experimental methodologies and findings for research studies presented in Table 4

Ref.	Methods	Findings
Feng et al. [8]	Linear polarization resistance (LPR)	Increasing corrosion inhibition efficiency (51 to 81%) with increasing imidazoline derivative (HASI) concentration from 0.19 to 1.89 mM. HASI behaved as a cathodic inhibitor
	Electrochemical impedance spectroscopy (EIS)	Increased resistance against chloride attack, as evidenced by reduced double layer capacitance, increased charge transfer resistance, and increased resistance at film-solution interface. These changes indicated the formation of a more compact passive film.
	Scanning electron microscopy (SEM)	Rebar immersed in simulated concrete pore solution (SCPS) added with 0.76 mM HASI showed no corrosion. Rebar immersed in control SCPS (no corrosion inhibitor) showed formation of blister
	Quantum chemical calculation (QC) and molecular dynamic simulation (MD)	N=C=N bond of imidazoline ring was the adsorption center via electron sharing between nitrogen atoms and vacant d-orbitals of iron. HASI adsorbed on steel surface at near parallel configuration to maximize surface contact
Asipita et al. [17]	Water permeability using initial surface absorption test (ISAT)	Water absorption of less than 0.07 mL/m^2 after 2 hours, fulfilling the 'low permeability' requirement of ISAT standard

Bolzoni et al. [20]	Potentiodynamic polarization (PD) Potentiostatic polarization Natural corrosion test	Similar performances (pitting potential, chloride threshold concentration, and initiation time of corrosion) between tested carboxylic acids and sodium nitrite (a positive control)
	LPR	Higher chloride threshold concentration of concrete containing glutamine and triethylenetetramine than control concrete (no corrosion inhibitor)
Jiang et al. [59]	Stereo microscope	Significant corrosion damage on rebar without corrosion inhibitor Almost no corrosion damage on rebar protected by 0.0025% deoxyribonucleic acid (DNA), rebars protected by other DNA concentrations showed pitting corrosion
	PD	0.0025 and 0.0050% DNA reduced current density by two-log compared to control (no corrosion inhibitor)
	LPR	0.0025 and 0.0050% DNA had the highest corrosion inhibition efficiency Corrosion inhibition efficiency of 0.0025 and 0.0050% DNA against 0.07 M NaCl were 78-79%; other DNA concentrations showed no inhibition Against 0.10 M NaCl, the corrosion inhibition efficiency of 0.0025 and 0.0050% DNA were 59 and 46%
	EIS	Up to 0.07 M NaCl, 0.0025 and 0.0050% DNA significantly increased film resistance at rebar interface from 0.50 $k\Omega.cm^2$ (for control) to 10.67 and 8.47 $k\Omega.cm^2$

		Increase of NaCl concentration to 0.10 M significantly reduced the film resistance to 0.34 and 0.52 kΩ.cm^2 vs. 0.27 kΩ.cm^2 for control
	X-ray photoelectron spectroscopy (XPS)	XPS suggested the presence of iron oxides (FeO and Fe_2O_3) and possible adsorption of DNA on rebar surface
Okeniyi et al. [118]	LPR	Increasing corrosion inhibition efficiency with increasing extract concentration (81% at 0.16% inhibitor and up to 97% at 0.42% inhibitor) Adsorption of extract on steel obeyed Langmuir isotherm, with a dominant effect of chemical interaction (chemisorption)
Jiang et al. [120]	LPR	Increased polarization resistance after 20 wetting-drying cycles from 200 Ω/cm^2 for control mortar (no corrosion inhibitor) to 3,200 and 1,800 Ω/cm^2 for 0.0025% deoxyribonucleic acid (DNA)-based mortar and 0.0050% DNA-based mortar 2% commercial phosphate inhibitor increased polarization resistance to 9,200 Ω/cm^2)
	EIS	Increased charge transfer resistance after 20 wetting-drying cycles, from 100 Ω.cm^2 for control mortar to 2,800 and 1,600 Ω.cm^2 for 0.0025% DNA-based mortar and 0.0050% DNA-based mortar 2% commercial phosphate inhibitor increased charge transfer resistance to 8,900 Ω/cm^2

	Mercury intrusion porosimetry (MIP)	DNA reduced percentage of macropores (10% reduction for 0.0025% DNA-based mortar, similar percentage of macropores for 0.0050% DNA-based mortar and control mortar) DNA reduced percentage of micropores (approximately 10% reductions for both 0.0025% DNA-based mortar and 0.0050% DNA-based mortar) DNA increased percentage of gel pores (50% and 15% for 0.0025% DNA-based mortar and 0.0050% DNA-based mortar)
	Compressive strength	DNA reduced 3-day compressive and flexural strength
	Flexural strength	DNA exerted negligible effects on 28-day compressive and flexural strength
Abdel-Gaber et al. [121]	PD	Increase in corrosion potential from -660 mV for control (no corrosion inhibitor) to -610 mV Extract behaved as an anodic inhibitor
	EIS	Increase in total resistance after 62-day from 14,000 Ω/cm^2 (for control) to 21,000 Ω/cm^2 Increase in Warburg resistance to diffusion was more profound than the increase in charge transfer resistance.
	Visual inspection (optical images)	No sign of corrosion damage after 18 months

Etteyeb and Novoa [147]	Mott-Schottky (MS)	MS suggested formation of passive layer, as indicated by the reduction in donor density at the interface of passive film-electrolyte and the increase in the thickness of passive layer
	EIS	EIS suggested that plant extracts increased corrosion resistance, as indicated by the increase in electrical resistance and decrease in capacitance
	SEM and energy dispersive X-ray spectroscopy (EDX)	SEM and EDX supported MS and EIS results by showing deposit formation on rebar surface
	PD	Extracts of *Eucalyptus globulu*s leaves, *Punica granatum* trunk, and *Olea europaea* secondary rods demonstrated corrosion inhibition efficiency of 88, 93, and 92%
Asaad et al. [148]	Thermal gravimetric analysis (TGA/DTA)	Complex of silver nanoparticle and palm oil leaf extract (EG/AgNP) promoted consumption of Portlandite to produce calcium silicate hydrate and formation of denser concrete matrix
	X-ray diffraction spectroscopy (XRD)	Lower Portlandite in EG/AgNP-modified concrete
	LPR PD	LPR and PD showed that EG/AgNP increased polarization resistance and reduced corrosion rate (maximum corrosion inhibition efficiency of 94.74%) PD suggested that EG/AgNP was a mixed-type corrosion inhibitor
	Concrete resistivity	EG/AgNP significantly increased concrete resistivity, particularly at later exposure stage (up to 365 days)
	SEM with EDX	SEM of EG/AgNP-modified concrete displayed a more compact matrix

		EDX of EG/AgNP-modified concrete showed the absence of chloride compared to 15% for control concrete (no corrosion inhibitor) SEM showed a smoother surface of rebar extracted from EG/AgNP-modified reinforced concrete. Rebar extracted from control reinforced concrete (no corrosion inhibitor) exhibited corroded surface and cracks after 365-day EDX showed no chloride at steel reinforcement level for EG/AgNP-modified reinforced concrete compared to 13.6% for rebar from control reinforced concrete
Shanmugapriya et al. [149]	PD	Turmeric extract reduced corrosion current density compared to control (no corrosion inhibitor), from 1.57×10^{-6} to 1.06×10^{-6} A/cm^2
	EIS	Turmeric extract reduced double layer capacitance from 10.9×10^{-10} F/cm (for control) to 7.51×10^{-10} F/cm Turmeric extract increased charge transfer resistance from 4.68 kΩ.cm^2 (for control) to 6.79 kΩ.cm^2 Turmeric extract increased polarization resistance from 2.68 kΩ.cm^2 (for control) to 3.87 kΩ.cm^2

2.5 Natural antioxidants as potential corrosion inhibitors and justifications for selecting green tea as the source of natural antioxidants

Natural antioxidants are organic compounds which are abundant in nature, particularly in plants and plant products such as fruits and vegetables [150]. Benefits of the antioxidants have been utilized in several industrial sectors, particularly in food and health industries [151]. Natural antioxidants are rich in polar atoms and electron-rich bonds [39]. These functional groups help the antioxidants to inhibit oxidation process by chelating metal ions which catalyze the oxidation, or donating protons and/or electrons to directly reduce the oxidation of target substrates [151]. The electron donation properties of natural antioxidants are potentially beneficial for an anti-corrosion activity, because the donated electrons will form coordinate bonds with vacant d-orbital of iron atoms, and promote the adsorption of antioxidant molecules on rebar surface [8, 146]. The adsorption plausibly confers the natural antioxidants an anti-corrosion activity as mixed-type corrosion inhibitors [22].

Green tea has one of the highest contents of natural antioxidants [40-43]. The antioxidant activity of green tea is ten to thirty-fold higher than that of berries, which are notably the other rich sources of natural antioxidants (Table 6) [44]. The antioxidant activity of green tea is contributed by the potent antioxidants from catechin derivatives (Figure 8) [40], which constitute approximately 70% of total polyphenols in green tea [152]. Given the extraordinarily higher antioxidant activity of green tea relative to other sources of natural antioxidants, the authors believe that this material is favorable (as a proof of concept) and it stands the best chance at preventing rebar corrosion. Therefore, the authors have selected green tea to be used as the source of natural antioxidants in this study.

Table 6: Antioxidant activity ratio of green tea to berries. Adapted and modified from Borges et al. [44] and Benzie and Szeto [153].

Berries	Antioxidant activity ratio of green tea to berries
Black currants	12
Blueberries	22
Raspberries	23
Red currants	26
Cranberries	34

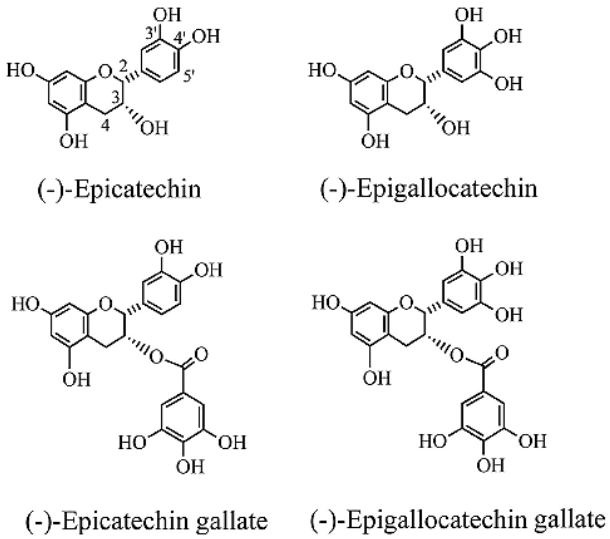

Figure 8: Potent antioxidants in green tea (Adapted from Stewart et al. [40])

2.6 Novelty of study

There has been no study reporting on the IE of GT in alkaline pH of concrete, nor compared the IE with the IE of a commercial corrosion inhibitor (i.e. CI). The novelty of these findings is further compounded by the scarcity of studies relating to natural organic corrosion inhibitors.

2.7 Summary

Rebar corrosion harms the safety of RC structures and bears significant socio-economic consequences. Rebar corrosion due to chloride is particularly detrimental, because it has a high corrosion propagation rate and short propagation time. At present, CP and SS are the best methods to protect steel rebar from corrosion. However, they are expensive. Corrosion inhibitors are simpler and more cost-effective than CP and SS. Existing corrosion inhibitors can be categorized as inorganic and organic corrosion inhibitors. The inorganic corrosion inhibitors, in particular CI, have been reported to be more effective than the organic corrosion inhibitor counterparts. However, several studies have reported arguable efficiency of CI. Moreover, the use of inorganic corrosion inhibitors arises environmental and health concerns. Therefore, green alternatives to existing inorganic and organic corrosion inhibitors are required. Unfortunately, while studies on green corrosion inhibitors in acidic media are abundant, similar studies on the alkaline pH within concrete matrix are still scarce. Hence, the authors contribute towards the limited studies by investigating the efficiency of natural antioxidants from green tea to inhibit rebar corrosion in alkaline pH of concrete. This study continues with the investigation on corrosion inhibition efficiency of green tea in simulated concrete pore solution, which is presented in the Chapter 3.

CHAPTER 3: CORROSION TESTS IN SOLUTION

3.1 Introduction

Corrosion inhibitors are added into reinforced concrete (RC) structures during concrete mixing to prevent corrosion initiation (admixed corrosion inhibitors) or being applied on the surface of hardened concrete to reduce ongoing corrosion (migrating corrosion inhibitors). In this study, green tea was applied as an admixed corrosion inhibitor against chloride-induced corrosion. Chloride-induced corrosion propagates faster than carbonation-induced corrosion (up to ten-times). Thus, when chloride-induced corrosion initiates, service life of RC structure is often assumed to reach the end (Tuutti's model) [20, 110, 154-156]. Consequently, preventing corrosion to prolong the structural service life is prioritized over remediating corrosion, and admixed corrosion inhibitor is preferred to migrating corrosion inhibitor from a service-life perspective [20]. In addition, the active compounds of migrating corrosion inhibitors are small and volatile to enable penetration through hardened concrete [18]. In comparison, potent antioxidant compounds in green tea are larger and less volatile than the typical active compounds of migrating corrosion inhibitors. Hence, considering the physicochemical properties of green tea compounds and the importance of preventing corrosion to prolong structural service life, green tea was applied as an admixed corrosion inhibitor against chloride-induced corrosion.

As reported by Feng et al. [8], electron donation promotes inhibitor adsorption on rebar surface as mixed-type corrosion inhibitor. Therefore, the electron donation capacity of green tea was initially measured with single electron transfer antioxidant activity (SET-AA) assays: the 2,2-diphenyl-1-picrylhydrazyl (DPPH) radical scavenging activity and ferric reducing power assay. The assays were performed following the study by Chan et al. [157]. Afterwards, the physical form (dry admixture or aqueous extract [17, 20, 118, 121, 133, 148, 149, 158-160]) to apply green tea as an

admixed corrosion inhibitor was determined. The physical form which did not significantly change the 7-day compressive strength of green tea-based mortar relative to the strength of control mortar (no corrosion inhibitor) was selected to apply green tea for corrosion tests in simulated concrete pore solution (SCPS).

3.2 Material properties and sample preparations

The next sections describe the preparations for SET-AA, compressive strength, and corrosion measurements. These preparations include the antioxidant extraction from green tea, mortar mix design for compressive strength measurements, as well as the preparations of steel rebars and SCPS for corrosion tests.

3.2.1 Preparations of green tea

Green tea was procured from a commercial Japanese green tea supplier (Figure 9). Green tea for SET-AA measurements was prepared as green tea extract, by hot-water extraction of 1 g green tea leaves on orbital shaker [157]. On the other hand, green tea for mortar compressive strength measurements and corrosion tests were prepared in four different forms [17, 118, 121, 133, 148, 149, 158-160]:

(a) dry admixture of 1% green tea (by cement weight),

(b) dry admixture of 2% green tea (by cement weight),

(c) aqueous extract of 1% green tea (by cement weight), and

(d) aqueous extract of 2% green tea (by cement weight)

Figure 9: Green tea

The aqueous extract of 1% green tea and aqueous extract of 2% green tea for compressive strength measurements were prepared by hot-water extraction on orbital shaker (Figure 10). On the other hand, the aqueous green tea extracts for corrosion tests were prepared by ultrasonic-assisted extraction (Figure 11).

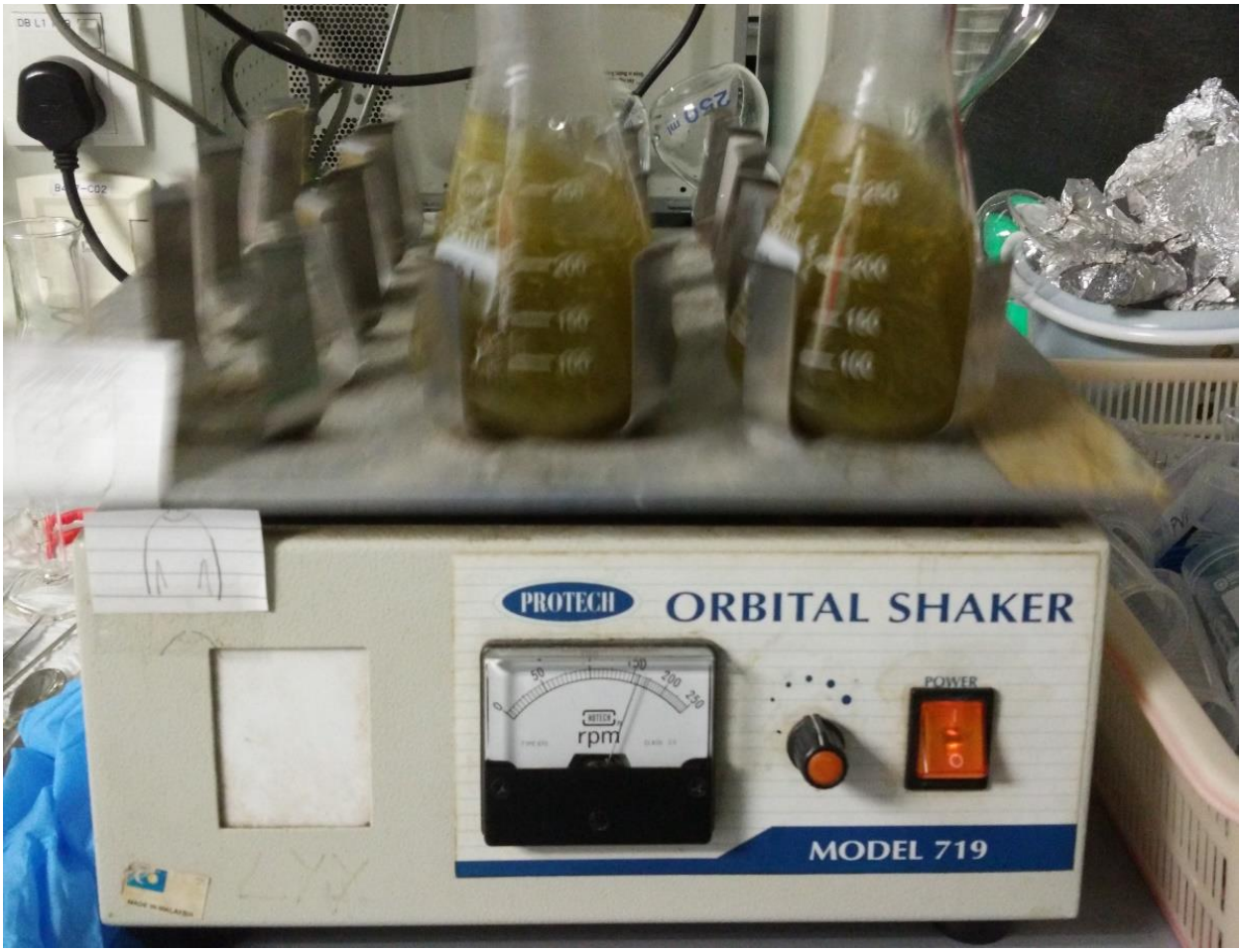

Figure 10: Hot-water extraction of green tea on orbital shaker with the shaking speed of 150 rpm

Figure 11: Ultrasonic-assisted extraction of green tea with an ultrasonic bath

A higher amount of green tea was extracted for the corrosion tests in SCPS, than for the SET-AA and mortar compressive strength measurements. Regardless of the extraction method, green tea suspension is produced during the extraction. The suspension absorbs and retains some portion of the green tea extract, leading to unavoidable extract loss. The higher is the amount of the extracted green tea, the thicker is the suspension, and the higher is the loss of the green tea extract. Therefore, the green tea extracts for corrosion tests were extracted by ultrasonic-assisted method, to eliminate the use of multiple apparatuses (conical flasks in this case, see Figure 10), which is necessary for extracting the increasing amount of green tea on orbital shaker. The use of multiple apparatuses would otherwise contribute to a higher loss of the green tea extract as some leaf suspension may remain in the container and retain the green tea extract. This suspension can only be recovered by rinsing the container with water. Unfortunately, extract recovery through water rinsing is not recommended as the water dilutes the extract. Therefore, with incorporation of multiple apparatuses, the leaf suspension which retains some portion of green tea extract is distributed over the apparatuses, hence producing a higher loss of the extract.

3.2.1.1 Preparations of green tea for SET-AA measurements

Green tea for SET-AA measurements was prepared as green tea extract, by hot-water extraction of 1 g green tea leaves with 50 mL ultra-pure water (UPW) on orbital shaker for 1 hour (shaking speed of 150 rpm) [157]. During the extraction, the extract was continuously shaken and allowed to cool down naturally. Afterwards, the extract was vacuum-filtered to obtain the green tea extract (GT), as illustrated in Figure 12.

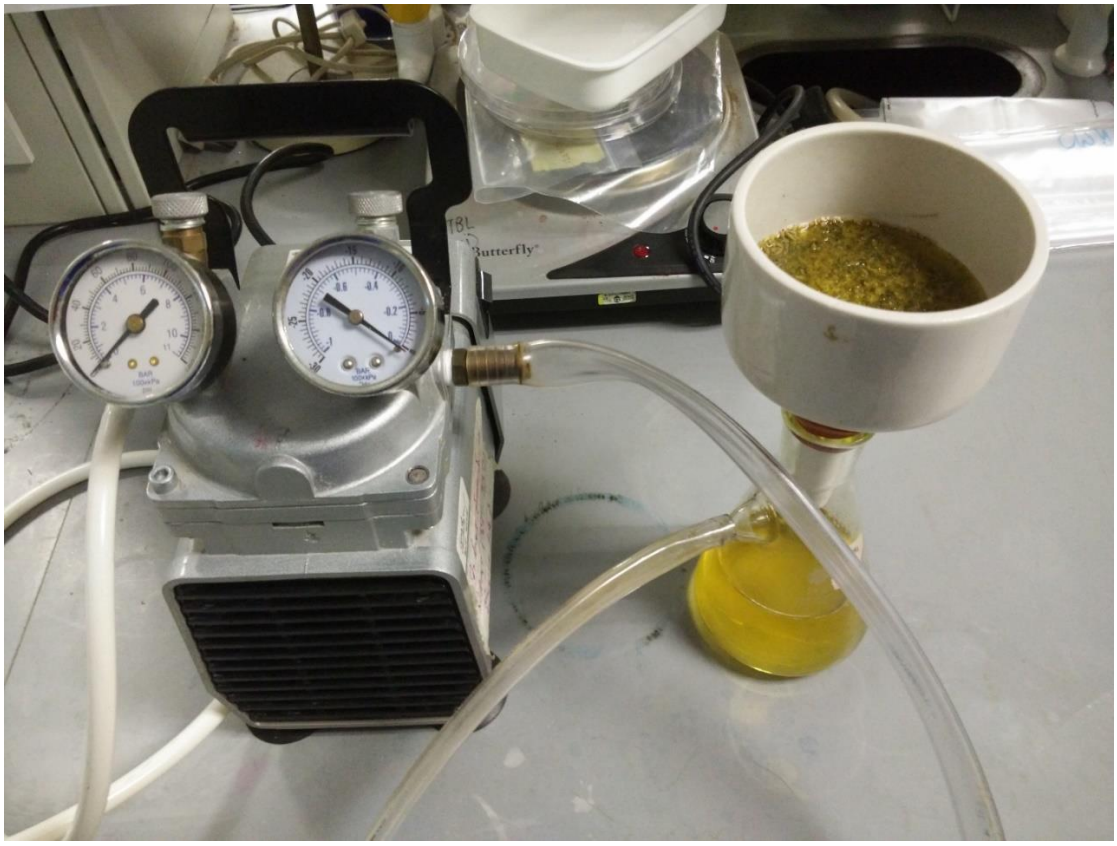

Figure 12: Vacuum filtration to obtain green tea extract

3.2.1.2 Preparations of green tea for mortar compressive strength measurements

Green tea for compressive strength measurements was prepared in four different forms, based on the physical forms of corrosion inhibitors reported in literatures [17, 118, 121, 133, 148, 149, 158-160]:

(a) dry admixture of 1% green tea leaves (by cement weight)

(b) dry admixture of 2% green tea leaves (by cement weight)

(c) GT of 1% green tea leaves (by cement weight) and

(d) GT of 2% green tea leaves (by cement weight).

The percentage by cement weight is a common expression for the dosage of a commercial corrosion inhibitor [133, 158-160].

The GT of 1% green tea leaves (by cement weight) was produced extracting the 1% green tea leaves with hot UPW on orbital shaker for 1 hour (shaking speed of 150 rpm), at leaves-to-water ratio (w/v) of 1% [153, 157, 161, 162]. On the other hand, the

GT of 2% green tea leaves (by cement weight) was produced by extracting the 2% green tea leaves with hot UPW on orbital shaker for 1 hour (shaking speed of 150 rpm), at leaves-to-water ratio (w/v) of 2%. Continuous shaking was applied during the extraction and the extracts were allowed to cool down naturally. Afterwards, the extracts were vacuum-filtered to obtain the GT.

3.2.1.3 Preparations of green tea for corrosion tests in SCPS

Green tea for corrosion tests in SCPS was prepared similarly to the green tea for compressive strength measurements, except for the extraction method. The GT of 1% green tea leaves (by cement weight) for the corrosion tests was prepared by ultrasonic-assisted extraction of the 1% green tea leaves with hot UPW for 15 minutes, at leaves-to-water ratio (w/v) of 1%. On the other hand, the GT of 2% green tea leaves (by cement weight) for the corrosion test was prepared by ultrasonic-assisted extraction of the 2% green tea leaves with hot UPW for 15 minutes, at leaves-to-water ratio (w/v) of 2%.

3.2.2 Preparations for compressive strength measurements

Portland Cement CEM II/B-S 42.5N and fine aggregate passing 600 µm sieve were used to prepare mortar for compressive strength measurements, according to compositions presented in Table 7. Chemical compositions of the cement are presented in Table 8. The size of the fine aggregate was standardized to obtain a better comparison on the compressive strength of control and green tea-based mortar. On the other hand, an optimum water/cement ratio (w/c) was selected to avoid the use of other chemical admixture (particularly superplasticizer) which may interfere with the evaluation on the efficiency of green tea during corrosion tests in mortar (presented in Chapter 4). Moreover, the w/c was selected to enable the completion of the corrosion tests in mortar within the reasonable timeframe of this study (under twelve months), similar to the studies by Andrade et al. [158, 163]. Dosages of green tea admixed into mortar are shown in Table 9.

Table 7: Constituents of mortar mixture

Constituent	Proportion (kg/m^3)
Cement	420.0
Water	210.0
Fine aggregate	619.2
Water/cement (w/c) = 0.50	

Table 8: Chemical compositions of cement

Constituent	Percentage weight
SiO_2	23.56
Al_2O_3	6.80
CaO	57.61
MgO	1.36
SO_3	2.87
K_2O	0.66
Na_2O	0.11
Loss on ignition	2.70

Table 9: Dosages of green tea added into mortar

Corrosion inhibitor	Inhibitor physical form	Percentage water replacement with inhibitor	Weight of inhibitor (kg/m^3)
No inhibitor (control)	-	-	-
1% green tea (by cement weight)	Dry admixture	-	4.20
	Green tea extract	20	24.36
		40	48.72
		60	73.08
		80	97.44
		100	121.80
2% green tea (by cement weight)	Dry admixture	-	8.40
	Green tea extract	20	24.36
		40	48.72
		60	73.08
		80	97.44
		100	121.80

3.2.3 Preparations for corrosion tests in SCPS

Preparations for corrosion tests in SCPS involved the preparations of steel rebars and SCPS.

3.2.3.1 Preparations of steel rebars

Steel rebars of 12 mm diameter and 130 mm length were cut from commercial carbon steel rebars (high tensile deformed steel rebars grade 500B) [10]. Chemical compositions of the rebar are presented in Table 10. Prior to use, the rebars were mechanically cleaned with grade-400 silicon carbide paper and down to grade-800 and grade-1000. The rebars were degreased with acetone, cleaned with UPW, air-dried [10, 164], and painted with epoxy [8]. Only 1,571 mm^2 (at the middle) and 943 mm^2 (at the top) surface areas of the rebars were unpainted for exposure to chloride and electrical

connection. The remaining surface of the rebars were painted with epoxy. The painted and unpainted sections of the rebar are illustrated in Figure 13.

Table 10: Chemical compositions of steel reinforcing bar

Element	Percentage weight
C	0.210
Si	0.300
Mn	0.420
P	0.046
S	0.042
N	0.003
Fe	98.979

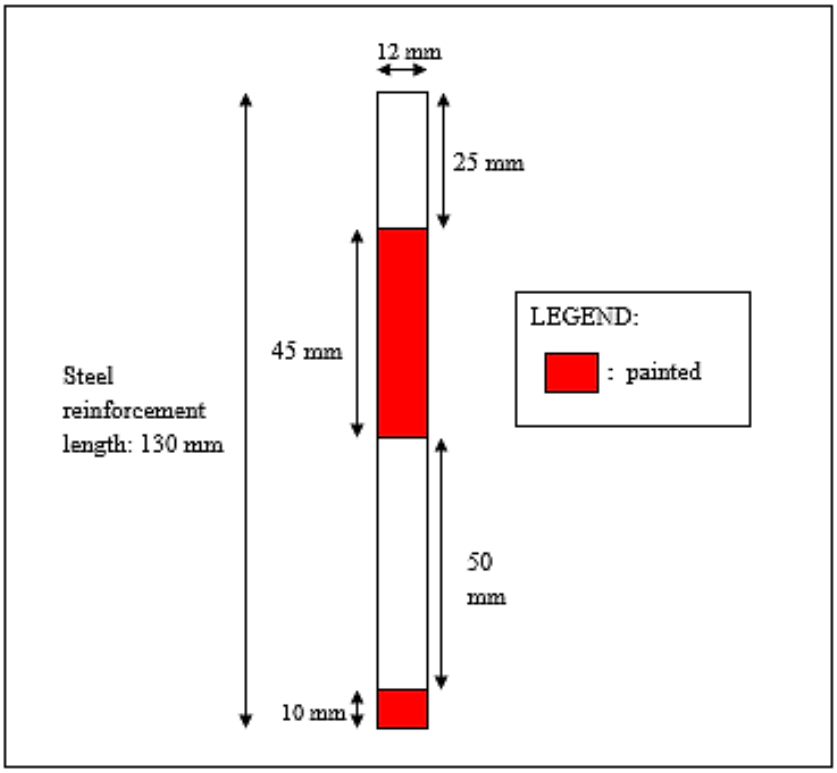

Figure 13: Steel reinforcing bar for corrosion test

3.2.3.2 Preparations of SCPS

Saturated calcium hydroxide solution (2 g/L) was used to simulate the alkaline liquid of concrete pore [8, 10, 59, 158]. The simulated concrete pore solution (SCPS) which contained green tea is referred to as GT-SCPS. On the other hand, SCPS without green tea is referred to as C-SCPS. Dosages of green tea selected to prepare the GT-SCPS are presented in Table 11. Final pH of C-SCPS and GT-SCPS were adjusted to 12.7 with 2 M sodium hydroxide [20, 165]. Upon pH adjustment, 3.5% (w/v) sodium chloride (NaCl) was introduced into the SCPS, to simulate the exposure to seawater [4, 8, 118, 166-168].

Table 11: Dosages of green tea in simulated concrete pore solution

Corrosion inhibitor	Percentage water replacement with inhibitor	Volume of green tea extract (mL)	Volume of ultra-pure water (mL)
No inhibitor (control)	-	-	200
Extract of 1% green tea (by cement weight)	100	200	0
Extract of 2% green tea (by cement weight)	60	120	80

3.3 Methodologies

The following sections describe the procedures for SET-AA measurements, mortar casting and compressive strength measurements, and corrosion measurements.

3.3.1 SET-AA measurements

Two antioxidant assays were employed to measure the electron donation capacity of green tea: the ferric reducing power and DPPH radical scavenging assay. Procedures for performing the assays were adapted from the study by Chan et al. [169].

3.3.1.1 Ferric reducing power assay

For ferric reducing power assay, three different volume of GT were pipetted into test tubes, one test tube for each volume, and made up to 1 mL with UPW. Afterwards, 2.5 mL phosphate buffer (0.2 M, pH 6.6) and 2.5 mL of 1% (w/v) potassium ferricyanide were added into each test tube. The aliquots were mixed and incubated at 50°C for 20 minutes. The reaction was brought to a halt by the addition of 2.5 mL of 10% (w/v) trichloroacetic acid. The 8.5 mL mixture in each test tube was separated into three test tubes (i.e. three replicates), each containing 2.5 mL solution. Each of the 2.5 mL solution was diluted with 2.5 mL UPW, and 500 µL of 0.1% (w/v) ferric chloride was subsequently added. The solution was mixed and incubated in the dark for 30 minutes prior to absorbance measurement at 700 nm. The ferric reducing power was expressed as mg gallic acid equivalent (GAE) per g of green tea. The calibration equation for gallic acid standard was y = 17.085x where y was the absorbance value at 700 nm and x was the gallic acid concentration in mg/mL.

3.3.1.2 DPPH radical scavenging assay

For DPPH radical scavenging assay, three different volume of GT were pipetted into test tubes, three test tubes (i.e. three replicates) for each volume, and made up to 1 mL with UPW. In each test tube, the diluted GT was added with 2 mL of 5.9 mg/100 mL of DPPH. The solution was mixed and incubated in the dark for 30 minutes prior to absorbance measurement at 517 nm. Three replicates of 1 mL UPW added with 2 mL DPPH were prepared as the negative controls. The average absorbance of the negative controls was used to calculate the required green tea concentration to scavenge 50% of DPPH radical (IC_{50}), based on the % scavenging activity calculation:

$$\%\ scavenging\ activity = \left(1 - \frac{Average\ absorbance\ of\ GT}{Average\ absorbance\ of\ negative\ control}\right) \times 100\% \qquad (10)$$

The calculated % scavenging activities were plotted against mg green tea in 3 mL solution, and the equation obtained was used to calculate the IC_{50}. The DPPH radical scavenging activity was expressed as ascorbic acid equivalent antioxidant capacity

(AEAC). The AEAC was calculated as $\frac{IC_{50} ascorbic\ acid}{IC_{50}\ green\ tea} \times 10^5$, with IC_{50} of ascorbic acid was 0.003885 mg/mL.

3.3.2 Mixing and casting of mortar

Mortar was mixed with a laboratory-scale mixer (KitchenAid heavy duty mixer), based on the procedures described by Gencel et al. [86] and Karahan and Atis [52] with modifications. The cement and fine aggregate were initially mixed for one minute; for mortar containing dry green tea admixture, the dry admixture was mixed together with the cement and fine aggregate. Subsequently, UPW or mixture of UPW and GT was added into the dry mixtures. The mortar was mixed for two minutes at the lowest mixer speed (60 rpm), rested for two minutes, and mixed for a further two minutes. The fresh mortar mixture was filled into PVC pipe molds (diameter: 33 mm, height: 70 mm) in three-equal layers, and each layer was compacted on a vibrating table for 25 seconds. Three specimens were prepared for control mortar and mortar added with each dosage of green tea (Table 12). After 24 hours, the hardened mortar specimens were de-molded and cured for 7 days [52] in saturated limewater following ASTM C 511.

Table 12: Number of specimens prepared for control mortar and green tea-based mortar

Corrosion inhibitor	Inhibitor physical form	Percentage water replacement with inhibitor	Weight of inhibitor (kg/m^3)	Number of mortar specimens
No inhibitor (control)	-	-	-	3
1% green tea (by cement weight)	Dry admixture	-	4.20	3
	Green tea extract	20	24.36	3
		40	48.72	3
		60	73.08	3
		80	97.44	3
		100	121.80	3
2% green tea (by cement weight)	Dry admixture	-	8.40	3
	Green tea extract	20	24.36	3
		40	48.72	3
		60	73.08	3
		80	97.44	3
		100	121.80	3

3.3.3 Corrosion measurements

There are two commonly used methods to measure rebar corrosion: the gravimetric and electrochemical methods. Gravimetric method quantifies rebar weight loss due to corrosion damage. Thus, this method requires the removal of rebar from the concrete (i.e. destructive method) and is time-consuming [110, 154, 158]. On the other hand, the electrochemical method is non-destructive and less time-consuming. Electrical potential is applied to the rebar and the generated current is measured, which is converted into corrosion rate by applying the Faraday law [170]. Hence, the

electrochemical method is preferred over the gravimetric method, due to its shorter measurement time and non-destructive nature [155, 158, 171, 172].

In this study, linear polarization resistance (LPR) was adopted to measure rebar corrosion. LPR is a popular electrochemical measurement technique which applies a small potential (±20 mV) to the rebar, resulting in short measurement time (10-15 minutes) and no alteration to the electrochemical processes of rebar corrosion [158, 173-176]. Thus, LPR enables multiple measurements over time, to determine the time-to-corrosion initiation and the efficiency of an admixed corrosion inhibitor [10, 164, 165].

LPR was performed based on the study by Feng et al. [8], using Metrohm Autolab potentiostat (model M204) with a three-electrode setup: saturated calomel electrode as the reference electrode (RE), platinum electrode as the counter electrode (CE), and steel rebar as the working electrode (WE) [59, 120, 149]. The CE, WE, and RE were located approximately 3 mm away from each other to prevent ohmic drop. The LPR measurement was conducted at laboratory temperature (26.4± 1.7°C, 70.3± 7.5% relative humidity). Prior to LPR measurement, open circuit potential (OCP) of the rebar was measured. OCP indicates the rebar potential in absence of interference from external potential/current. When the OCP had reached a stable value [172] (fluctuations less than 10 mV, reached within 10 minutes), OCP value was determined and the rebar was polarized with a scan potential of ±20 mV from OCP and scan rate of 0.166 mV/s. Electrochemical parameters such anodic and cathodic slopes, polarization resistance, and corrosion rate were obtained by analyzing the resulted plots of potential vs. log current with Nova software version 1.11. The corrosion rate was used to calculate the corrosion inhibition efficiency according to:

$$\% \text{ inhibition efficiency} = \frac{CR\ control - CR\ inhibitor}{CR\ control} \times 100\% \quad (11)$$

where $CR_{control}$ is the corrosion rate in absence of green tea and $CR_{with\ inhibitor}$ is the corrosion rate in presence green tea.

OCP and LPR measurements were performed periodically: after immersion for 1, 3, 7, 14 and 21 days [165]. In addition, OCP after immersion for 1 and 8 hours were also determined [8, 177]. The periodic measurements (i.e. measurements over time) illustrate the time-dependent formation of passive layer, and determine the time-to-corrosion initiation which was used to evaluate the efficiency of green tea as an admixed corrosion inhibitor [20, 54].

3.3.4 Compressive strength measurements

After 7 days of moist curing, mortar compressive strength was measured with NL Scientific compression machine (ECO-SMARTZ Fully Automatic Compression Machine 3000 kN). The loading rate was 0.25±0.05 MPa/s, based on ASTM C 39.

3.3.5 Statistical analyses

Results are expressed as mean ± standard deviation of three samples. Significant differences in the results were evaluated with one-way analysis of variance (one-way ANOVA) followed by Tukey HSD post hoc test using SPSS 20 software [178]. Within a single set of data, the significant differences are represented by superscripted letters after the presented values. The superscripted letters ‘a’ until ‘c’ represent different statistical groupings, and each group is significantly different based on p-value of 0.05. Therefore, values followed by different superscripted letters are significantly different from each other.

3.4 Results and discussion

Results on SET-AA, 7-day mortar compressive strength, and electrochemical parameters are presented in the next sections.

3.4.1 SET-AA

The SET-AA of green tea are presented and compared with the SET-AA of black tea and fruits with high antioxidant contents, in Table 13.

Table 13: Antioxidant activity of green tea, fruits with high antioxidant contents, and black tea

Sample	DPPH (mg AEAC/100 g)	FRP (mg GAE/g)
Green tea	9,623 ± 517	43.3 ± 1.8
Guava	218 ± 79	2.1 ± 0.2
Orange	69 ± 17	0.6 ± 0.1
Mangosteen	32 ± 10	0.3 ± 0.1
Black tea	9,764 ± 2,068	44.4 ± 8.1

Values are presented as mean ± standard deviation of three samples. Abbreviations: DPPH = 2,2-diphenyl-1-picrylhydrazyl**,** FRP= ferric reducing power, AEAC = ascorbic acid equivalent antioxidant capacity, GAE = gallic acid equivalent

Currently, there is no standardized method to measure antioxidant activity. Unfortunately, the lack of standardized method makes the antioxidant activity reported in literatures often not comparable, due to the differences in assay procedures [179-181]. Thus, the SET-AA of green tea were compared with the SET-AA of black tea and fruits having high antioxidant contents (guava, orange, and mangosteen), which were measured previously using the same procedures in our research laboratory (Table 13) [157, 182, 183]. Fruits and black tea are rich in natural antioxidants [153, 184-187]. Fruits have high contents of vitamin C and polyphenols, which are well-established antioxidants [43, 153, 179-183, 186, 188]. On the other hand, black tea contains thearubigins and theaflavins. Similar to the (-)-epigallocatechin gallate in green tea, thearubigins and theaflavins are known potent antioxidants [43, 153, 157].

As shown in Table 13, green tea has a 40 to 300-fold higher electron donation capacity than fruits with high antioxidant contents, and a comparable electron donation capacity to black tea. This indicates a very high electron donation capacity, which is potentially beneficial to confer green tea an anti-corrosion activity [8].

3.4.2 Mortar compressive strength

7-day compressive strength of control and green tea-based mortar are presented in Table 14. As shown in Table 14, there was no significant difference in 7-day compressive strength of control and green tea-based mortar, at any percentage of water replacement with GT. Compressive strength of the green tea-based mortar was at least as high as 90% of the control mortar's compressive strength; thus satisfying ASTM requirement on the use of uncommon water for concrete mixing [189]. On the other hand, when green tea was applied as dry admixtures, compressive strength of the green tea-based mortar was significantly lower than that of control mortar. Hence, green tea was used as GT to replace water during the corrosion tests in SCPS.

Table 14: 7-day compressive strength of mortar

Corrosion inhibitor	Inhibitor physical form	Percentage water replacement with inhibitor	Inhibitor weight (kg/m^3)	7-day compressive strength (MPa)
Control	-	-	-	16.38±1.22[a]
1% green tea (by cement weight)	Dry admixture	-	4.20	10.16±2.87[b]
	Green tea extract	20	24.36	15.94±1.59[a]
		40	48.72	16.40±0.98[a]
		60	73.08	16.57±1.16[a]
		80	97.44	17.15±2.97[a]
		100	121.80	16.74±2.85[a]
2% green tea (by cement weight)	Dry admixture	-	8.40	2.58±0.35[c]
	Green tea extract	20	24.36	16.28±2.65[a]
		40	48.72	15.64±2.36[a]
		60	73.08	15.34±1.79[a]
		80	97.44	17.61±1.91[a]
		100	121.80	14.92±1.78[a]

Values are presented as mean ± standard deviation of three samples. Within the same column, values followed by different superscripted letters are significantly different from the other based on Tukey-HSD test with p-value of 0.05.

3.4.3 Corrosion measurements

As indicated in the previous section, there was no significant difference in 7-day compressive strength of control and green tea-based mortar at any percentage of water replacement with the extracts of 1% and 2% green tea. This indicates that any percentage of the water replacement with the green tea extracts could be selected for the corrosion tests in SCPS. In this study, the authors have selected 100% water replacement with extract of 1% green tea and 60% water replacement with extract of 2% green tea for corrosion tests in SCPS. 60% was selected over the 80 and 100% water replacements, because the hardened mortar prepared with the 60% water replacement had a more similar consistency to control mortar than the 80 and 100%

water replacement mortar. The 100% water replacement with extract of 1% green tea and 60% water replacement with extract of 2% green tea are referred to as 1% GT and 2% GT. Electrochemical parameters of rebars in SCPS containing 3.5% NaCl are presented in Tables 15 to 20.

Table 15: Corrosion rate of steel reinforcing bars in simulated concrete pore solution containing 3.5% sodium chloride

Corrosion inhibitor	Corrosion rate (µm/year)				
	1 day	3 days	7 days	14 days	21 days
Control	47.97±3.41^{a}	32.15±9.21^{a}	17.94±3.48^{a}	89.92±7.78^{a}	112.10±35.51^{a}
Extract of 1% green tea (by cement weight)	3.40±1.64^{b}	10.50±2.74^{b}	15.62±3.91^{a}	51.32±4.21^{b}	60.17±6.67^{a}
Extract of 2% green tea (by cement weight)	3.75±2.43^{b}	3.67±1.25^{c}	10.78±3.76^{a}	53.87±9.28^{b}	70.05±25.22^{a}

Values are presented as mean ± standard deviation of three samples. Within the same column, values followed by different superscripted letters are significantly different from the other based on Tukey-HSD test with p-value of 0.05.

As shown in Table 15, GT inhibited rebar corrosion, as reflected by the reduction in corrosion rate and the delay in sudden increase of the corrosion rate (indicating corrosion initiation) [165]. In absence of GT (i.e. in C-SCPS), corrosion rate of immersed rebars was high (10-100 µm/year) throughout 14 days and increased to very high (>100 µm/year) after 21 days [45]. After 7 days, corrosion rate was reduced, plausibly due to the formation of a protective layer on rebar surface which reduced the rate of anodic and cathodic reactions (i.e. anodic and cathodic slopes), and increased polarization resistance (Tables 16-18) [10, 133]. However, longer immersion

periods (14 and 21 days) damaged the layer, thus significantly decreasing polarization resistance and increasing corrosion rate. On the other hand, addition of GT maintained rebar corrosion rate at low and moderate levels during early immersion days. The 1% GT maintained a low (<5 µm/year) and moderate (5-10 µm/year) corrosion rate for one and three days [45]. Meanwhile, 2% GT maintained the corrosion rate within moderate level for 7 days. Sudden increase in corrosion rate occurred at 14 days in both the SCPS which contained 1% GT and the SCPS which contained 2% GT. This indicated that both GT were equally effective in inhibiting rebar corrosion induced by 3.5% NaCl.

Table 16: Anodic slope of steel reinforcing bars in simulated concrete pore solution containing 3.5% sodium chloride

Corrosion inhibitor	Anodic slope (mV/decade)				
	1 day	3 days	7 days	14 days	21 days
Control	73.37±26.94[a]	51.61±26.86[a]	24.39±4.63[a]	18.52±4.34[a]	22.48±7.89[a]
Extract of 1% green tea (by cement weight)	20.46±8.08[b]	30.01±1.52[a]	42.73±7.16[b]	19.47±0.74[a]	22.80±0.25[a]
Extract of 2% green tea (by cement weight)	17.55±4.17[b]	25.97±9.41[a]	24.47±2.64[a]	23.07±12.77[a]	17.28±0.98[a]

Values are presented as mean ± standard deviation of three samples. Within the same column, values followed by different superscripted letters are significantly different from the other based on Tukey-HSD test with p-value of 0.05.

Table 17: Cathodic slope of steel reinforcing bars in simulated concrete pore solution containing 3.5% sodium chloride

Corrosion inhibitor	Cathodic slope (mV/decade)				
	1 day	3 days	7 days	14 days	21 days
Control	104.80±31.04[a]	84.36±24.43[a]	50.60±5.83[a]	44.55±0.94[a]	51.55±0.79[a]
Extract of 1% green tea (by cement weight)	66.12±10.78[a]	52.04±4.30[a]	61.17±5.61[a]	67.50±5.50[b]	73.50±13.98[b]
Extract of 2% green tea (by cement weight)	74.99±16.22[a]	51.40±6.63[a]	58.43±3.30[a]	63.10±2.54[b]	69.83±4.71[b]

Values are presented as mean ± standard deviation of three samples. Within the same column, values followed by different superscripted letters are significantly different from the other based on Tukey-HSD test with p-value of 0.05.

Table 18: Polarization resistance of steel reinforcing bars in simulated concrete pore solution containing 3.5% sodium chloride

Corrosion inhibitor	Polarization resistance (Ω)				
	1 day	3 days	7 days	14 days	21 days
Control	378±38[a]	1047±241[a]	993±179[a]	156±38[a]	152±27[a]
Extract of 1% green tea (by cement weight)	5746±3772[b]	2043±676[a]	1830±686[a]	316±22[b]	311±53[a]
Extract of 2% green tea (by cement weight)	4830±1852[b]	5050±287[b]	1835±542[a]	319±80[b]	231±79[a]

Values are presented as mean ± standard deviation of three samples. Within the same column, values followed by different superscripted letters are significantly different from the other based on Tukey-HSD test with p-value of 0.05.

The highest corrosion inhibition efficiency (IE) of 1% and 2% GT were observed after 1 day (Table 19), during which polarization resistance significantly increased (Table 18) while corrosion rate and anodic slope significantly decreased (Tables 15 and 16). In addition, cathodic slope was also reduced (Table 17). These changes in electrochemical parameters occurred without a significant change in open circuit potential (Table 20), indicating that GT behaved as a mixed-type inhibitor [164, 190-193]. As a mixed-type inhibitor, the adsorption of GT compounds on rebar surface reduced anodic and cathodic slopes simultaneously without significantly changing the open circuit potential. Moreover, the adsorption increased the polarization resistance [164, 191, 192, 194]. Nonetheless, IE of both GT decreased over 7 days, with a more pronounced reduction for the 1% GT. This IE reduction was the consequence of corrosion propagation, as indicated by the low open circuit potential values shown in Table 20 [7, 54, 195].

Overall, 1% and 2% GT were equally effective against 3.5% NaCl. However, the 2% GT exhibited a higher overall IE than the 1% GT (46.31±15.97% and 37.50±6.97% after 21 days). Therefore, the extract of 2% green tea was selected for corrosion tests in mortar, which will be presented in Chapter 4.

Table 19: Corrosion inhibition efficiency of green tea extracts in simulated concrete pore solution containing 3.5% sodium chloride

Corrosion inhibitor	Corrosion inhibition efficiency (%)				
	1 day	3 days	7 days	14 days	21 days
Extract of 1% green tea (by cement weight)	92.92±2.91[a]	67.33±4.08[a]	12.93±5.90[a]	42.93±0.18[a]	46.31±15.97[a]
Extract of 2% green tea (by cement weight)	92.17±4.38[a]	88.58±1.06[b]	39.91±10.33[b]	40.09±5.11[a]	37.50±6.97[a]

Values are presented as mean ± standard deviation of three samples. Within the same column, values followed by different superscripted letters are significantly different from the other based on Tukey-HSD test with p-value of 0.05.

Table 20: Open circuit potential of steel reinforcing bars in simulated concrete pore solution containing 3.5% sodium chloride

Corrosion inhibitor	Open circuit potential (mV vs. saturated calomel electrode)						
	1 hour	8 hours	1 day	3 days	7 days	14 days	21 days
Control	-471±22[a]	-509±29[a]	-524±22[a]	-535±4[a]	-548±3[a]	-577±38[a]	-594±10[a]
Extract of 1% (by cement weight) green tea	-522±21[b]	-513±14[a]	-529±30[a]	-540±5[a]	-526±10[a]	-588±17[a]	-572±1[a]
Extract of 2% (by cement weight) green tea	-538±11[b]	-555±8[a]	-559±14[a]	-562±11[a]	-552±2[a]	-559±36[a]	-561±13[a]

Values are presented as mean ± standard deviation of three samples. Within the same column, values followed by different superscripted letters are significantly different from the other based on Tukey-HSD test with p-value of 0.05.

3.5 Summary

In summary, it is evident that green tea inhibited rebar corrosion in SCPS. When green tea was used as extracts of 1% and 2% green tea to replace water, there was no significant difference in 7-day compressive strength of control mortar and green tea-based mortar, at any percentage of the water replacement (20-100% in 20% increments). Moreover, compressive strength of the green tea-based mortar fulfilled ASTM requirement on the use of uncommon water for concrete mixing. On the other hand, when green tea was applied as dry admixtures, compressive strength of green tea-based mortar was significantly lower than the control mortar. Therefore, green tea was used as GT to replace water during corrosion tests in SCPS. The dosages were 100% water replacement with extract of 1% green tea and 60% water replacement with extract of 2% green tea. The two dosages were referred to as 1% GT and 2% GT. GT inhibition on rebar corrosion was confirmed through an observed reduction in the corrosion rate and a delay in the sudden increase of the corrosion rate (which indicated the initiation of rebar corrosion). Against 3.5% NaCl, highest IE was observed after 1 day (±92%) for both GT, with the following changes in electrochemical parameters indicated that GT behaved as a mixed-type corrosion inhibitor: changes in anodic and cathodic slopes without a significant change in open circuit potential. Overall, the 2% GT showed a higher overall IE throughout the entire corrosion test (46.31± 15.97% vs. 37.50± 6.97% after 21 days). Thus, the extract of 2% green tea was deemed suitable for the corrosion tests in mortar, presented in Chapter 4.

CHAPTER 4: CORROSION TESTS IN MORTAR

4.1 Introduction

In Chapter 3, it has been shown that green tea inhibited the corrosion of steel reinforcing bar (rebar) in simulated concrete pore solution (SCPS), as indicated by a reduced rebar corrosion rate and delayed initiation of rebar corrosion. This chapter investigates green tea's inhibition on corrosion of rebar embedded in mortar (steel reinforced mortar). Green tea was added as aqueous extract of 2% green tea (by cement weight), which exhibited the lowest rebar corrosion rate in SCPS.

Corrosion inhibition efficiency (IE) of the green tea extract (GT) was compared with the IE of commercial calcium nitrite corrosion inhibitor (CI). As mentioned in Chapter 2, CI is widely accepted as the current most effective corrosion inhibitor for concrete [16-19]. Both CI and GT were added as admixed corrosion inhibitors, and the dosages of both inhibitors were kept similar to allow a justification on selected GT dosages, IE comparison between both inhibitors, and indirect adjustment of GT dosages to chloride concentration [17, 20, 35, 118, 121].

Corrosion studies in mortar/concrete commonly adopt an accelerated corrosion regime because natural corrosion will entail years to obtain the required corrosion level [196-200]. Thus, accelerated corrosion was adopted for the corrosion tests in mortar. Unfortunately, there is no standardized method to accelerate rebar corrosion [200]. Noneheless, there are three commonly used methods: impressed techniques (impressed current and impressed voltage), admixing chloride into concrete, and cyclic wetting-drying exposure [200, 201]. Admixing chloride into concrete used to be popular, to emulate the early chloride contamination of concrete from the aggregate and the addition of calcium chloride as concrete set accelerator. The concrete contamination with chloride from the aggregate was common (such as in Japan), due to the lack of

good aggregate which led to the use of marine sand in construction [7, 133, 156, 199, 202]. Nonetheless, the incorporation of marine sand and calcium chloride into reinforced concrete have been banned [203], to avoid the undesirable introduction of chloride into concrete. Therefore, impressed techniques and cyclic wetting-drying exposure are more commonly used today, and were employed during the accelerated corrosion tests in mortar.

4.2 Material properties and sample preparations

This section describes the preparations for corrosion tests in mortar: preparations of CI and GT, preparations of mortar mixture, and preparations of steel rebars.

4.2.1 Preparations of CI and GT

CI was procured from BASF company (i.e. MasterLife® CI 30), and is composed of 30% (w/w) calcium nitrite as the active constituent. Dosage of CI is commonly expressed as a chloride-to-nitrite ratio [20]. Manufacturer recommends a range of chloride-to-nitrite ratio between 1.2 and 1.5 for an effective IE of using CI. Thus, in this study, CI dosages were selected to encompass the recommended dosages (ratios of 1.2 and 1.5) and a wider range of dosages (ratios of 0.9 and 1.8). The selected chloride-to-nitrite ratios conformed with published literature [20], which reported that CI is effective at chloride-to-nitrite ratio lower than 2.0. The ratio of 0.9 was the lowest recommended ratio for exposure to a very aggressive (i.e. corrosive) environment.

GT was produced by ultrasonic-assisted extraction of 2% (by cement weight) green tea leaves with hot water for 30 minutes, at leaves-to-water ratio of 10% (w/v). The ratio was selected to simulate CI concentration (30%) the closest possible, while maintaining the extract-ability and filter-ability of GT. Upon extraction, large particles were removed from the aqueous extract by filtration and GT concentration was determined by oven-drying method at 100°C [147]. The concentration ranged from 2.0-3.0% (w/w) and was used to determine the water content of GT.

4.2.2 Dosages of CI and GT at equal volume

GT was added into mortar at equal volume to CI (Table 21) [35, 204]. The IE of GT and CI were investigated against 3.5% sodium chloride (NaCl) solution, which simulated the seawater [20, 110, 115, 118, 120, 197, 201, 205-207].

The volume of CI presented in Table 21 was calculated based on CI concentration (i.e. total solid) of 30%, CI density of 1.22 kg/m^3, and concrete density of 2,350 kg/m^3. The concentration and density were obtained from the specification sheet of selected CI product (MasterLife® CI 30).

Table 21: Volume of calcium nitrite corrosion inhibitor (CI) and green tea extract (GT)

Corrosion inhibitor	Chloride-to-nitrite ratio	Volume of inhibitor (L/m^3)
CI	0.9	40.14
	1.2	30.11
	1.5	24.10
	1.8	20.08
GT	Not applicable	40.14
		30.11
		24.10
		20.08

4.2.3 Dosages of CI and GT at similar concentration

At equal volume, GT had a lower concentration than CI (30% vs. 2-3%) Therefore, in addition to the comparison at equal volume, IE of GT and CI were compared at similar inhibitor concentration, to address the lower concentration of GT. Hence, concentration of CI was diluted to the similar concentration as GT. However, the dilution of CI changed the chloride-to-nitrite ratios. Thus, the NaCl concentration was diluted based on the dilution factor of CI, to maintain the chloride-to-nitrite ratios identical to those shown earlier in Table 21.

Table 22 shows the weight of CI, when CI concentration was diluted from 30% to 3%. The table also shows the weight of GT at the similar concentration to CI. The NaCl concentration was diluted ten-fold to 0.35% (w/v), based on the dilution factor of CI. Despite the dilution, the NaCl concentration was within the range of concentration used in other studies [20, 59, 165].

Table 22: Weight of calcium nitrite corrosion inhibitor (CI) and green tea extract (GT)

Corrosion inhibitor	Chloride-to-nitrite ratio	Weight of inhibitor (kg/m^3)
CI	0.9	48.97
	1.2	36.73
	1.5	29.40
	1.8	24.50
GT	Not applicable	48.97
		36.73
		29.40
		24.50

4.2.4 Preparations of mortar mixture

Mortar mixture was prepared with Portland Cement CEM II/B-S 42.5N and fine aggregate according to mix design shown in Table 23. Chemical compositions of the cement are identical to those reported in Chapter 3, Table 8. On the other hand, properties of the fine aggregate are presented in Table 24. The water/cement (w/c) shown in Table 23 was adjusted for the moisture content of the fine aggregate. The w/c of 0.54 has been widely used in other studies [110, 156, 163, 198-201, 208, 209], and was selected to provide suitable permeability for completing corrosion investigation within the available timeframe of this study (under twelve months). Additionally, no chemical admixture (e.g. superplasticizer) was added into mortar for the w/c, since the mortar had exhibited an acceptable workability. Thus, there was no interference from other chemical admixture during the evaluation on IE of corrosion inhibitors.

During mixing of CI-based and GT-based mortar, additional water contributed into mortar by the inhibitors was taken into account, to maintain a consistent w/c in control, CI-based, and GT-based mortar [23, 34]. Water content of the inhibitor was the difference between total inhibitor weight per liter (i.e. density) and inhibitor concentration (i.e. total solid) per liter.

Table 23: Constituents of mortar mixture

Constituent	Proportion (kg/m^3)
Cement	420.00
Water	226.51
Fine aggregate	1084.28
Water/cement (w/c) = 0.54	

Table 24: Properties of fine aggregate

Properties	Remarks
Effective size	1.5-3.0 mm
Uniformity coefficient	1.5 ± 8%
Average fineness modulus	2.19 ± 0.08
Main composition	Quartz crystalline silica (approximately 94% of total composition)
Appearance	Fine to coarse sand grains with brown/grey to light grey color
Specific gravity	Approximately 2.6

4.2.5 Preparations of steel rebars

Steel rebars of 12 mm diameter and 130 mm length were cut from commercial carbon steel rebars (high tensile deformed steel rebars grade 500B) [8, 20, 147]. Prior to use, the rebars were sandblasted, degreased with acetone, cleaned with ultra-pure water, and wiped dry [20, 210]. Only surface area of 1,886 mm^2 (at the middle) and

943 mm^2 (at the top) were unpainted for exposure to NaCl solution and electrical connection [211, 212]. The remaining surface areas of the rebars were painted with epoxy [8]. The painted steel rebars were aligned at the center of PVC pipe molds as illustrated in Figure 14. Distance between the lower end of the rebar and the lower end of the mold was 30 mm, to prevent the exposure of unpainted-electrical connection section to NaCl and to ensure a good access to oxygen [213].

4.3 Methodologies

This section describes the procedures for casting mortar and steel reinforced mortar, accelerating rebar corrosion, measuring rebar corrosion, and measuring mortar compressive strength.

4.3.1 Casting mortar and steel reinforced mortar

Procedures for mixing and casting steel reinforced mortar specimens were adopted and modified from the study by Gencel et al. [86] and Karahan and Atis [52] with modifications. In brief, a laboratory-scale mixer was used for the mortar mixing. Upon mixing, the fresh mortar was filled into PVC pipe molds (Figure 14) in three-equal layers. Each layer was compacted on a vibrating table for 25 seconds. Three control specimens (no corrosion inhibitor) and three specimens for each dosage of CI and GT were prepared. After 24 hours, the hardened steel reinforced mortar specimens were de-molded and cured for 28 days [52] in saturated limewater following ASTM C 511.

Mixing and casting of mortar for compressive strength measurements were performed similarly to the mixing and casting of steel reinforced mortar, except for the absence of steel rebars aligned at the center of PVC pipe molds.

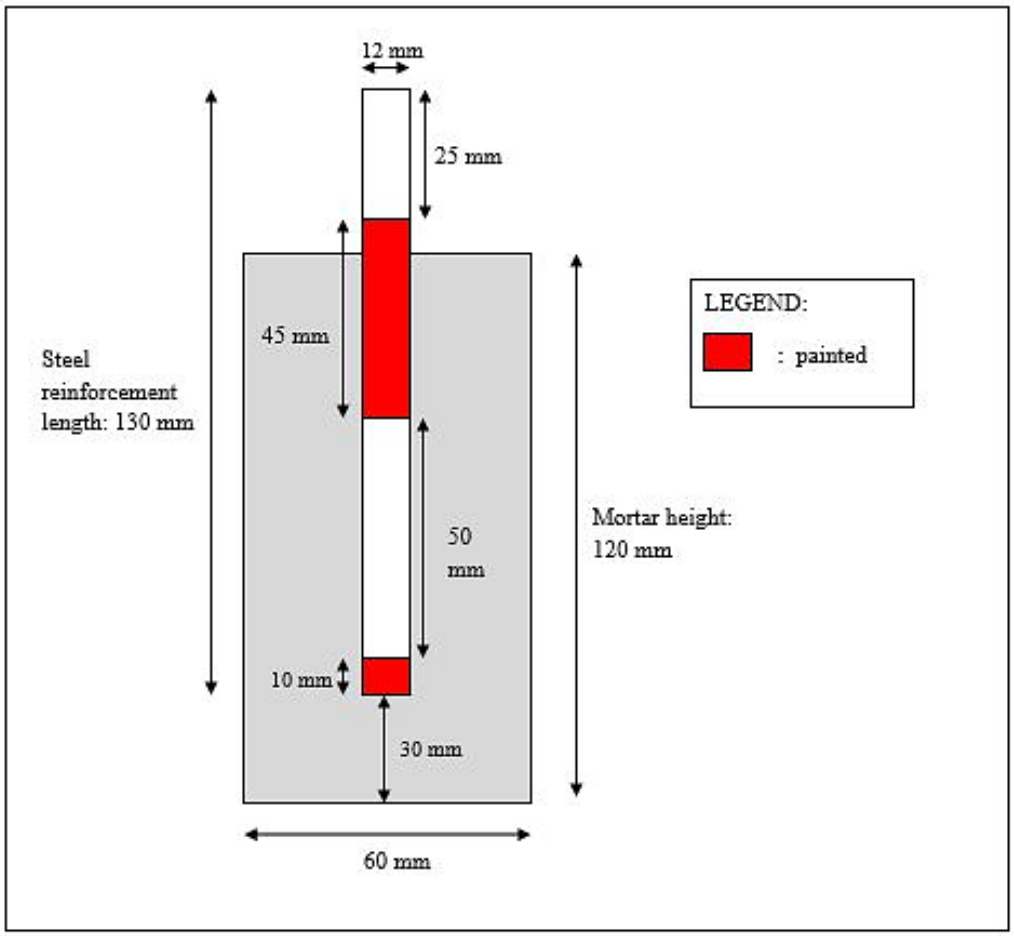

Figure 14: Steel reinforced mortar specimen (Adapted and modified from Alghamdi and Ahmad [171])

4.3.2 Accelerated corrosion

After 28 days of curing, steel reinforced mortar specimens were subjected to an accelerated corrosion employing a combination of impressed current and cyclic wetting-drying. The current density was 100 μA/cm^2, and the wetting-drying cycle was four days of wetting and three days of drying (twelve wetting-drying cycles in total) [110, 200, 214-216].

Fundamental purpose of accelerated corrosion is to obtain the required corrosion level within the shortest time and the least deviation from natural corrosion [217]. Accelerated corrosion studies employing impressed current used current

densities which were 3 to 100-times higher than the maximum values reported from field studies, ranging from 45 to 10,400 μA/cm^2 [199]. In this study, the selected current density was 100 μA/cm^2. This current density has been used in other studies [155, 156, 198, 199, 218-220] and was originally proposed by Andrade et al. [221] after collecting current density data from natural corrosion in various sizes of mortar and concrete specimens over 20 years. The authors reported the highest current density of 100-200 μA/cm^2 in a structure exposed to a very aggressive environment, against a more commonly encountered current density of 1-10 μA/cm^2. A further study by El Maaddawy and Soudki [199] investigated the effect of increasing current density from 100 to 500 μA/cm^2. The authors reported that at equivalent percentage of steel loss, increasing current density above 200 μA/cm^2 increased tensile strain and concrete crack width. This was due to the higher corrosion rate at higher current density, which exceeded the diffusion rate of corrosion products through concrete pores, resulting in accumulation of corrosion products. The accumulated corrosion products induced tensile strain and concrete cracks. According to Andrade et al. [221], percentage mass loss is a more accurate indicator of corrosion damage than crack width and diffusion of corrosion products. Therefore, by adopting percentage steel loss as the indicator of corrosion damage, maintaining current density below 200 μA/cm^2 prevents a false positive increase in crack width and tensile strain.

The accelerated corrosion employing impressed current was combined with cyclic wetting-drying to simulate the exposure of reinforced concrete structure to marine environment. Cyclic wetting-drying allowed the ingress of oxygen into mortar during drying period, which would otherwise be limited due to the saturation of concrete pore with water during wetting period and the low solubility of oxygen in water [222]. Therefore, due to the oxygen ingress, corrosion products formed under natural environment can be simulated by cyclic wetting-drying setup. The selected wetting-drying cycle was four wetting days and three drying days, to represent the long dry period on-field and allow sufficient time for development of corrosion products in the presence of oxygen [110, 200, 214-217].

The setup for the accelerated corrosion is shown in Figure 15. The accelerated corrosion was performed at laboratory temperature (26.4± 1.7°C, 70.3± 7.5% relative humidity). The anode was the steel rebar embedded in mortar, the cathode was AISI 304 stainless steel plate (120 x 100 x 10 mm), and the electrolyte was NaCl solution [211]. The steel reinforced mortar specimen and stainless steel plate were immersed up to 20 mm from the top of plate to reduce the corrosion of the crocodile clip holding the plate (Figure 15). The specimens were connected in series to subject all specimens to equal applied current [196, 199]. Nevertheless, mortar pores dry out during the drying period, which increases mortar resistivity to current flow. Therefore, applying 100 $\mu A/cm^2$ current density during drying period increased the total potential of connected specimens above the maximum potential of power supply. Hence, the impressed current was applied during the wetting period, and the specimens were allowed to corrode naturally during drying period. During the drying period, the specimens were removed from the NaCl solution and the corrosion was sustained by the ingress of oxygen. A similar setup was adopted by Malumbela et al. [208].

The accelerated corrosion test was conducted until the 12^{th} wetting-drying cycle, similar to the study period selected by Fayala et al [110]. At the end of the 12^{th} cycle, at least half of the total steel reinforced mortar specimens have satisfied ASTM G 109-07 requirement, having integrated electrical charge of 150 Coulomb or greater to ensure sufficient corrosion for visual inspection. Electrical charge values of the specimens are presented in Table 25. The values were calculated from the area under the curve of corrosion current measured at each cycle (average of three specimens, in Ampere) vs. time (second). In addition, at the end of the 12^{th} cycle, control and CI-based steel reinforced mortar specimens had shown a stable corrosion rate at 170-200 µm/year (Section 4.4.2.1, Figure 18), which fell under ‘very high’ corrosion rate category (corrosion rate >100 µm/year). On the other hand, GT-based steel reinforced mortar specimens showed ‘high’ corrosion rate values (corrosion rate between 10 and 100 µm/year) at 45-57 µm/year [45].

Table 25: Electrical charge of steel reinforced mortar admixed with equal volume of calcium nitrite corrosion inhibitor (CI) or green tea extract (GT)

Corrosion inhibitor	Volume of inhibitor (L/m^3)	Electrical charge (Coulomb)
Control	-	1,652
CI	40	1,319
CI	30	1,223
CI	24	1,268
CI	20	1,445
GT	40	244
GT	30	246
GT	24	260
GT	20	348

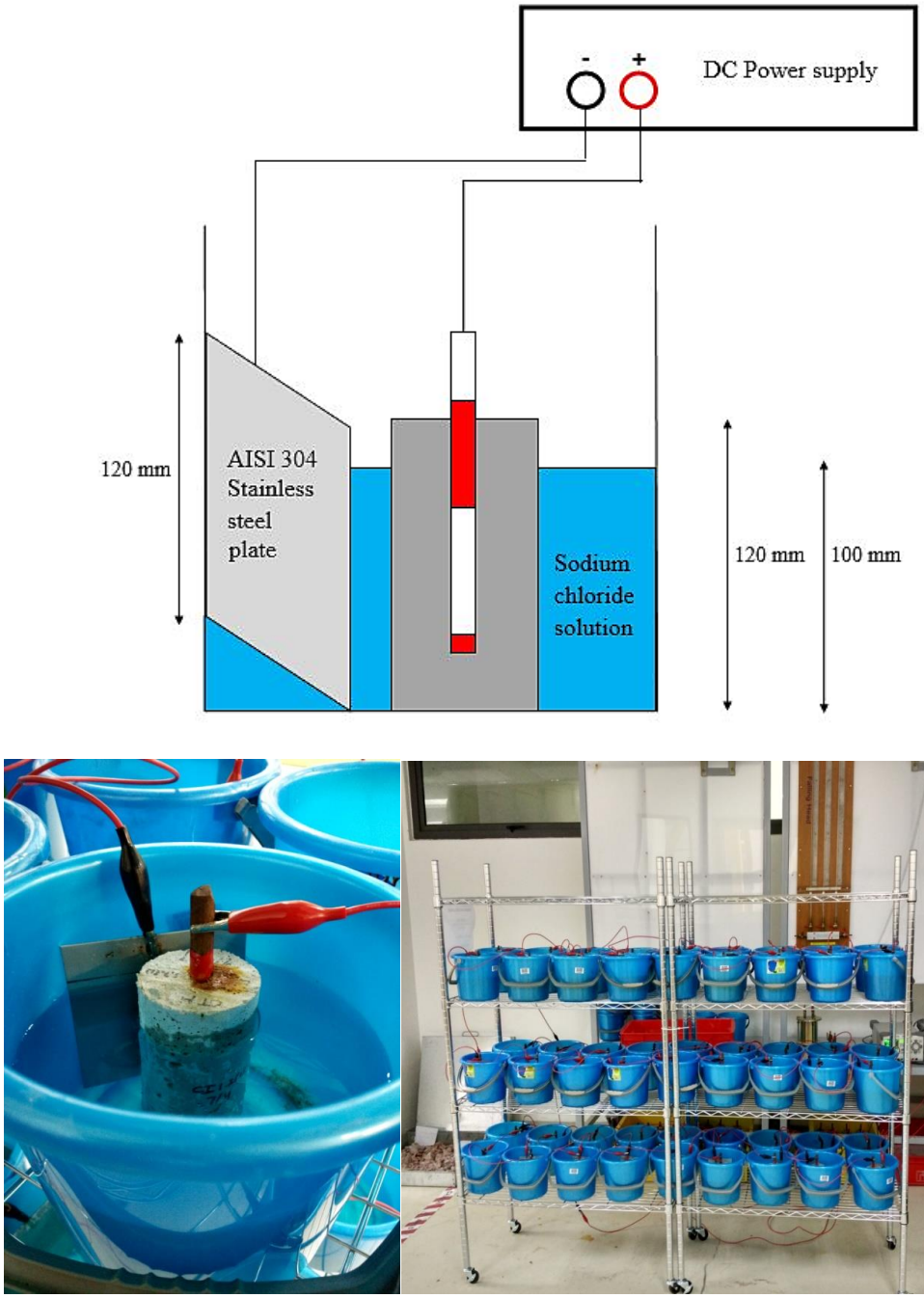

Figure 15: Accelerated corrosion setup employing impressed current and cyclic wetting-drying. The specimens were removed from sodium chloride solution during the drying period (Adapted and modified from Guneyisi and Gesoglu [211] and Fayala et al. [110])

4.3.3 Corrosion measurements

Corrosion development, as represented by electrochemical parameters, was measured with linear polarization resistance (LPR) technique at laboratory temperature (26.4± 1.7°C, 70.3± 7.5% relative humidity). The measurement was performed with a Metrohm Autolab M204 potentiostat employing three-electrode setup [110]. The working electrode (WE) was the steel rebar embedded in mortar, while the reference electrode (RE) and counter electrode (CE) were saturated calomel electrode and AISI 304 stainless steel plate (120 x 100 x 10 mm).

The corrosion measurement was performed at the end of a drying period and prior to the beginning of a new wetting period. Therefore, the specimens were in dry condition. Hence, electrical connection between RE and WE was established using a sponge wetted with diluted detergent [110, 154]. Prior to LPR measurement, open circuit potential (OCP) of the rebar was measured. When the OCP had been stable (fluctuations less than 10 mV, achieved within 10 minutes), OCP was determined and the rebar was polarized with a scan potential of ±20 mV from OCP and scan rate of 0.166 mV/s [8, 21]. The electrochemical parameters (anodic and cathodic slopes, corrosion rate, and polarization resistance) were obtained by analyzing the plots of log current vs. potential with Nova 1.11 software. The corrosion rate was used to calculate the IE of CI and GT, according to Equation 11 presented in Chapter 3. The corrosion rate in absence of CI and GT is defined as $CR_{control}$, while $CR_{inhibitor}$ denotes the corrosion rate in presence of CI and GT.

4.3.4 Compressive strength measurements

After 28 days of moist curing, mortar compressive strength was measured with NL Scientific compression machine (ECO-SMARTZ Fully Automatic Compression Machine 3000 kN). The loading rate was 0.25±0.05 MPa/s based on ASTM C 39.

4.3.5 Statistical analyses

Results are expressed as mean ± standard deviation of three samples. Results on electrochemical parameters are presented with error bars to represent the mean and standard deviation values. On the other hand, the compressive strength results are reported with their significant differences evaluated using one-way analysis of variance (one-way ANOVA) followed by a Tukey HSD post hoc test, by employing SPSS 20 software [178]. Within single set of data, the significant differences are represented by superscripted letters after the presented values. The superscripted letters 'a' until 'e' represent different statistical groupings, and each group is significantly different based on p-value of 0.05. Thus, values followed by different superscripted letters are significantly different from each other.

4.4 Results and discussion

Effects of CI and GT on electrochemical parameters and 28-day mortar compressive strength are presented in the next sections. The mortar compressive strength indicated the inhibitors' effects on the physical protection of mortar against corrosion. On the other hand, the electrochemical parameters indicate the inhibitors' effects on the corrosion resistance of the rebar.

The inhibitors' effects at similar concentration and equal volume are presented in Sections 4.4.1 and 4.4.2. The inhibitors' effects at similar concentration are presented earlier, to investigate the corrosion rate at similar inhibitor concentration before investigating the corrosion rate at equal inhibitor volume, at which GT had a lower concentration than CI.

4.4.1 Corrosion rate and mortar compressive strength at similar concentration of CI and GT

Effects of CI and GT at similar concentration on corrosion rate and mortar compressive strength are presented in Sections 4.4.1.1 and 4.4.1.2. As presented in Section 4.2.3, the inhibitors' dosages were expressed in terms of the inhibitor weight.

4.4.1.1 Corrosion rate at similar concentration of CI and GT

Corrosion rate of steel reinforced mortar specimens (control, CI-based, and GT-based specimens) and the IE of CI and GT at similar inhibitor concentration, are shown in Figures 16 and 17. As shown in Figure 16, there was neither a significant difference in corrosion rate of CI-based and GT-based specimens, nor an overall significant difference in corrosion rate of GT-based and control specimens. Therefore, the IE of CI and GT were not significantly different (Figure 17). Both inhibitors showed a similar IE at the end of the corrosion test, ranging from 51-70%.

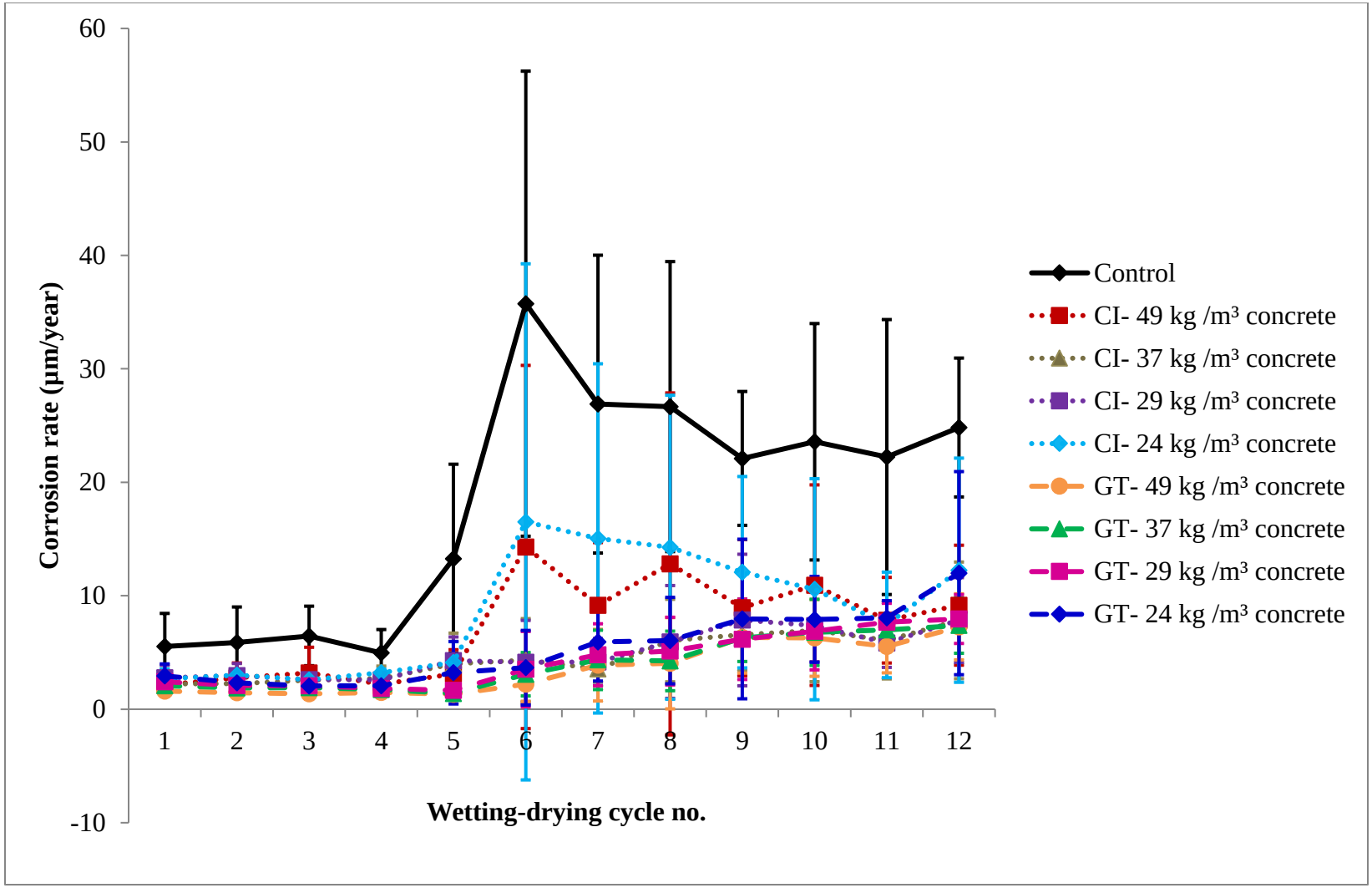

Figure 16: Mean ± standard deviation (n=3) in corrosion rate of steel reinforced mortar admixed with similar weight of calcium nitrite corrosion inhibitor (CI) or green tea extract (GT)

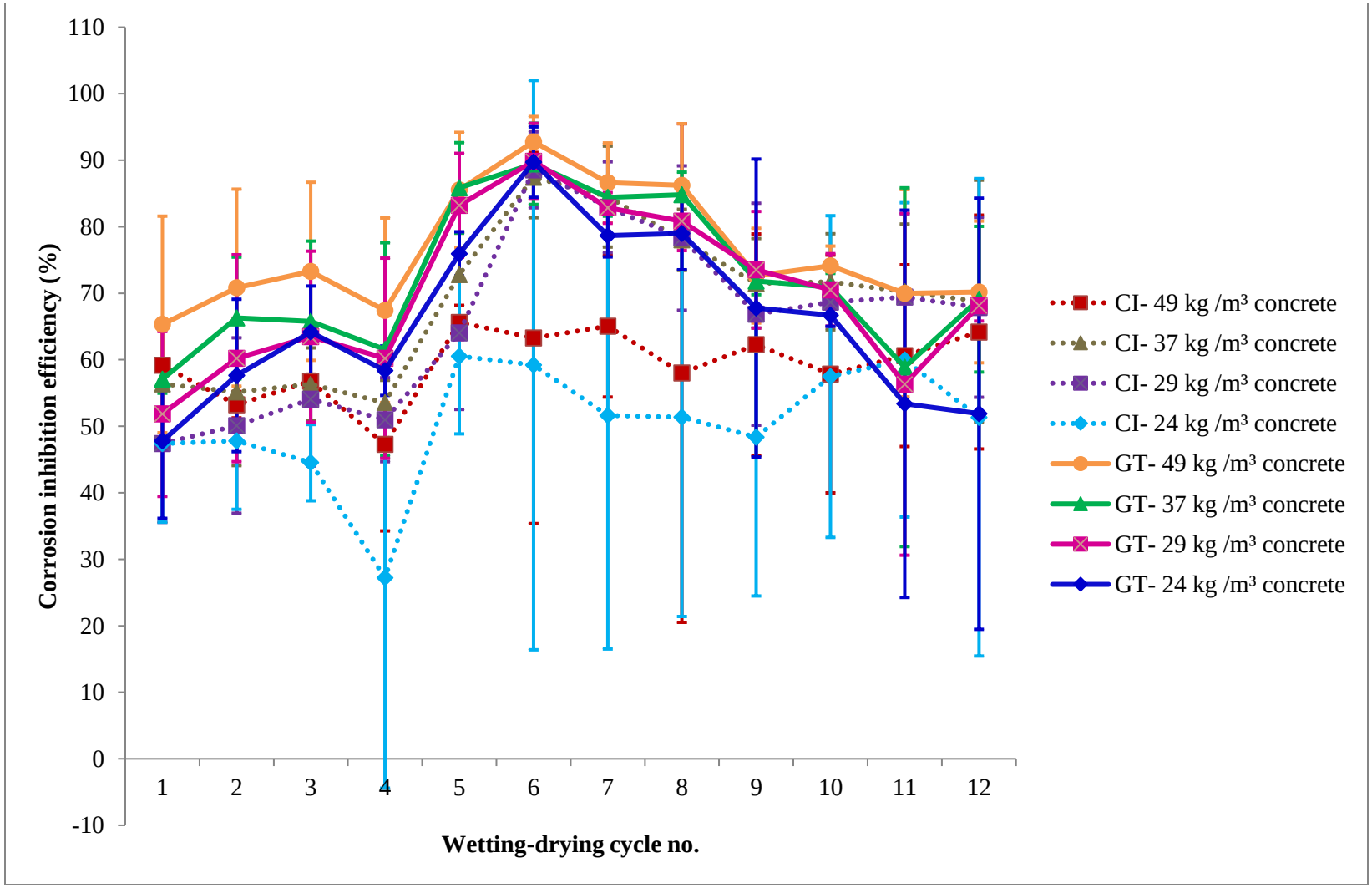

Figure 17: Mean ± standard deviation (n=3) in corrosion inhibition efficiency of calcium nitrite corrosion inhibitor (CI) and green tea extract (GT) at similar weight

4.4.1.2 Compressive strength at similar concentration of CI and GT

Compressive strength of control, CI-based, and GT-based mortar specimens, at similar inhibitor concentration are presented in Table 26. As shown in the Table 26, there was no overall significant difference in compressive strength of CI-based and GT-based specimens. On the other hand, only the strength of specimens added with GT at 49 and 37 kg/m^3 were significantly higher than the strength of control specimens.

Table 26: Compressive strength of mortar admixed with similar weight of calcium nitrite corrosion inhibitor (CI) or green tea extract (GT)

Corrosion inhibitor	Weight of inhibitor (kg/m^3)	Compressive strength (MPa)
Control	-	14.64 ± 1.31^{a}
CI	49	18.20 ± 2.29^{ac}
CI	37	14.74 ± 1.68^{acd}
CI	29	15.65 ± 3.18^{ac}
CI	24	17.43 ± 2.25^{ac}
GT	49	23.88 ± 4.83^{bce}
GT	37	23.98 ± 4.29^{bce}
GT	29	22.77 ± 0.79^{ac}
GT	24	23.18 ± 4.63^{ac}

Values are presented as mean ± standard deviation of three samples. Within the same column, values followed by different superscripted letters are significantly different from each other based on Tukey-HSD test with p-value of 0.05.

4.4.1.3 Overall effects of CI and GT on corrosion rate and mortar compressive strength at similar concentration

At similar inhibitor concentration, there was neither a significant difference in the corrosion rate of CI-based and GT-based specimens, nor a significant difference in the compressive strength of CI-based and GT-based specimens. This suggested the contribution of the physical protection by mortar against corrosion. More importantly, the absence of significant difference in the corrosion rate of CI-based and GT-based specimens at similar inhibitor concentration allowed the comparison on corrosion rate

of CI-based and GT-based specimens at equal inhibitor volume, at which GT had a lower concentration than CI. The effects of CI and GT on electrochemical parameters and mortar compressive strength at equal volume are presented in the next section.

4.4.2 Electrochemical parameters and mortar compressive strength at equal volume of CI and GT

Effects of CI and GT at equal volume on electrochemical parameters (corrosion rate, anodic slope, cathodic slope, polarization resistance, and open circuit potential) and mortar compressive strength are presented in Sections 4.4.2.1 to 4.4.2.6.

4.4.2.1 Corrosion rate at equal volume of CI and GT

Corrosion rate of steel reinforced mortar specimens (control, CI-based, and GT-based specimens), and the IE of CI and GT at equal inhibitor volume are shown in Figures 18 and 19. Figure 18 shows that GT-based specimens had a significantly lower corrosion rate than control and CI-based specimens. Therefore, GT demonstrated a significantly higher IE than CI (Figure 19). The IE ranged from 75-80% vs 14-24% at the end of corrosion test.

The estimated residual service life of the steel reinforced mortar specimens is presented in Table 27. The values were calculated from the average corrosion rate of the specimens at the end of corrosion test, using calculation methods described by Andrade et al. [221]. The rebar diameter was 12 mm and the residual service life was defined as the timespan to reach critical diameter loss, which leads to structure deterioration. According to Torres-Acosta [223], the critical diameter loss was 10%, which produced approximately 50% loss in structural strength.

Table 27: Residual service life of steel reinforced mortar added with equal volume of calcium nitrite corrosion inhibitor (CI) or green tea extract (GT)

Corrosion inhibitor	Volume of inhibitor (L/m^3)	Residual service life (years)
Control	-	5.25
CI	40	6.50
CI	30	6.83
CI	24	6.75
CI	20	6.10
GT	40	26.55
GT	30	25.86
GT	24	22.02
GT	20	21.16

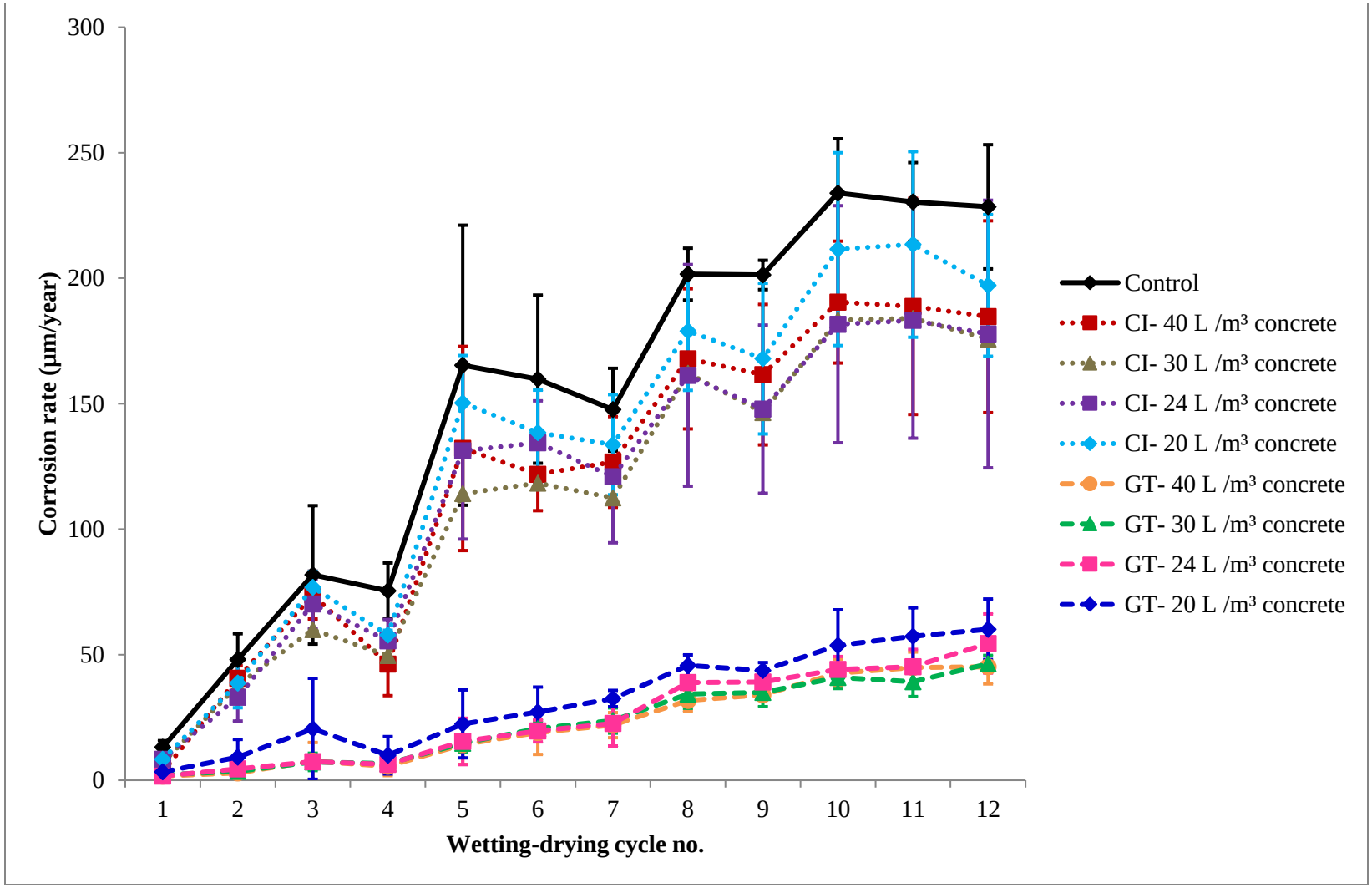

Figure 18: Corrosion rate (mean ± standard deviation, n=3) of steel reinforced mortar at equal volume of calcium nitrite corrosion inhibitor (CI) and green tea extract (GT)

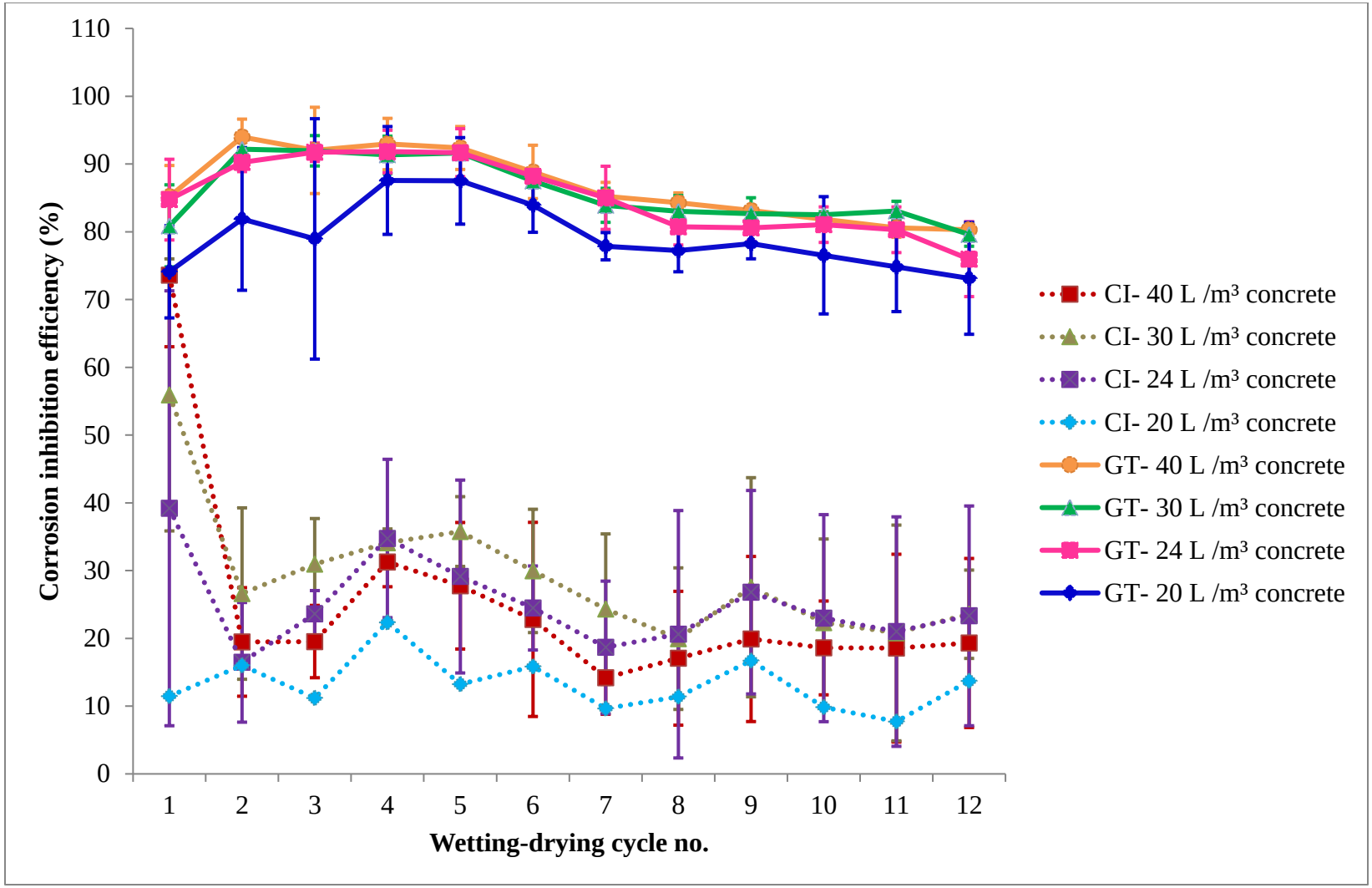

Figure 19: Corrosion inhibition efficiency (mean ± standard deviation, n=3) at equal volume of calcium nitrite corrosion inhibitor (CI) and green tea extract (GT)

4.4.2.2 Compressive strength at equal volume of CI and GT

At equal inhibitor volume, GT-based specimens showed a significantly lower corrosion rate than control and CI-based specimens. Therefore, effects of GT on factors which potentially elucidate the mechanism(s) by which GT reduced corrosion rate, were investigated.

The first factor was the mortar compressive strength, which indicated the physical protection of mortar against corrosion. Compressive strength of control, CI-based, and GT-based mortar specimens at equal inhibitor volume, are presented in Table 28. As shown in the Table 28, there was no overall significant difference in the strength of CI-based and GT-based specimens. On the other hand, only the strength of mortar specimens added with GT at 40 L/m^3 was significantly higher than the strength of control specimens.

Table 28: Compressive strength of mortar added with equal volume of calcium nitrite corrosion inhibitor (CI) or green tea extract (GT)

Corrosion inhibitor	Volume of inhibitor (L/m^3)	Compressive strength (MPa)
Control	-	14.91 ± 1.53^{a}
CI	40	19.72 ± 0.78^{ac}
CI	30	20.27 ± 4.12^{ac}
CI	24	21.46 ± 3.21^{ac}
CI	20	18.52 ± 2.96^{ac}
GT	40	23.01 ± 1.11^{bc}
GT	30	18.05 ± 2.21^{ac}
GT	24	19.28 ± 1.38^{ac}
GT	20	18.99 ± 2.84^{ac}

Values are presented as mean ± standard deviation of three samples. Within the same column, values followed by different superscripted letters are significantly different from each other based on Tukey-HSD test with p-value of 0.05

In order to investigate the effect of compressive strength on corrosion rate, the trends on compressive strength were correlated with the trends on corrosion rate. It was observed that despite the absence of significant difference in strength of CI-based and GT-based specimens, GT-based specimens showed a significantly lower corrosion rate than CI-based specimens. This implied that the lower corrosion rate of GT-based specimens was not due to an improved physical protection of mortar against corrosion. Hence, effect of GT on rebar corrosion resistance, as indicated by the electrochemical parameters, was investigated. The investigated electrochemical parameters were the anodic slope (Figure 20), cathodic slope (Figure 22), polarization resistance (Figure 23), and open circuit potential (Figure 25).

4.4.2.3 Anodic slope at equal volume of CI and GT

The effects of CI and GT on anodic slope are presented in Figure 20. Anodic slope represents the rate of iron oxidation during rebar corrosion (i.e. rate of anodic reaction) [22]. As shown in Figure 20, GT-based specimens had a significantly lower anodic slope than control and CI-based specimens, despite the significant reduction subsided after the sixth wetting-drying cycle.

A good correlation between anodic slope and corrosion rate is observed in Figure 21. The correlation suggests that the reduction in anodic slope contributed to the lower corrosion rate of GT-based specimens [22]. In addition, the correlation between anodic slope and corrosion rate explains the sudden increase in corrosion rate of CI-based specimens when the ability of CI to decrease anodic slope diminished (at the second wetting-drying cycle). CI inhibits rebar corrosion by forming passive film on rebar surface, and reduces the rate of anodic reaction [18, 20, 21]. Therefore, when the effect of CI to reduce anodic reaction rate decreased, IE of CI was reduced.

4.4.2.4 Cathodic slope at equal volume of CI and GT

Effects of CI and GT on cathodic slope are presented in Figure 22. Cathodic slope indicates the rate of oxygen reduction rate during rebar corrosion (i.e. rate of cathodic reaction) [22]. As shown in Figure 22, GT-based specimens displayed a lower

cathodic slope than the control and CI-based specimens for seven wetting-drying cycles. Nonetheless, there was no overall significant difference in cathodic slope among control, CI-based, and GT-based specimens.

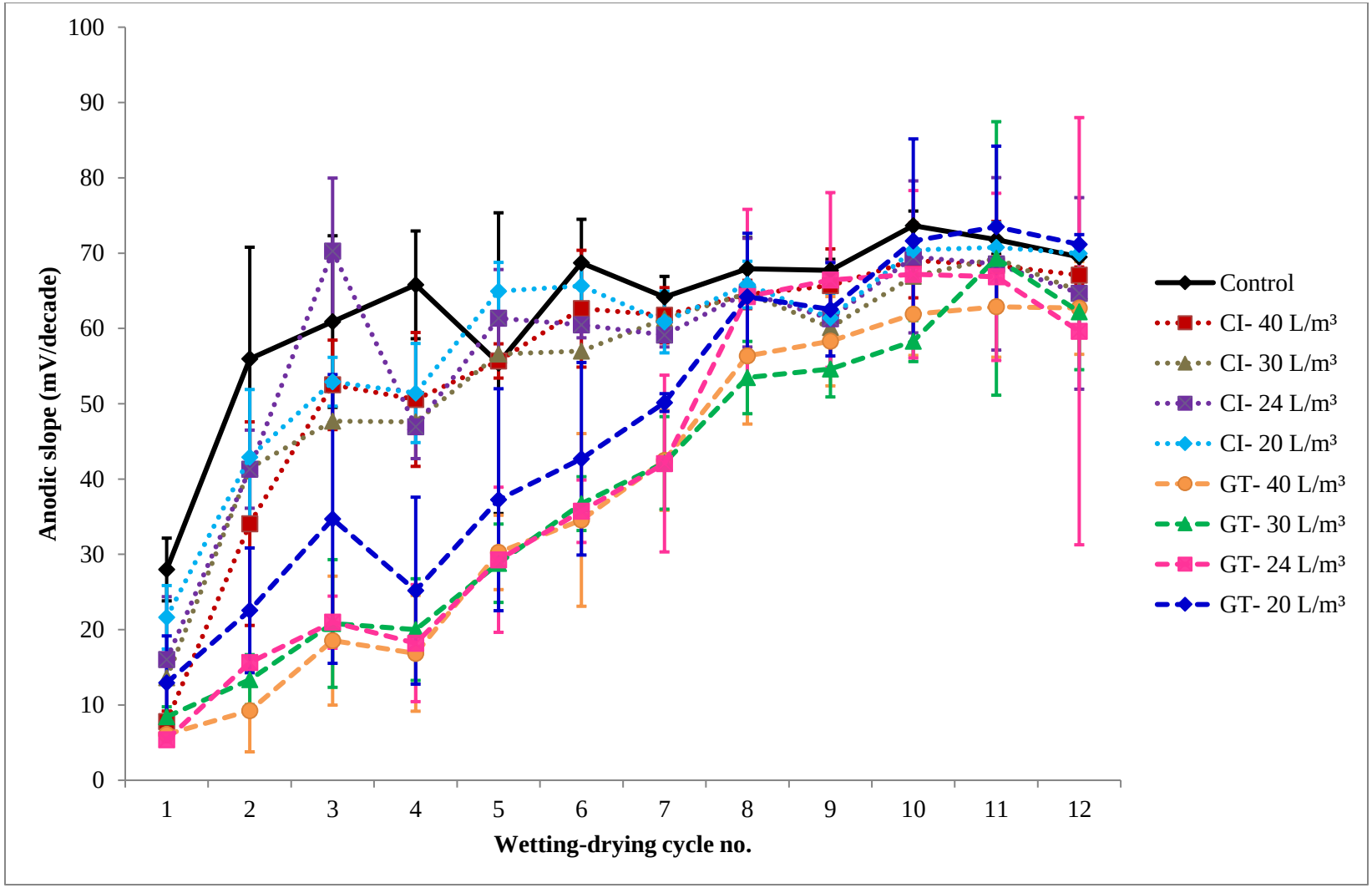

Figure 20: Anodic slope (mean ± standard deviation, n=3) of steel reinforced mortar at equal volume of calcium nitrite corrosion inhibitor (CI) and green tea extract (GT)

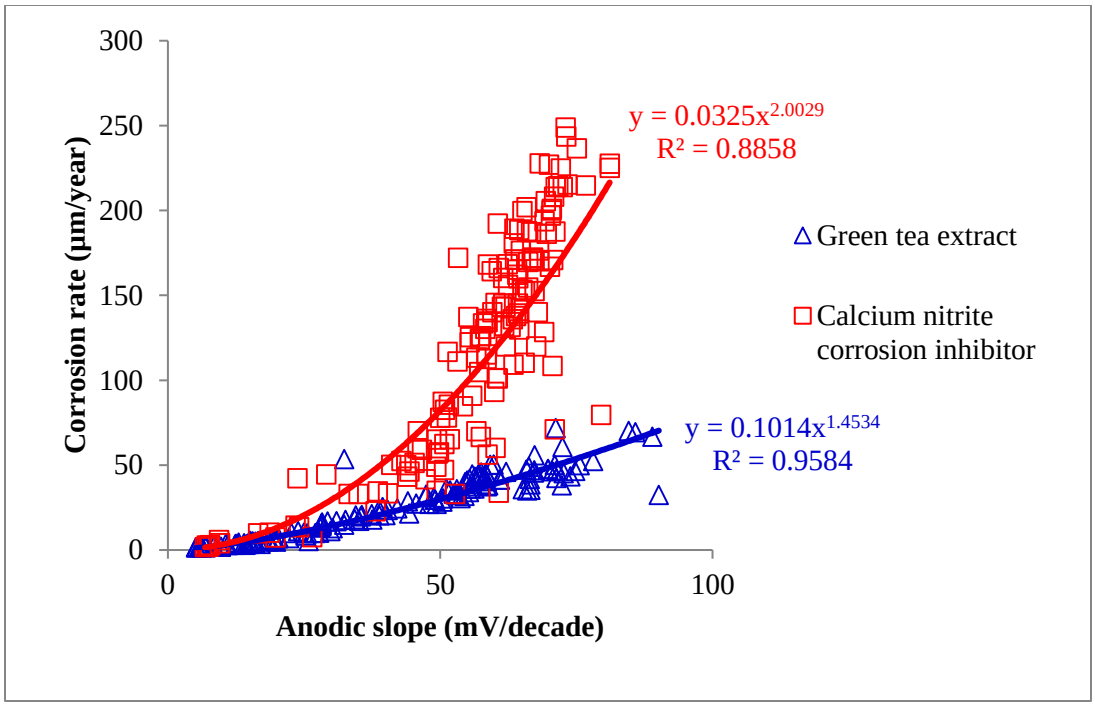

Figure 21: Anodic slope vs. corrosion rate at equal volume of calcium nitrite corrosion inhibitor (CI) and green tea extract (GT)

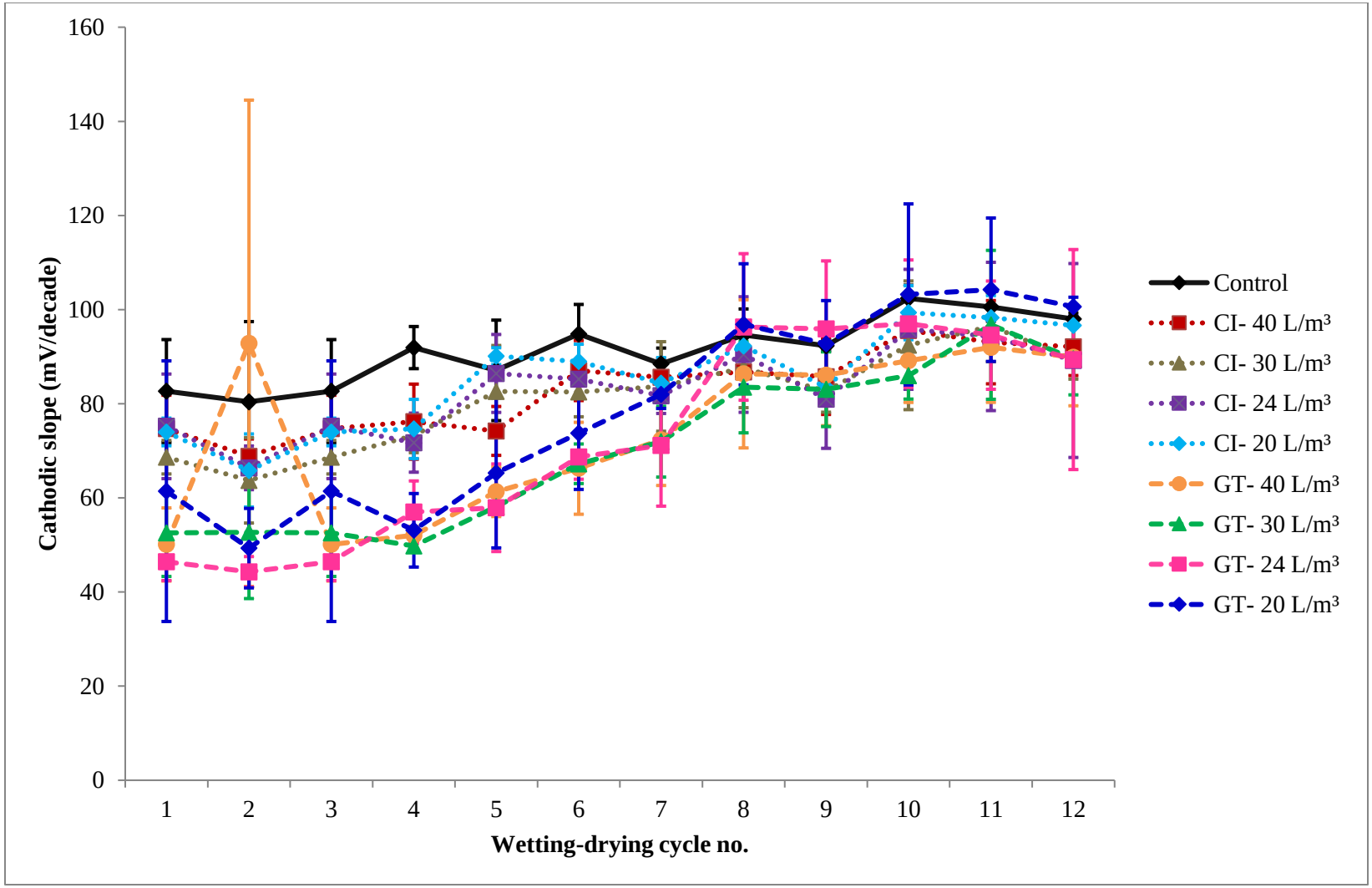

Figure 22: Cathodic slope (mean ± standard deviation, n=3) of steel reinforced mortar at equal volume of calcium nitrite corrosion inhibitor (CI) and green tea extract (GT)

4.4.2.5 Polarization resistance at equal volume of CI and GT

Figure 23 shows the effects of CI and GT on polarization resistance. Polarization resistance indicates the rebar resistance to potential/current which may change the electrochemical state of the rebar and induce rebar corrosion. Figure 23 shows that in overall, GT-based specimens had a significantly higher polarization resistance than control and CI-based specimens.

A strong correlation was observed between corrosion rate and polarization resistance, as presented in Figure 24. The strong correlation suggests that the increase in polarization resistance reduced the corrosion rate of GT-based specimens. In fact, the contribution of the increase in polarization resistance towards reduction in corrosion rate was more prominent than the contribution by the reduction in anodic slope. This is evidenced by the consistently higher polarization resistance of GT-based specimens than control and CI-based specimens until the end of corrosion test. On the other hand, the reduction in anodic slope decreased after midway through the test (Figure 20). Increase in polarization resistance is often associated with the formation of protective layer on rebar surface [3, 10, 64].

4.4.2.6 Open circuit potential at equal volume of CI and GT

Effects of CI and GT on open circuit potential are presented in Figure 25. Open circuit potential indicates rebar potential in absence of influence from external potential or current [8]. Figure 25 demonstrates the absence of significant difference in open circuit potential among control, CI-based, and GT-based specimens. A similar range of open circuit potential values was reported in a study by Care and Raharinaivo [198].

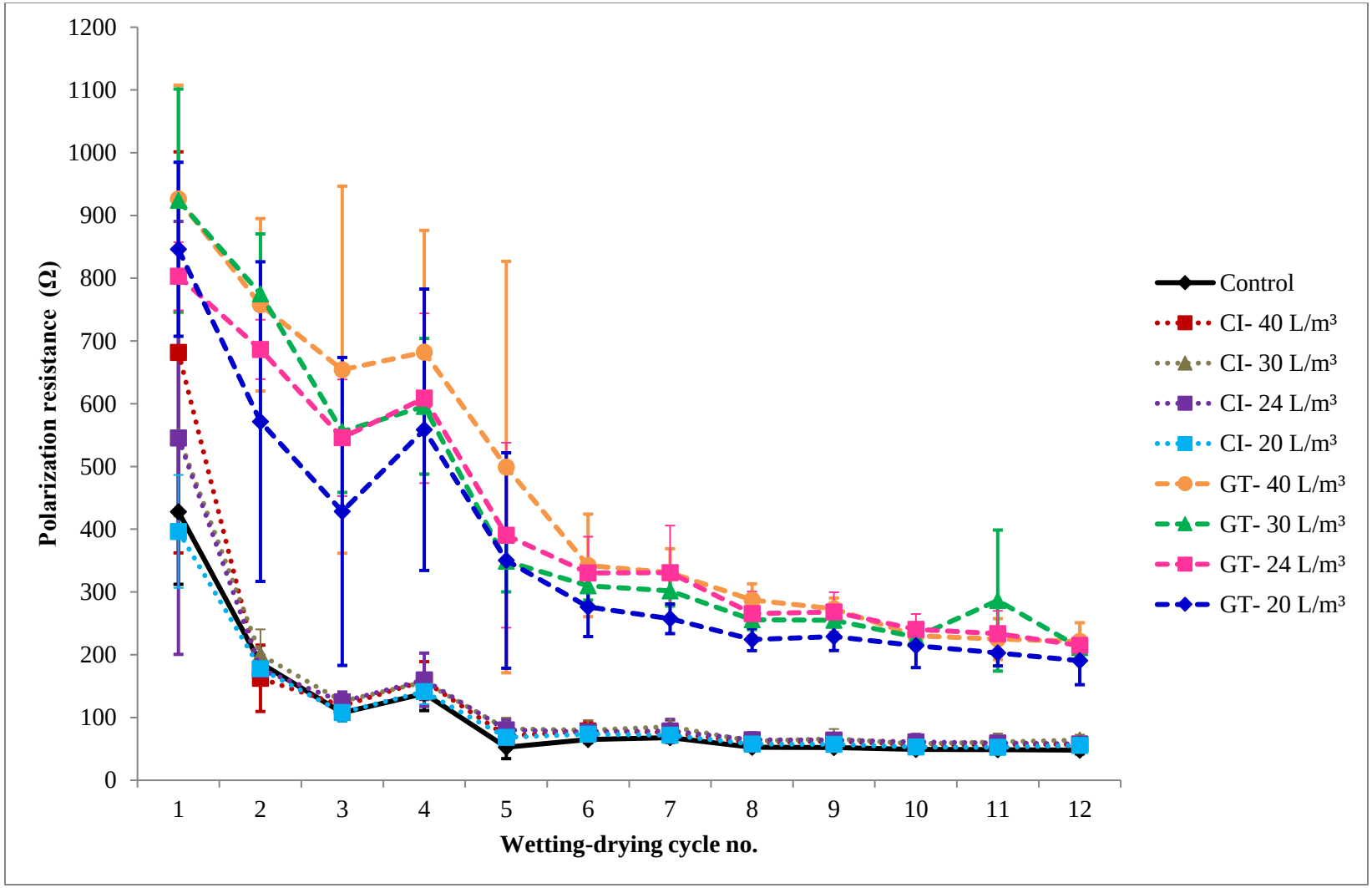

Figure 23: Polarization resistance (mean ± standard deviation, n=3) of steel reinforced mortar at equal volume of calcium nitrite corrosion inhibitor (CI) and green tea extract (GT)

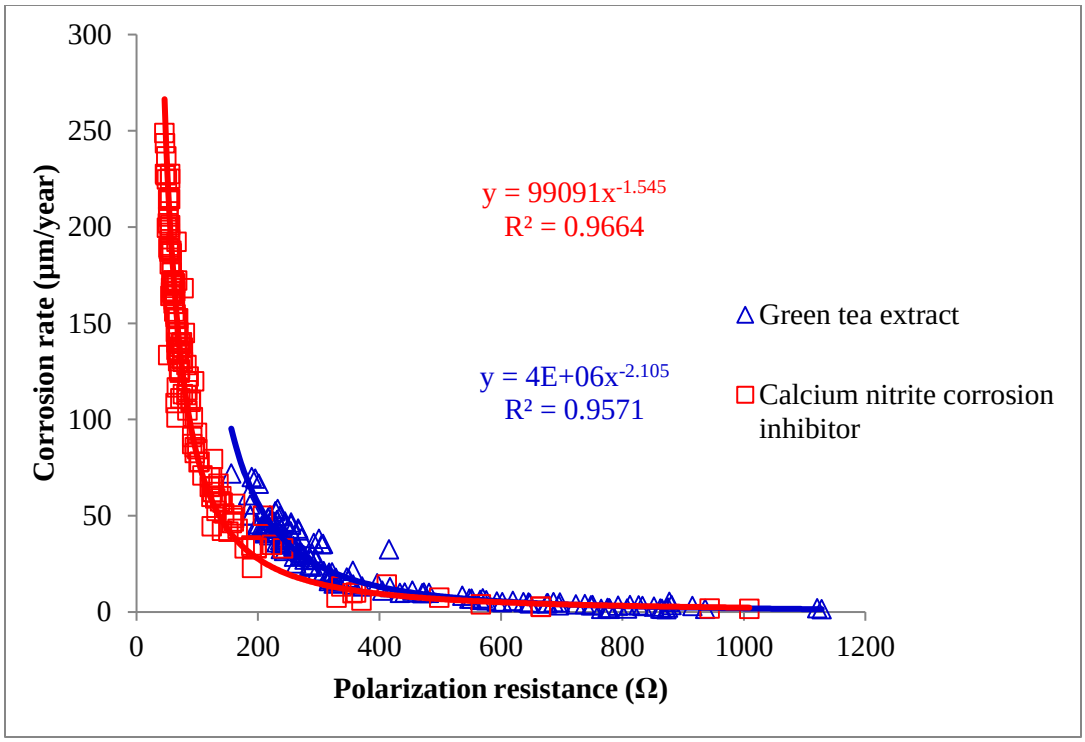

Figure 24: Polarization resistance vs. corrosion rate at equal volume of calcium nitrite corrosion inhibitor (CI) and green tea extract (GT)

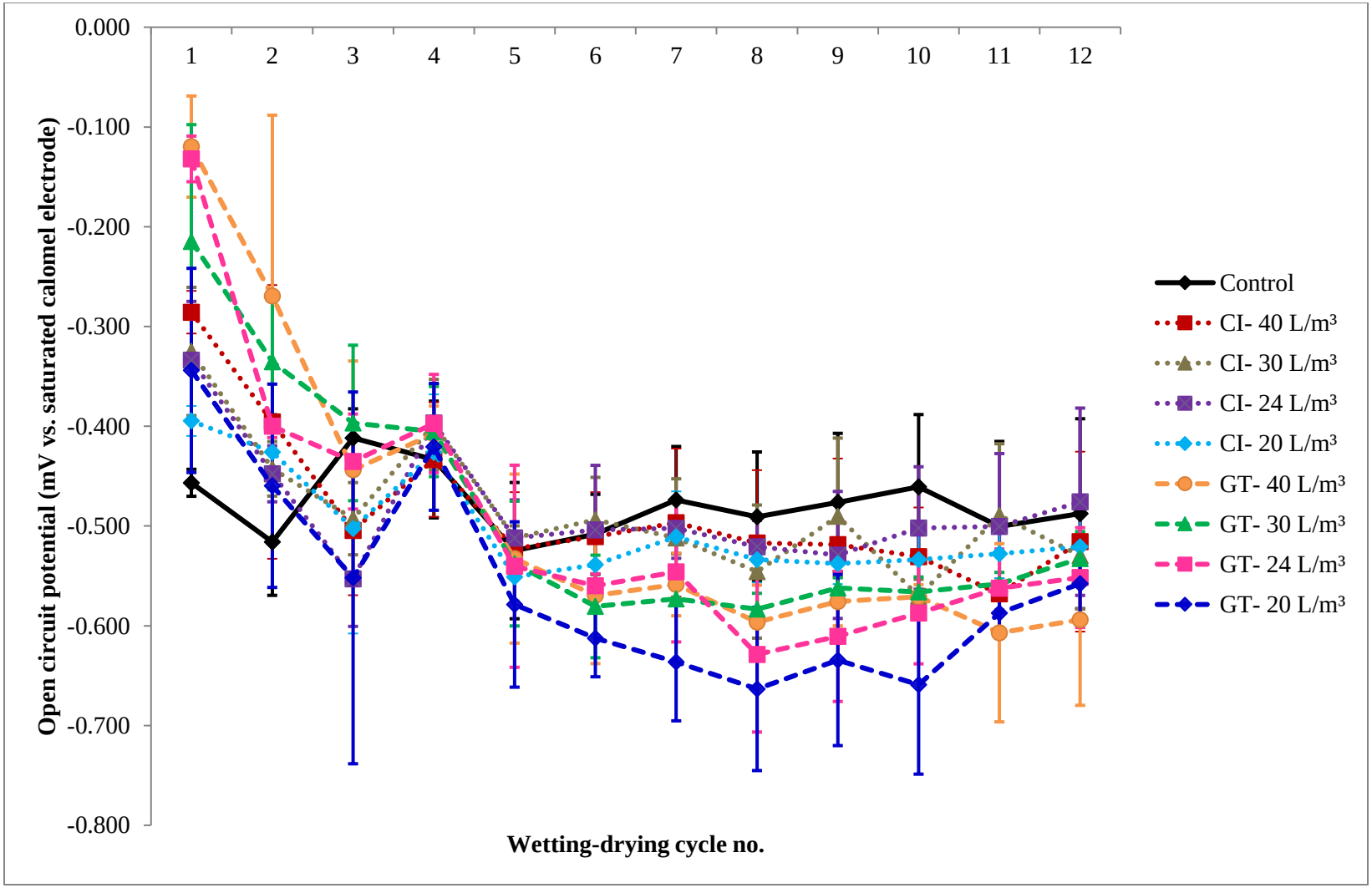

Figure 25: Open circuit potential (mean ± standard deviation, n=3) of steel reinforced mortar at equal volume of calcium nitrite corrosion inhibitor (CI) and green tea extract (GT)

4.4.2.7 Overall effects of CI and GT on electrochemical parameters and mortar compressive strength at equal volume

At equal inhibitor volume, GT-based specimens exhibited a significantly lower corrosion rate than control and CI-based specimens. The steel reinforced mortar specimens were subjected to 3.5% NaCl solution, which simulated the exposure to actual seawater. Therefore, the significantly lower corrosion rate of GT-based specimens than control and CI-based specimens demonstrated a better efficiency of GT as a corrosion inhibitor against the simulated seawater. Specifically, GT was a better admixed corrosion inhibitor than CI. This was illustrated by the sudden increase in corrosion rate (i.e. corrosion initiation) of CI-based specimens at the second wetting-drying cycle. In comparison, GT maintained the corrosion rate of GT-based specimens lower than control and CI-based specimens, until the end of corrosion test.

GT did not reduce corrosion rate by improving the physical protection of mortar against corrosion, as GT-based mortar displayed a comparable compressive strength to CI-based mortar. Instead, the lower corrosion rate was attributed to the improvement on the corrosion resistance of the rebar. GT reduced anodic and cathodic slopes, and increased polarization resistance without significantly changing the open circuit potential; indicating that GT behaved as a mixed type corrosion inhibitor [164, 190-193].

4.5 Summary

Results showed that the corrosion rate of CI-based and GT-based specimens were not significantly different at similar inhibitor concentration. Therefore, CI and GT demonstrated a comparable IE, ranging from 51 to 70% at the end of corrosion test. On the other hand, when comparisons were made based on equal inhibitor volume, GT-based specimens showed a significantly lower corrosion rate than control and CI-based specimens. Thus, GT exhibited a significantly higher IE than CI (75-80% vs. 14-24% at the end of corrosion test). The higher IE of GT was not merely due to an improved physical protection of mortar, as there was no significant difference in compressive strength of CI-based and GT-based mortar. Instead, the higher IE of GT was due to the

effect of GT which significantly increased polarization resistance and reduced anodic slope. Meanwhile, the reduction in cathodic slope and change in open circuit potential were insignificant. The reduction in anodic and cathodic slopes without a significant change in open circuit potential indicated that GT behaved as a mixed-type corrosion inhibitor. As a mixed-type corrosion inhibitor, GT inhibited rebar corrosion by increasing polarization resistance. The increase in polarization resistance was the most prominent factor contributing to the higher IE of GT, as illustrated by the consistently higher polarization resistance of GT-based specimens than CI-based specimens, until the end of corrosion test (191-221 and 56-64 Ω at the end of the test). The formation of protective layer on rebar surface, as suggested by the increase in polarization resistance is further investigated in Chapter 5.

CHAPTER 5: STUDIES ON CORROSION-INHIBITING MECHANISMS OF GREEN TEA

5.1 Introduction

In Chapter 4, it has been shown that steel reinforcing bars (rebars) embedded in mortar admixed with green tea extract (GT) had a significantly lower corrosion rate than the rebars embedded in control mortar, and mortar admixed with calcium nitrite corrosion inhibitor (CI). Therefore, GT demonstrated a higher corrosion inhibition efficiency (IE) than CI. GT behaved as a mixed-type corrosion inhibitor which increased polarization resistance, suggesting that it formed a protective layer on rebar surface [3, 10, 64].

In this chapter, the formation of a protective layer is investigated through visual inspections and microscopic examinations (optical microscope and scanning electron microscope). Corrosion inhibition by the layer was investigated by comparing rebar weight loss in presence and absence of the layer. On the other hand, the plausible corrosion inhibition due to an improved physical protection of mortar/concrete was further examined by comparing chloride permeability of control and GT-based concrete. Meanwhile, composition of the protective layer was elucidated by analyses with energy-dispersive X-ray spectroscopy, X-ray diffraction spectroscopy, and Fourier transform infrared spectroscopy. In addition, effect of GT's antioxidant activity on corrosion rate and polarization resistance of steel reinforced GT-based mortar was investigated. Lastly, the corrosion-inhibiting compounds of GT were proposed based on liquid chromatography-mass spectrometry (LCMS) and liquid chromatography-tandem mass spectrometry (LCMS-MS) analyses.

5.2 Material properties and sample preparations

In this section, preparations for accelerated corrosion tests in mortar and rapid chloride permeability tests (RCPT) are described.

5.2.1 Materials and sample preparations for accelerated corrosion

Accelerated corrosion was performed to investigate the corrosion rate of steel reinforced mortar which incorporated the residual solid of GT, and to study the effect of GT's antioxidant activity on the corrosion rate and polarization resistance of steel reinforced GT-based mortar. Materials and samples for the accelerated corrosion were prepared as previously described in Chapter 4 Section 4.2, except for the chloride concentration and inhibitor dosages. The accelerated corrosion presented in this chapter was only performed against 3.5% sodium chloride (NaCl) solution, to simulate the actual exposure of a reinforced concrete structure to seawater [20, 110, 115, 118, 120, 197, 201, 205-207]. On the other hand, the inhibitor dosages are described in Sections 5.2.1.1 and 5.2.1.2.

5.2.1.1 Dosages of CI and GT

Corrosion rate of steel reinforced GT-based mortar was investigated at equal volume of GT and CI. The corrosion rate was investigated to study the effect of GT's antioxidant activity on the increase in polarization resistance and decrease in corrosion rate of steel reinforced GT-based mortar, which were observed at the equal inhibitor volume. The volume of CI and GT are identical to those presented in Chapter 4, Table 21.

5.2.1.2 Dosages of resuspended GT solid

GT is composed of the supernatant (i.e. the liquid) and fine residual solid. The residual solid lacks in the active compounds contained in supernatant, which are hypothesized to be responsible for the electron donation and anti-corrosion activity of GT as a mixed-type corrosion inhibitor.

Corrosion rate of steel reinforced mortar which incorporated the residual solid of GT (i.e. without the supernatant) was studied to investigate the anti-corrosion activity of the solid. In the absence of GT's active compounds contained in supernatant, the plausible reduction in corrosion rate is attributed to the effect of the residual solid

which fills up mortar pores and creates denser mortar matrix, hence improving the physical protection of mortar against corrosion. Therefore, the investigation on the corrosion rate of steel reinforced mortar incorporating residual GT solid is deemed appropriate to determine whether GT reduces corrosion rate by improving the physical protection of mortar against corrosion, in addition to increasing rebar polarization resistance.

For the investigations on corrosion rate of steel reinforced mortar incorporating residual GT solid, GT was initially prepared according to volume shown in Table 21, and centrifuged to separate the supernatant and the residual solid. The supernatant was discarded, and the solid was resuspended in ultra-pure water (UPW) to the original volume shown in Table 21. The resuspended residual solid was added into mortar as an admixed corrosion inhibitor, similar to GT.

5.2.2 Materials and sample preparations for RCPT

The preparations for RCPT involved the preparations of concrete mixture as well as the preparations of CI and GT.

5.2.2.1 Preparations of concrete mixture

Concrete specimens for RCPT were prepared according to the mix design shown in Table 29. Properties of the fine aggregate are identical to those shown earlier in Chapter 4, Table 24. On the other hand, the coarse aggregates were 10-mm crushed gravels. The w/c was adopted from the w/c used for accelerated corrosion (w/c = 0.54), with an additional adjustment for the moisture content of coarse aggregates. During concrete mixing, additional water contributed by the inhibitors to the concrete mixture was taken into account, to maintain a consistent w/c among control, CI-based, and GT-based concrete.

Table 29: Constituents of concrete mixture

Constituent	Proportion (kg/m^3)
Cement	420.00
Water	234.59
Coarse aggregate	611.77
Fine aggregate	1083.19
Water/cement (w/c) = 0.56	

5.2.2.2 Preparations of CI and GT

Volume of CI and GT admixed into concrete are reported in Table 30. Only CI and GT volume which showed the highest IE (i.e. lowest corrosion rate) during accelerated corrosion, were selected for RCPT.

Table 30: Volume of calcium nitrite corrosion inhibitor (CI) or green tea extract (GT) admixed into concrete

Corrosion inhibitor	Volume of inhibitor (L/m^3)
Control	-
CI	30.11
GT	30.11

5.3 Methodologies

This section describes the procedures for performing accelerated corrosion, RCPT, antioxidant activity measurements, surface examinations of rebar, LCMS and LCMS-MS analyses, and statistical analyses.

5.3.1 Accelerated corrosion

Mixing and casting steel reinforced mortar specimens, accelerating rebar corrosion, and measuring rebar corrosion with electrochemical method were performed in accordance with the procedures described previously in Chapter 4, Sections 4.3.1 to 4.3.3. In addition to the electrochemical corrosion measurement, rebar corrosion was also measured with gravimetric (weight loss) method. For the gravimetric corrosion measurements, the steel reinforced mortar specimens were intentionally fractured at the end of accelerated corrosion test to extract the embedded steel rebars. Weight loss of the rebars was determined according to ASTM G 1-90.

5.3.2 RCPT

The methodologies for RCPT elaborate the procedures for casting concrete specimens and performing RCPT.

5.3.2.1 Casting concrete

The mixing and casting procedures of concrete specimens were similar to the procedures for the steel reinforced mortar specimens described in Chapter 4 Section 4.3.1, except for the absence of steel rebars. Moreover, a larger concrete mixer (20 L capacity) and cylindrical steel molds (diameter 100 mm and height 200 mm) were used in place of the smaller laboratory-scale mixer (5 L capacity) and PVC pipe molds. Three specimens were prepared for each of control (no corrosion inhibitor), CI-based, and GT-based concrete.

5.3.2.2 RCPT

After 28 days of moist curing, concrete specimens were subjected to RCPT according to ASTM C 1202 [47]. Prior to testing, the cylindrical concrete specimens of 100 mm diameter and 200 mm height were cut into discs of 100 mm diameter and 50 mm height. The discs were fitted into cells of *PROOVE'it* RCPT instrument, and potential difference of 60 V was applied across the discs for 6 hours. The magnitude of electrical charge passed through the discs after 6 hours was used to determine the chloride permeability of concrete specimens according to ASTM C 1202.

5.3.3 Antioxidant activity measurements

According to Feng et al. [8], electron donation promotes the adsorption of a mixed-type corrosion inhibitor on rebar surface. In Chapter 4, it was evident that GT behaved as mixed-type corrosion inhibitor. Hence, the electron donation capacity of GT was measured with ferric reducing power antioxidant assay [8, 150].

Procedures for performing the assay were adapted from a study by Chan et al. [169]. Antioxidant activity of GT volume adopted for accelerated corrosion were quantified by accounting for the dilution factor of each volume in mortar. For each of the diluted GT, three different volume were pipetted into test tubes; one test tube for each volume and made up to 1 mL with UPW. Subsequently, 2.5 mL phosphate buffer (0.2 M and pH 6.6) and 2.5 mL of 1% (w/v) potassium ferricyanide were added into each test tube. The aliquots were mixed and incubated at 50°C for 20 minutes. The reaction was stopped by adding 2.5 mL of 10% (w/v) trichloroacetic acid. The 8.5 mL mixture in each test tube was divided into three test tubes (i.e. three replicates), each containing of 2.5 mL solution. Each of the 2.5 mL solution was further diluted with 2.5 mL UPW, and added with 500 µL of 0.1% (w/v) ferric chloride. The solution was mixed and incubated in the dark for 30 minutes prior to absorbance measurement at 700 nm. The ferric reducing power results were expressed as mg gallic acid equivalent (GAE). The calibration equation for gallic acid standard was $y = 17.085x$ where y was the absorbance value at 700 nm and x was the gallic acid concentration in mg/mL.

5.3.4 Surface examinations of rebar

Rebar surface was examined visually and further examined with optical microscope and scanning electron microscope (SEM). The rebar surface was also subjected to elemental and mineral analyses with energy-dispersive X-ray spectroscopy (EDX) and X-ray diffraction spectroscopy (XRD). Additionally, the presence of organic functional groups on the rebar surface was detected by Fourier transform infrared spectroscopy (FTIR).

5.3.4.1 Optical microscope

Extracted rebars were observed with ZEISS Stemi 2000 stereo microscope complemented with Zen software. Magnifications of the objective and camera adapter were 1.0x and 0.5x.

5.3.4.2 SEM-EDX

Rebar surface was examined and analyzed with Hitachi SU8010 Field Emission scanning electron microscope (FE-SEM) equipped with EDX. Hitachi S3400N-II variable-pressure scanning electron microscope (VP-SEM) was used for the examination of rebar surface at lower magnification. The accelerating voltage was 15 kV.

5.3.4.3 XRD

Homogenous (i.e. non-*localized*) layer was scraped from rebar surface with a scalpel, and analyzed in powder form with Bruker D8 Discover X-ray diffractometer [224]. The 2θ ranged from 5 to 90°. A Cu-Kα radiation source and Lynxeye detector were employed for the analyses (40 kV, 40 mA, 0.15418 nm) [224, 225]. The peaks were identified with data files from Joint Committee on Powder Diffraction Standards-International Centre for Diffraction Data (JCPDS-ICDD), and confirmed with published literatures.

5.3.4.4 FTIR

Rebar surface was analyzed with Nicolet iS10 FTIR equipped with ATR Smart iTR Diamond. The resolution was 4 cm^{-1} and number of scans were 64 [226, 227]. The wavenumber ranged from 525 to 4,000 cm^{-1} [227]. Background spectrum was collected prior to collection of every rebar spectrum, and being subtracted from the rebar spectrum to eliminate the effect of accumulated carbon dioxide and water vapor during spectra collections [226].

5.3.5 LCMS and LCMS-MS analyses of GT

It is widely accepted that the antioxidant activity of GT is contributed by potent antioxidants from flavan-3-ol class (i.e. catechin derivatives, see Figure 8, Chapter 2) specifically the catechin, (-)-epicatechin, (-)-epigallocatechin, (-)-epicatechin gallate, and (-)-epigallocatechin gallate [40, 152, 153, 157, 162, 228-233]. Therefore, the presence of these compounds in GT was investigated by LCMS and LCMS-MS analyses, to suggest the likely constituents contributing to the corrosion-inhibiting activity of GT. The GT dosage was 30.11 L/m^3 (see Table 21) and was diluted based on the dilution factor of the GT in mortar.

LCMS analyses were performed based on the procedures described in the study by Saleem et al. [234] with modifications, using Agilent 1290 Infinity RP-UHPLC system coupled to Agilent 6520 Accurate-Mass Q-TOF mass spectrometer incorporating dual ESI source. The column was Agilent Zorbax Eclipse XDB- C18, narrow-bore 2.1 x 150 mm, 3.5 µm (P/N: 930990- 902). The column and auto-sampler temperature were maintained at 25 and 4°C. The flow rate was 0.5 mL/min and the injection volume was 3 µL. The mobile phases consisted of A: 0.1% formic acid in water and B: 0.1% formic acid in acetonitrile. A linear gradient of mobile phases was applied: 5% B at 0-5 minutes, 5 to 100% B at 5-20 minutes, and 100% B at 20-25 minutes (total run time and post-run time were 25 and 5 minutes respectively). Full-scan LCMS analyses were performed with the mass-to-charge ratio (m/z) ranged from 50-700 using electrospray ion source in negative mode [40, 232, 235, 236]. Nitrogen was supplied as the nebulizing and drying gas at flow rate of 25 and 600 L/hour. The drying gas temperature was set at 300°C. Fragmentation voltage was fixed at 125 V and the analyses were performed at capillary voltage of 3,500 V. Data were processed with Agilent Mass Hunter Qualitative Analysis B.05.00 (Method: Metabolomics-Default- Jan2018.m). Compounds were identified with Search Database METLIN_AM_PCDL-N-170502.cdb with the parameters: match tolerance of 5 ppm; positive ions of +H, +Na, $+NH_4$; and negative ion of -H.

LCMS-MS analyses were performed to further ascertain the presence of targeted compounds by structural elucidation [236]. Procedures for LCMS-MS analyses were similar to the procedures for LCMS analyses except for some

modifications. The injection volume was 6 µL and full-scan LCMS-MS analyses were performed with the m/z ranged from 50-750 using electrospray ion source in negative mode. Acquisition rate and acquisition time were 4 spectra/s and 250 ms/spectrum. The transients/spectrum was 2288 and the collision energy was 20 V. Data were processed with Agilent Mass Hunter Qualitative Analysis B.05.00 (Method: Metabolomics-Default- Jan2018.m). Compounds were identified with Search Library METLIN_AM_PCDL-N-170502.cdb with following parameters: precursor ion m/z expansion ±10 ppm + 2 mDa, product ion m/z expansion ±20 ppm + 2 mDa, and minimum reverse score of 80. Targeted LCMS-MS were searched with MS-MS integrator selection and maximum chromatogram peak width of 1.0 min. Identities of target compounds were confirmed by comparing the fragmentation patterns of targeted compounds with the fragments reported in METLIN Database (http://metlin.scripps.edu) and published literatures.

5.3.6 Statistical analyses

Results are expressed as mean ± standard deviation of three samples. Results on corrosion rate are presented with error bars to represent the mean and standard deviation values. On the other hand, results on antioxidant activity, elemental analyses, and rebar weight loss are presented with the significant differences in the results being evaluated with one-way analysis of variance (one-way ANOVA) followed by Tukey HSD post hoc test, by employing SPSS 20 software [178]. Within single set of data, the significant differences are represented by superscripted letters after presented values. The superscripted letters ‘a’ until ‘e’ represent different statistical groupings, and each group is significantly different based on p-value of 0.05. Therefore, values followed by different superscripted letters are significantly different from each other.

5.4 Results and discussion

The following sections present the results on corrosion rate, chloride permeability, antioxidant activity, examinations of rebar surface, rebar weight loss, and the hypothesized compounds contributing to corrosion inhibition by GT.

5.4.1 Effect of residual GT solid on corrosion rate

As discussed in Section 5.2.1.2, the residual GT solid lacks in the active compounds which are hypothesized to be responsible for the anti-corrosion activity of GT as a mixed-type corrosion inhibitor. Therefore, in the absence of GT's active compounds contained in supernatant, reduction in corrosion rate is attributed to the effect of the residual solid which fills up mortar pores and creates denser mortar matrix, hence improving the physical protection of mortar against corrosion. Thus, corrosion rate of steel reinforced mortar which incorporated residual GT solid (i.e. without the supernatant) demonstrates whether GT reduces corrosion rate by improving the physical protection of mortar against corrosion, in addition to increasing rebar polarization resistance.

A similar corrosion rate between steel reinforced control mortar and steel reinforced mortar admixed with residual GT solid is observed in Figure 26. This indicates a similar protective quality of the mortar in the steel reinforced control mortar and steel reinforced mortar incorporating GT solid. More importantly, the similar corrosion rate suggests that the active compounds in supernatant are responsible for the anti-corrosion of GT, and GT reduces rebar corrosion rate by increasing polarization resistance.

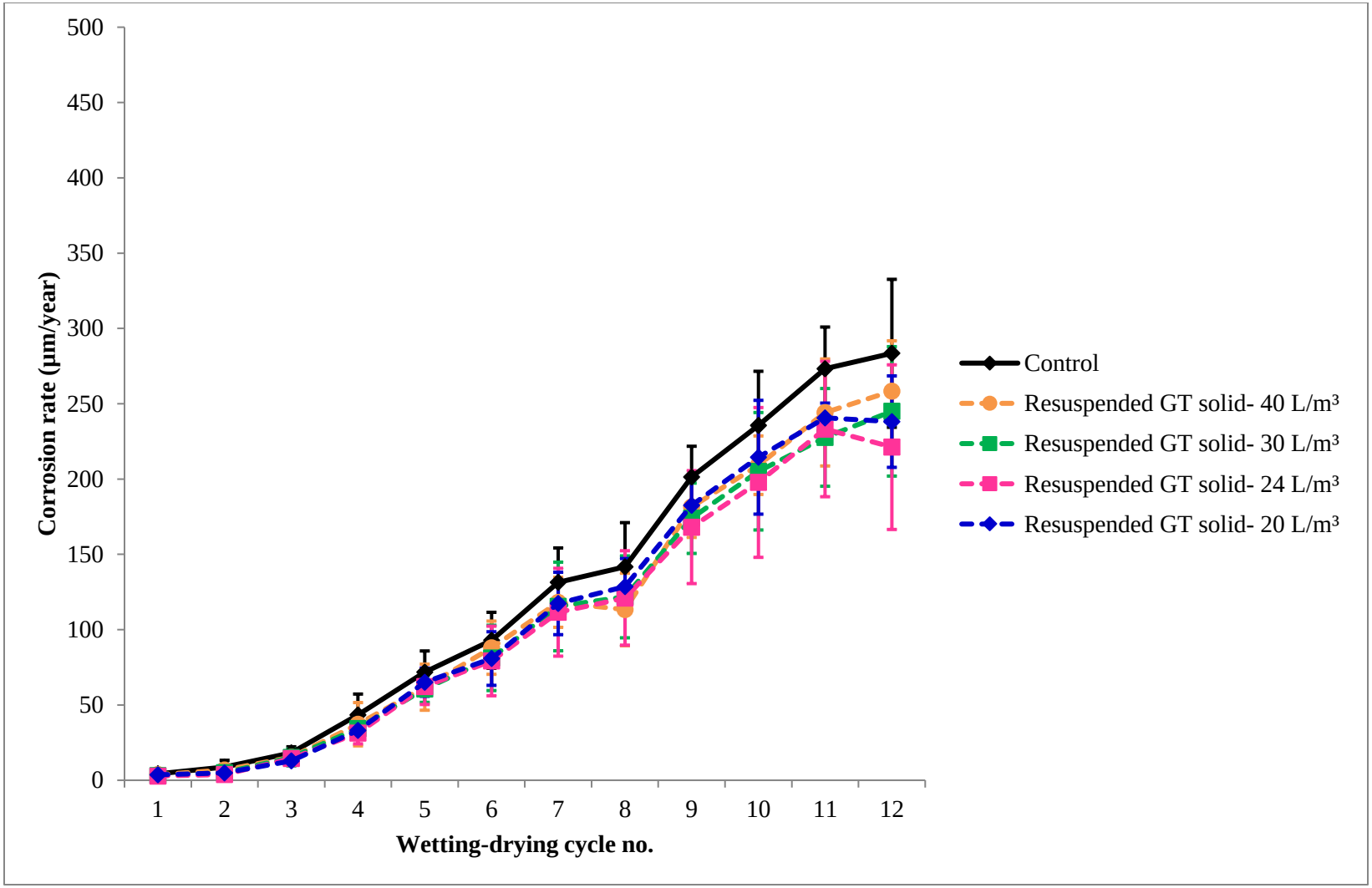

Figure 26: Mean ± standard deviation in corrosion rate (n= 3) of steel reinforced control mortar and steel reinforced mortar admixed with resuspended residual solid of green tea extract (GT)

5.4.2 RCPT

Values of electrical charge passed through concrete after 6 hours are presented in Table 31. All concrete specimens exhibited 'high' chloride permeability according to ASTM C 1202 (electrical charge >4000 Coulomb) [49]. However, the magnitude of electrical charge passed through GT-based concrete was not significantly different from the magnitude of charge passed through control concrete. This suggests a similar chloride permeability of the control and GT-based concrete. Hence, the similar chloride permeability further validated that the lower corrosion rate of steel reinforced GT-based mortar observed in Chapter 4, Figure 18 was not due to an improved physical protection of mortar/concrete against corrosion.

Table 31: Magnitude of electrical charge passed through concrete after 6 hours

Corrosion inhibitor	Volume of inhibitor (L/m^3)	Electric charge (Coulomb)
Control	-	5114 ± 586^a
Calcium nitrite corrosion inhibitor	30	8628 ± 995^b
Green tea extract	30	5177 ± 569^a

Values are expressed as mean ± standard deviation of three samples. Within the same column, values followed by different superscripted letters are significantly different from each other based on Tukey HSD test with p-value of 0.05.

5.4.3 Relationship among antioxidant activity, corrosion rate, and polarization resistance

Effect of GT's antioxidant activity on corrosion rate and polarization resistance of steel reinforced GT-based mortar are presented in Table 32**.** As shown in Table 32, antioxidant activity of GT affects the corrosion rate and polarization resistance of steel reinforced GT-based mortar. Nonetheless, accurate correlation coefficients among the parameters could not be drawn due to the larger variations in corrosion rate and polarization resistance, than the variation in antioxidant activity. This discrepancy might be the effect of the different working pH: accelerated corrosion at alkaline pH of mortar and antioxidant assay at normal pH.

Table 32: Effect of green tea extract's (GT's) antioxidant activity on polarization resistance and corrosion rate of steel reinforced GT-based mortar

Ferric reducing power (mg GAE)	Corrosion rate (μm/year)	Polarization resistance (Ω)
109.51 ± 4.30^{a}	45.18 ± 6.80^{a}	221.18 ± 29.85^{a}
84.27 ± 2.75^{b}	46.37 ± 3.34^{a}	211.14 ± 7.16^{a}
75.91 ± 1.87^{c}	54.48 ± 11.78^{a}	214.75 ± 16.11^{a}
66.49 ± 3.91^{c}	60.14 ± 12.07^{a}	190.50 ± 38.26^{a}
25.44 ± 0.82^{d}	134.25 ± 41.15^{b}	76.18 ± 11.10^{b}
21.47 ± 0.52^{e}	195.88 ± 42.16^{b}	64.49 ± 5.85^{b}

Values are expressed as mean ± standard deviation of three samples. Within the same column, values followed by different superscripted letters are significantly different from each other based on Tukey HSD test with p-value of 0.05. Abbreviations: GAE= gallic acid equivalent.

A study by Muzolf et al. [152] clearly shows that pH affects the electron-donating ability: at pH higher than the pKa of potent antioxidant compounds in GT namely (-)-epicatechin, (-)-epigallocatechin, (-)-epicatechin gallate, and (-)-epigallocatechin gallate, the compounds are deprotonated. The deprotonation increases the electron donation capacity of the compounds, and thereby enhancing antioxidant activity with increasing pH. Unfortunately, to our knowledge, there is yet an analytical method to quantify the electron donation capacity of crude plant extract in alkaline pH of concrete (pH 12-13) [152, 229, 230, 237]. Increasing the working pH of ferric reducing power assay to pH 12-13 reduced the absorbance values of gallic acid standard, indicating that the assay was not suitable to measure antioxidant activity at such a high pH. Therefore, the ferric reducing power values presented in Table 32 were reported at the original working pH of the assay. Nonetheless, despite the absence of accurate correlation coefficients, it can be observed that the magnitude of antioxidant activity influenced the ability of GT to increase polarization resistance and reduce corrosion rate: the higher is the electron donation capacity of GT measured with ferric reducing power assay, the higher is the polarization resistance and the lower is the corrosion rate of steel reinforced GT-based mortar.

5.4.4 Surface examinations of rebar

Visual inspections, optical microscope examinations, SEM examinations complemented with EDX analyses, XRD analyses, and FTIR analyses of steel rebars extracted after accelerated corrosion are presented in the next sections.

5.4.4.1 Visual inspections

Figure 27 shows an example of three steel rebars extracted from each mortar group (control, CI-based, and GT-based mortar). In each mortar group, a similar finding was observed on the three rebars. Therefore, only one rebar extracted from each mortar group is presented in Figure 27. Moreover, only rebars extracted from CI-based and GT-based mortar added with 30 L inhibitor/m^3 are presented, because this volume exhibited the highest IE during accelerated corrosion. Nonetheless, a similar result was also observed on rebars extracted from mortar added with other volume CI and GT.

As illustrated in Figure 27, rebar extracted from GT-based mortar exhibited the least corrosion damage (i.e. largest uncorroded area). A white layer was observed on the uncorroded area of the rebar, and this layer was also observed on the uncorroded area of rebar extracted from CI-based mortar. Further examinations of this layer with microscopic methods and analyses of the layer with EDX, XRD, and FTIR are presented in the next sections.

5.4.4.2 Optical microscope examinations

Optical microscope images of the white layer observed on uncorroded areas of rebars extracted from GT-based and CI-based mortar are presented in Figure 28. In comparison, rebar extracted from control mortar is mostly covered with brownish-black corrosion product. More importantly, the rebar does not exhibit the white layer observed on rebars extracted from GT-based and CI-based mortar.

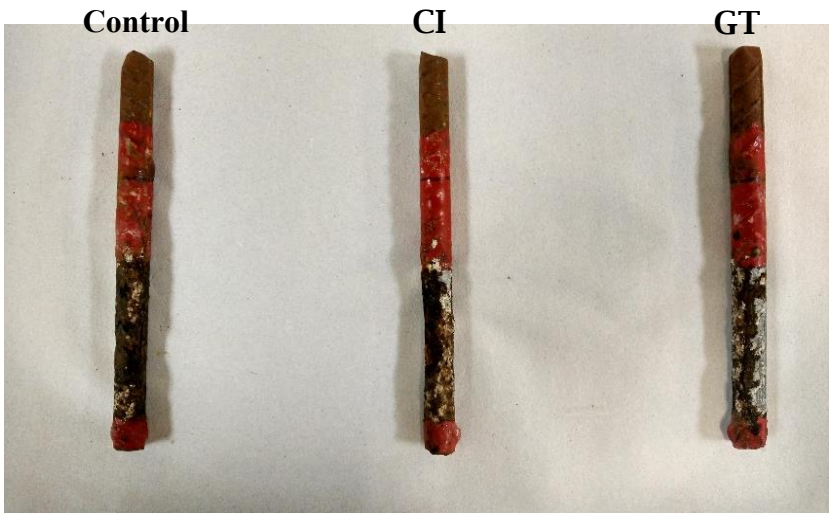

(a) Front side

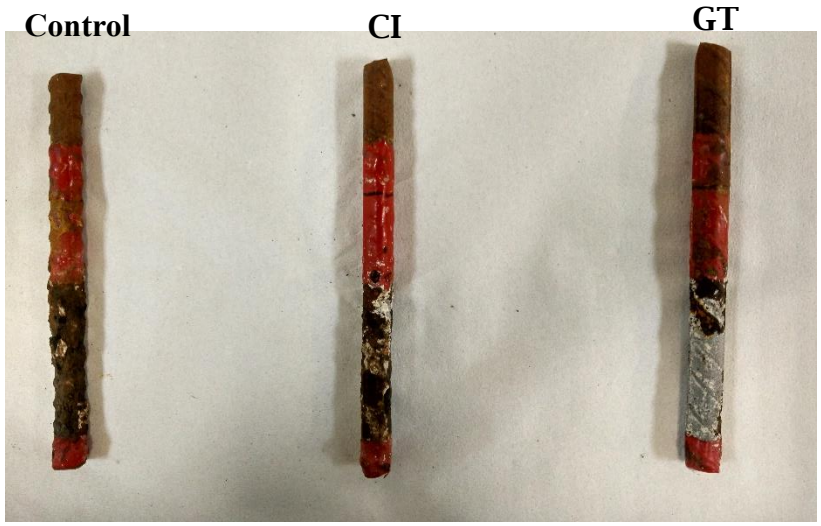

(b) Reverse side

Figure 27: Steel reinforcing bars extracted from control mortar, mortar admixed with 30 L/m^3 of calcium nitrite corrosion inhibitor (CI), and mortar admixed with 30 L/m^3 of green tea extract (GT)

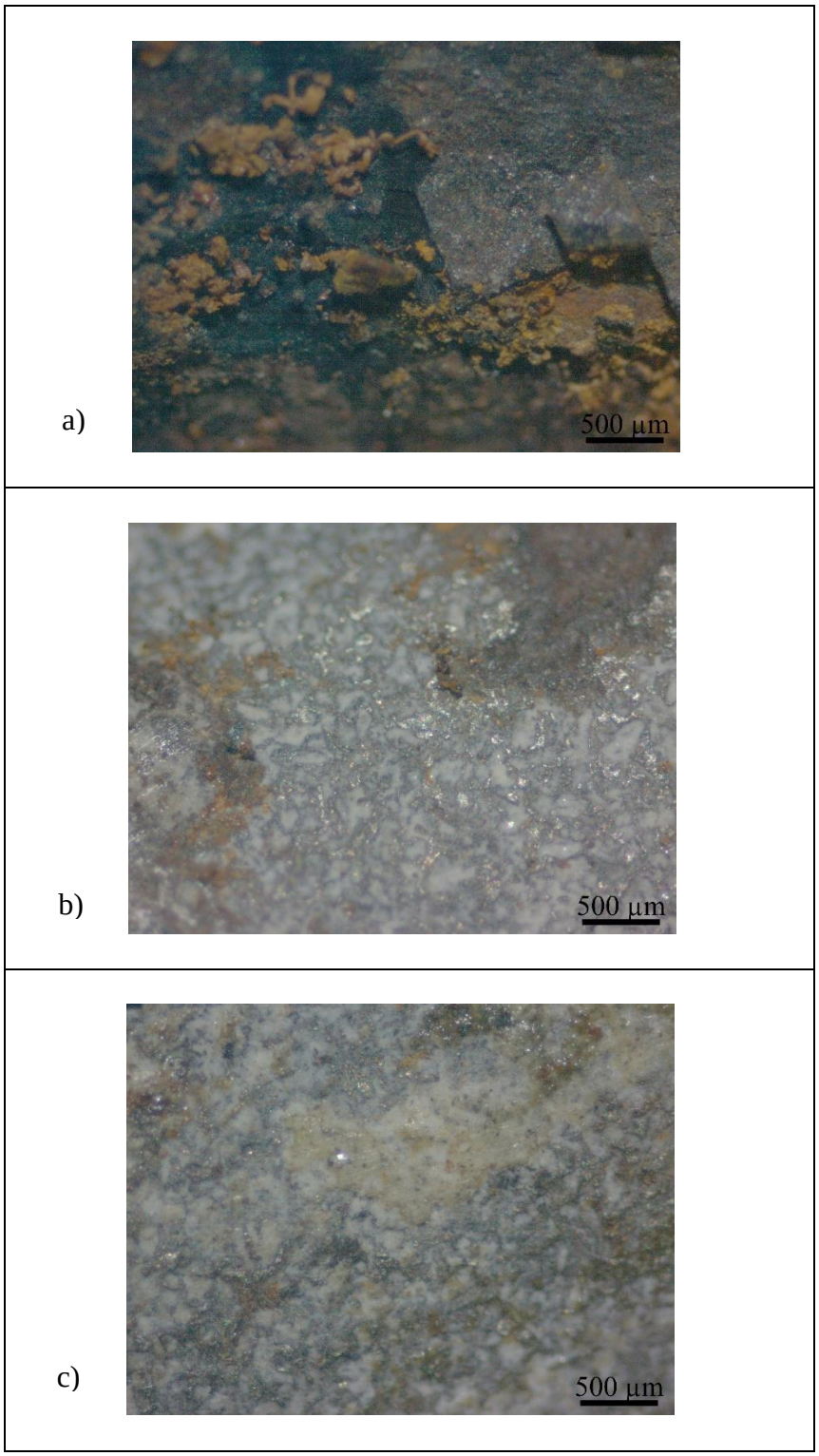

Figure 28: Optical microscope images of steel reinforcing bars extracted from (a) control mortar, (b) mortar admixed with 30 L/m^3 of calcium nitrite corrosion inhibitor, and (c) mortar admixed with 30 L/m^3 of green tea extract.

5.4.4.3 SEM-EDX

White layer on the surface of rebars extracted from GT-based and CI-based mortar was further examined with VP-SEM, and analyzed with FE-SEM equipped with EDX to elucidate the elemental compositions of the layer. The VP-SEM images are shown in Figure 29 and the elemental analyses are presented in Table 33.

As shown in Table 33, oxygen constitutes 40-60% of all rebar surface (except for the surface of untested rebars), suggesting the formation of iron oxides [225]. Moreover, Table 33 suggests that the white layer on rebars extracted from GT-based mortar was enriched with calcium, as evidenced by the significantly lower calcium content on rebars extracted from control mortar, on which the white layer was absent. Furthermore, the calcium was derived from mortar, as calcium was not detected on surface of untested rebars. The presence of this calcium-enriched layer significantly reduced the iron content on the rebars extracted from GT-based mortar than on rebars extracted from control mortar and untested rebars. The white layer on rebars extracted from CI-based mortar was similarly enriched with calcium. Results of XRD and FTIR analyses, which elucidated the mineral compositions of the layer on rebars extracted from GT-based mortar, are presented in the next sections.

a)

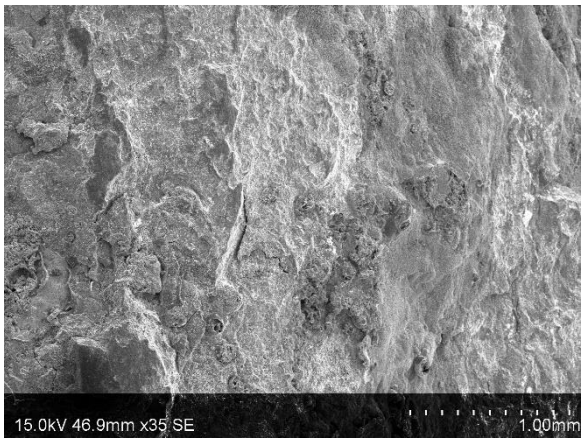

b)

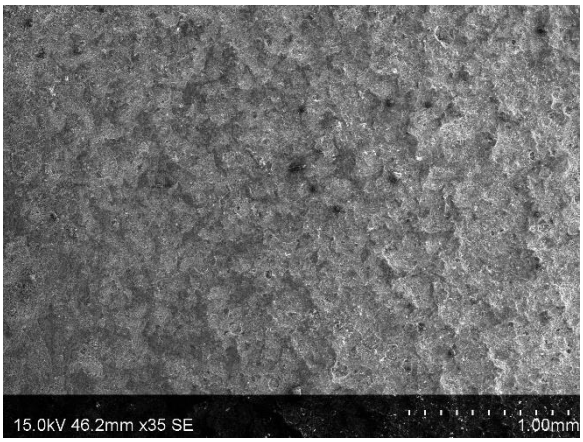

c)

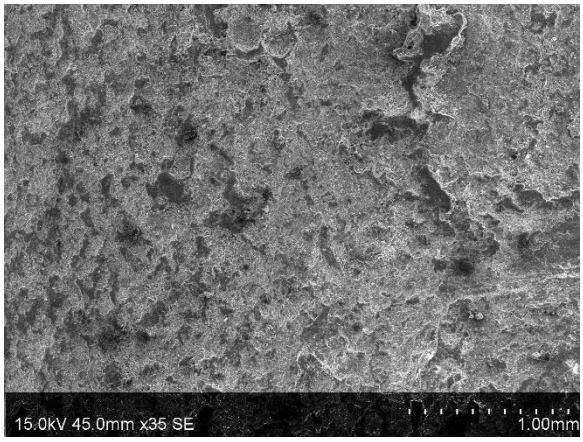

Figure 29: Scanning electron microscope images of steel reinforcing bars extracted from (a) control mortar, (b) mortar admixed with 30 L/m^3 of calcium nitrite corrosion inhibitor, and (c) mortar admixed with 30 L/m^3 of green tea extract.

Table 33: Elemental analyses on surface of untested steel reinforcing bars, reinforcing bars extracted from control mortar, and reinforcing bars extracted from mortar admixed with calcium nitrite corrosion inhibitor (CI) or green tea extract (GT)

Corrosion inhibitor for reinforcing bar	Inhibitor volume (L/m^3)	Percentage weight			
		Oxygen	Chloride	Calcium	Iron
Control	-	41.52 ± 5.98^{a}	3.60 ± 2.84^{a}	1.94 ± 1.49^{a}	52.94 ± 4.10^{a}
CI	30	44.60 ± 6.38^{a}	4.49 ± 0.67^{a}	20.38 ± 7.60^{b}	30.54 ± 12.33^{bc}
GT	30	59.11 ± 10.26^{bc}	3.52 ± 0.98^{a}	22.98 ± 5.43^{b}	14.39 ± 11.06^{bd}
Untested/original	-	11.16 ± 3.75^{bd}	-	-	88.83 ± 3.75^{be}

Values are expressed as mean ± standard deviation of three samples. Within the same column, values followed by different superscripted letters are significantly different from each other based on Tukey HSD test with p-value of 0.05.

5.4.4.4 FTIR and XRD

Calcium enrichment of the white layer on rebar extracted from GT-based mortar was further confirmed with XRD and FTIR analyses (Figures 30 and 31). As suggested by XRD spectra shown in Figure 30, the white layer on uncorroded area of rebar extracted from GT-based mortar was enriched with three major calcium carbonate polymorphs namely calcite, aragonite, and vaterite [238-241]. The main peaks of aragonite, vaterite, and calcite are indicated by peaks 1-3. Although the main peaks of aragonite and vaterite (peaks 1 and 2) [240-244] overlap with the peaks of corrosion products [206, 225, 245-247], the main calcite peak (peak 3) was attributed to calcite alone (JCPDS PDF 00-005-0586 and Ref. [240, 243, 244, 248, 249]) and was not detected on rebar extracted from control mortar. Moreover, the presence of the three calcium carbonate polymorphs on rebar extracted from GT-based mortar was also supported by the FTIR spectra shown in Figure 31.

The FTIR absorption bands corresponding to the three calcium carbonate polymorphs are: 1,405 and 711 cm^{-1} for calcite, 961 and 871 cm^{-1} for aragonite and vaterite, and 871 cm^{-1} for calcite and vaterite [226, 227, 242, 244, 250, 251]. The aforementioned bands represent different vibrations of carbonate ions: asymmetrical stretching vibration (ν_3) at 1,405 cm^{-1}, symmetrical stretching vibration (ν_1) at 961 cm^{-1}, out-of-plane bending vibration (ν_2) at 871 cm^{-1}, and in-plane bending vibration (ν_4) at 711 cm^{-1} [226]. On the other hand, the bands at 1,641 cm^{-1}, 2,337-2,361 cm^{-1}, and 3,402 cm^{-1} correspond to vibrations of O-H bending, CO_2, and O-H stretching respectively [248, 252, 253].

Overall, XRD and FTIR analyses illustrated that GT induces the formation of protective layer enriched with calcium carbonate polymorphs (calcite, aragonite, and vaterite) on rebar surface. The corrosion inhibition by this layer is presented in next section, whereby rebar weight loss in presence and absence of this layer are compared.

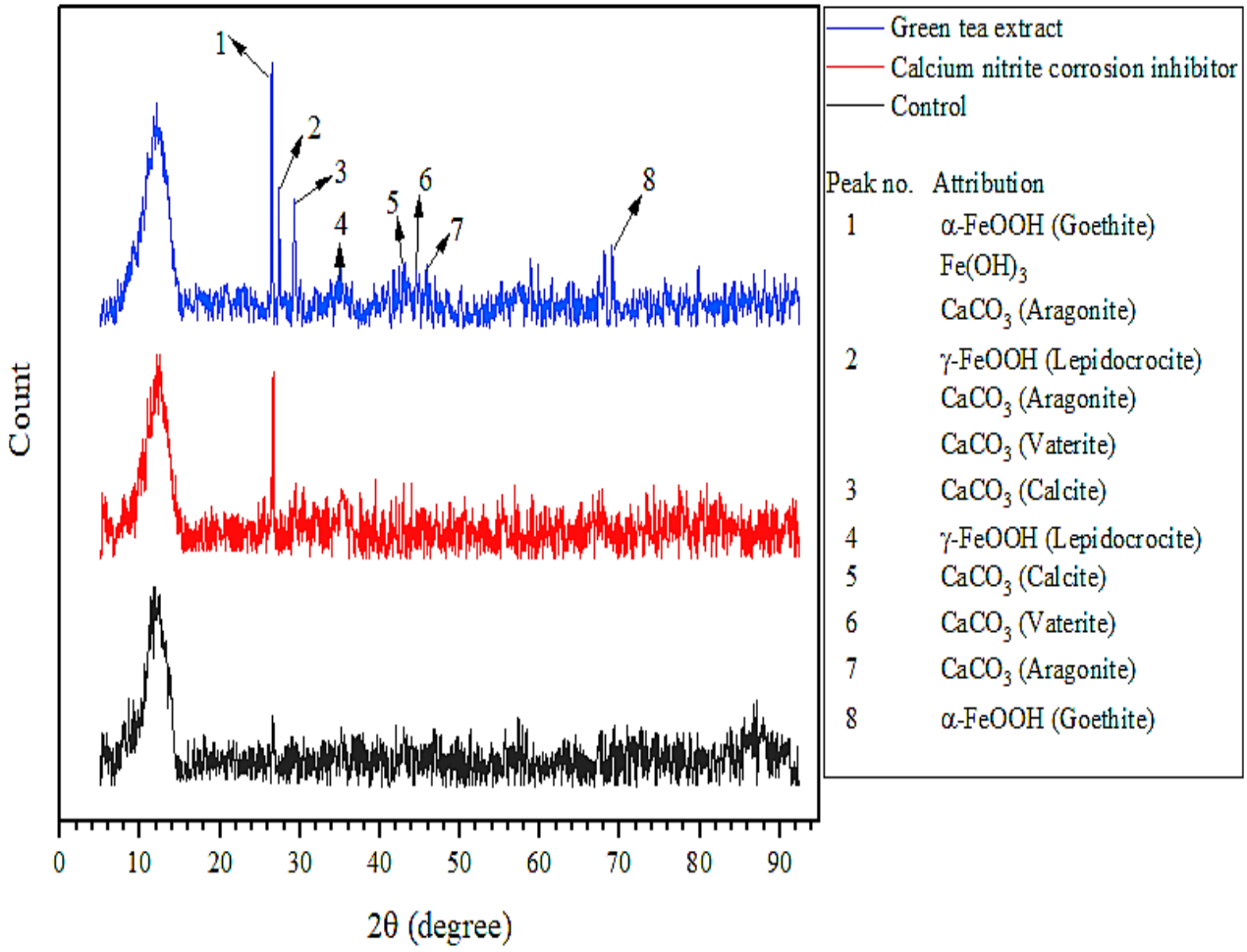

Figure 30: XRD spectra of steel reinforcing bars extracted from control mortar and mortar admixed with calcium nitrite corrosion inhibitor or green tea extract

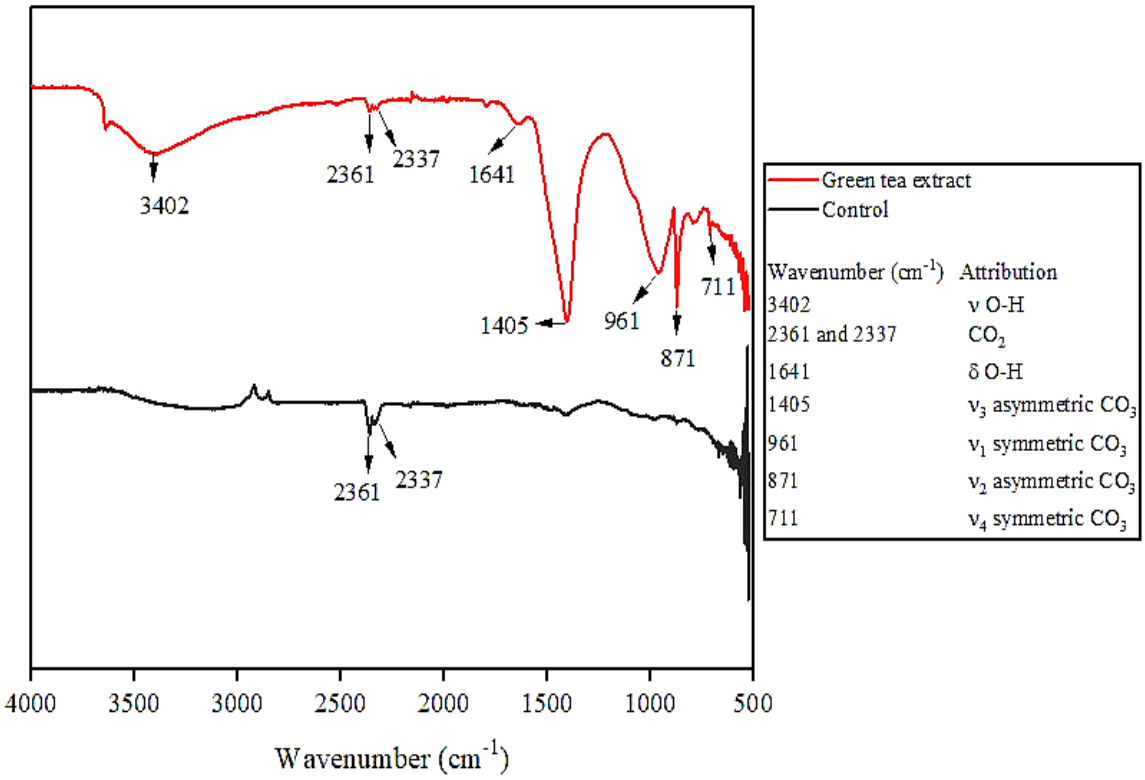

Figure 31: FTIR spectra of steel reinforcing bars extracted from control mortar and mortar admixed with green tea extract

5.4.5 Rebar weight loss

Weight loss of rebars extracted from control mortar and mortar admixed with corrosion inhibitors (CI, GT, and resuspended GT solid) are presented in Table 34. The rebars extracted from GT-based mortar had a lower weight loss than the rebars extracted from control and CI-based mortar. This is in agreement with the presented corrosion rate values. In particular, the rebars extracted from mortar added with GT at 30 L/m^3 showed a significantly lower weight loss than the rebars extracted from control and CI-based mortar. On the other hand, there was no significant difference in weight loss between rebars extracted from control mortar and rebars extracted from mortar admixed with resuspended GT solid. This behavior is in line with the absence of significant difference in the corrosion rate as illustrated in Figure 26 and Table 34. In summary, the presence of protective layer enriched with calcium carbonate polymorphs

(calcite, aragonite, and vaterite) on rebars extracted from GT-based mortar decreases rebar corrosion, as demonstrated by the reductions in measured rebar weight loss.

Table 34: Weight loss of steel reinforcing bars

Corrosion inhibitor	Volume of inhibitor (L/m^3)	Final corrosion rate (μm/year)	Weight loss (%)
Control	-	393 ± 117^{a}	2.94 ± 0.40^{a}
Calcium nitrite corrosion inhibitor	40	331 ± 48^{a}	2.88 ± 0.32^{a}
	30	293 ± 62^{ac}	2.68 ± 0.38^{ac}
	24	280 ± 43^{ad}	2.62 ± 0.25^{ad}
	20	294 ± 48^{a}	2.88 ± 0.23^{a}
Green tea extract	40	154 ± 30^{bcd}	2.09 ± 0.18^{bcd}
	30	134 ± 41^{b}	1.82 ± 0.16^{b}
	24	197 ± 38^{a}	2.24 ± 0.17^{a}
	20	196 ± 42^{a}	2.39 ± 0.20^{a}
Residual solid of green tea extract resuspended in water	40	258 ± 33^{a}	2.76 ± 0.23^{a}
	30	245 ± 43^{a}	2.55 ± 0.27^{a}
	24	221 ± 55^{a}	2.59 ± 0.36^{a}
	20	238 ± 30^{a}	2.62 ± 0.32^{a}

Values are expressed as mean ± standard deviation of three samples. Within the same column, values followed by different superscripted letters are significantly different from each other based on Tukey HSD test with p-value of 0.05.

5.4.6 Detection of proposed corrosion-inhibiting compounds in GT

Having evidenced that GT reduced rebar corrosion, the compounds responsible for the corrosion inhibition by GT are proposed, based on LCMS and LCMS-MS results presented in Figure 32 and Table 35. Figure 32 shows the LCMS spectra which indicated the presence of catechin derivatives in GT, based on the mass/charge ratios (m/z) of the parent ions: catechin or its stereoisomer (-)-epicatechin at m/z 289, (-)-epicatechin gallate at m/z 441, and (-)-epigallocatechin gallate at m/z 457 [40, 232, 235, 236, 254]. Fragmentation patterns of these parent ions detected by LCMS-MS are

presented in Table 35. These fragmentation patterns were in agreement with the reported fragments in METLIN Database and published literatures [40, 231, 235, 236]. Thus, LCMS and LCMS-MS analyses supported the presence of catechin or (-)-epicatechin, (-)-epicatechin gallate, and (-)-epigallocatechin gallate in GT.

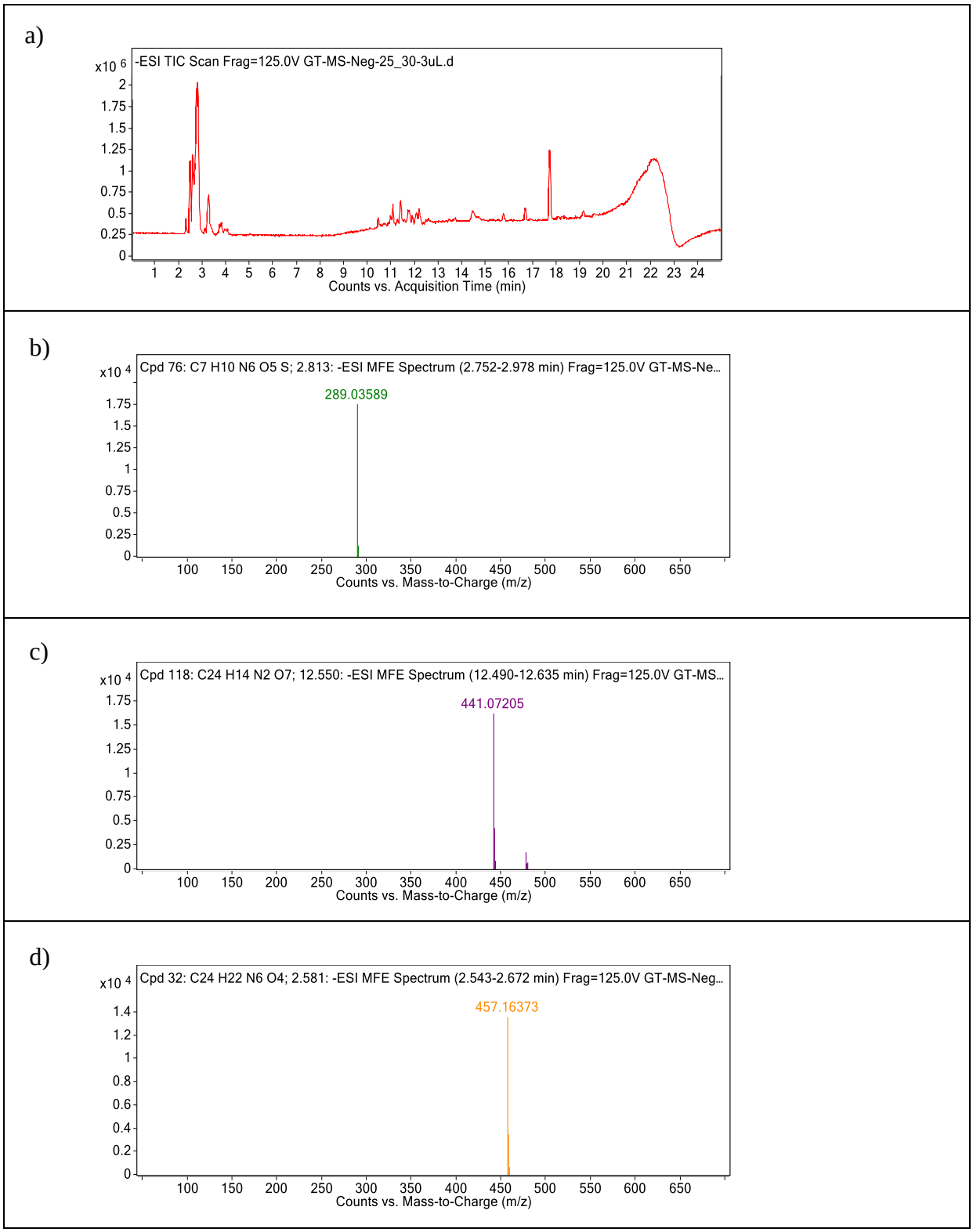

Figure 32: Liquid chromatography-mass spectrometry spectra of green tea extract: full-scan (a) and the spectra indicating the presence of catechin or (-)-epicatechin (b), (-)-epicatechin gallate (c), and (-)-epigallocatechin gallate (d) based on the mass-to-charge ratios of parent ions

Table 35: Mass-to-charge ratios (m/z) of ion fragments from targeted compounds in green tea extract detected by liquid chromatography-tandem mass spectrometry

Targeted compound	m/z of parent ion	m/z of ion fragment
Catechin or (-)-epicatechin	289	109, 125, 179, 203, 205, 245, 289
(-)-Epicatechin gallate	441	125, 169, 271, 289, 331
(-)-Epigallocatechin gallate	457	125, 169, 305, 331

It is observed in Table 35 that the ion fragments with m/z of 125 were detected from all parent ions, and corresponded to the fragmentations of the A-rings of catechin derivatives. On the other hand, the fragments with m/z 289 were attributed to the catechin moieties, of which the loss of water from these moieties arose the fragment with m/z 271. The fragments with m/z 169 distinguished (-)-epicatechin gallate and (-)-epigallocatechin gallate from catechin and (-)-epicatechin, and corresponded to the neutral losses of galloyl esters from (-)-epicatechin gallate and (-)-epigallocatechin gallate as gallic acid moieties. The (-)-epigallocatechin gallate fragment with m/z 305 corresponded to the epigallocatechin moiety after the loss of the galloyl ester [231, 236].

Green tea contains complex mixtures of chemicals such as polyphenols, alkaloids, carbohydrates, proteins, volatile compounds, minerals, and trace elements [255]. Among the chemicals, catechin derivatives are the major constituents of green tea [40, 41, 229, 232, 235, 255], constituting approximately 70% of total polyphenols in green tea [152] and 16-30% dry green tea weight [157, 236, 255]. (-)-Epigallocatechin gallate has been reported to be the most abundant among the catechin derivatives [40, 233, 235, 236, 254, 255]. In addition to being the major constituents of green tea, Stewart et al. [40] have reported that catechin derivatives are the major contributors to the total antioxidant activity of green tea (70-90%), 30% of which was contributed by (-)-epigallocatechin gallate. On the other hand, despite being less abundant than (-)-epigallocatechin gallate [40, 235, 255], (-)-epicatechin gallate demonstrated a comparable total antioxidant activity to (-)-epigallocatechin gallate [40, 152].

The potent antioxidant activity of catechin derivatives is contributed by the absence of 4-oxo function (i.e. double bond at 2,3 position and carbonyl group at 4-position) and the saturation of the heterocyclic ring. These structural characteristics promote the stabilization of the formed phenoxy radical upon electron donation, which enhances antioxidant activity [40, 152, 229]. In addition, the presence of di-hydroxyl groups (i.e. catechol) and tri-hydroxyl (i.e. pyrogallol) groups in the B-rings of (-)-epicatechin gallate and (-)-epigallocatechin gallate, as well as the presence of galloyl moieties attached to 3-positions of (-)-epicatechin gallate and (-)-epigallocatechin gallate further elevate the antioxidant activity of these compounds [40, 152, 229]. Therefore, given the major contribution of catechin derivatives to the total antioxidant activity of green tea, and considering the influence of antioxidant activity on anti-corrosion activity, it is reasonable to infer that the catechin derivatives specifically the (-)-epigallocatechin gallate, (-)-epicatechin gallate, and catechin or (-)-epicatechin are responsible for the anti-corrosion activity of GT.

5.4.7 Overall effects of GT on rebar corrosion

It has been demonstrated that the rebars embedded in GT-based mortar had a lower corrosion rate than the rebars embedded in control and CI-based mortar. The lower corrosion rate was not due to an improved physical protection of mortar/concrete against corrosion, since control and GT-based concrete had a similar chloride permeability, and steel reinforced mortar which incorporated the residual solid of GT had a similar corrosion rate to steel reinforced control mortar. Instead of improving the physical protection of mortar/concrete, GT reduced corrosion rate by inducing the formation of a protective layer enriched with calcium carbonate. This layer inhibited rebar corrosion, as suggested by a decreased rebar weight loss in presence of this layer. Catechin or (-)-epicatechin, (-)-epicatechin gallate, and (-)-epigallocatechin gallate were suggested to be the constituents which contributed to the corrosion-inhibiting activity of GT.

5.5 Summary

Formation of protective layer on rebar extracted from GT-based mortar was confirmed with visual inspections and microscopic examinations (optical microscope and SEM). In presence of this layer, rebar weight loss was reduced, and analyses with EDX, XRD, and FTIR suggested that the layer was enriched with calcium, precisely the calcium carbonate polymorphs (calcite, aragonite, and vaterite). Corrosion inhibition by the layer was further demonstrated by a similar chloride permeability between control and GT-based concrete, and a similar corrosion rate between steel reinforced control mortar and steel reinforced mortar incorporating residual solid of GT. These similarities ruled out the plausible reduction in corrosion rate due to an improved physical protection of mortar/concrete against corrosion. Despite the formation of protective layer and increase in polarization resistance were influenced by the magnitude of antioxidant activity, in this study GT has shown a better IE than CI, especially at the higher range of volume. It was hypothesized that the catechin or (-)-epicatechin, (-)-epicatechin gallate, and (-)-epigallocatechin gallate were responsible for the anti-corrosion activity of GT.

CHAPTER 6: CONCLUSIONS AND RECOMMENDATIONS FOR FUTURE STUDIES

6.1 Conclusions

In this study, the potential of natural antioxidants as non-toxic and environmentally-friendly ('green') corrosion inhibitors has been investigated. The main objective of this study is to evaluate the efficiency of natural antioxidants (extracted from green tea) as admixed corrosion inhibitors against the chloride-induced corrosion of steel reinforcing bar (rebar). There are three key areas of this study, namely: (a) the inhibition efficiency of natural antioxidants against chloride-induced corrosion, compared to a commercial corrosion inhibitor, (b) corrosion-inhibiting mechanisms of the natural antioxidants, and (c) the relationship between antioxidant activity and corrosion rate of rebar embedded in mortar added with the natural antioxidants, particularly in relation to the change in polarization resistance.

This study began with the investigation on corrosion inhibition efficiency of green tea in simulated concrete pore solution (SCPS). The SCPS was added with 3.5% (w/v) sodium chloride (NaCl) to simulate the exposure to seawater. The physical form to administer green tea (dry admixture or aqueous extract) and the selected dosage of green tea for the corrosion tests in SCPS were determined by comparing the 7-day compressive strength of control and green tea-based mortar. The corrosion tests were conducted for 21 days, and electrochemical parameters which indicated corrosion development (anodic and cathodic slopes, polarization resistance, corrosion rate, and open circuit potential) were monitored at regular intervals. The following conclusions were drawn from the corrosion tests in SCPS:

- At any percentage of water replacement (20-100%) with aqueous extracts of 1% and 2% (by cement weight) green tea, there was no significant difference in compressive strength of control and green tea-based mortar.
- Adding green tea as dry admixtures at 1% and 2% (by cement weight) significantly reduced the compressive strength of green tea-based mortar.
- Therefore, green tea was added as aqueous extracts of 1% and 2% green tea to replace water during the corrosion tests in SCPS.
- In SCPS, the green tea extracts reduced rebar corrosion rate and delayed the sudden increase in corrosion rate (which indicated corrosion initiation).
- The reduction in corrosion rate was expressed in terms of corrosion inhibition efficiency (IE).
- Against 3.5% NaCl, highest IE was observed after 1 day (±92% inhibition) for both the extracts of 1% and 2% green tea.
- Both green tea extracts behaved as mixed-type corrosion inhibitors, as indicated by the changes in the anodic slope (i.e. rate of iron oxidation) and cathodic slope (i.e. rate of oxygen reduction), without a significant change in open circuit potential.
- The extracts of 1% and 2% green tea were equally effective as admixed corrosion inhibitors against 3.5% NaCl: both extracts delayed the corrosion initiation until 14 days
- However, the extract of 2% green tea showed a higher overall IE throughout the corrosion test (46.31± 15.97% vs. 37.50± 6.97% after 21 days). Thus, the extract was selected for further studies.

Upon the completion of corrosion tests in SCPS, IE of green tea extract (GT) was investigated in mortar, and compared with the IE of commercial calcium nitrite corrosion inhibitor (CI). CI dosages were selected encompassing the recommended dosages by the manufacturer (chloride-to-nitrite ratios of 1.2 and 1.5), and a wider range of dosages (ratios of 0.9 and 1.8). On the other hand, GT dosages were selected similar to CI dosages. IE of both inhibitors were compared at similar concentration and equal volume. Corrosion of the rebar embedded in mortar was accelerated by a

combination of impressed current and cyclic wetting-drying exposure. The accelerated corrosion was conducted for 12 wetting-drying cycles, of which each cycle consisted of four wetting days and three drying days. The electrochemical parameters (anodic and cathodic slopes, polarization resistance, corrosion rate, and open circuit potential) were monitored weekly. 28-day compressive strength of mortar added with GT or CI was also measured. The following are the conclusions of the corrosion tests in mortar:

- At similar concentration, GT and CI showed a similar IE (51-70%).
- However, at equal volume GT exhibited a significantly higher IE than CI (75-80% vs. 14-24%).
- The higher IE of GT was not due an improved physical protection of mortar, as GT-based mortar showed a comparable compressive strength to CI-based mortar.
- The higher IE was due to a significant increase in polarization resistance and decrease in anodic slope.
- Changes in cathodic slope and open circuit potential were insignificant.
- The changes in anodic and cathodic slopes without a significant open circuit potential change suggested that GT was a mixed-type corrosion inhibitor which formed a protective layer on rebar surface and increased polarization resistance.

Having shown that GT reduced rebar corrosion rate in mortar, the corrosion-inhibiting mechanisms of GT were investigated. The main focus was the formation of protective layer on rebar surface, as indicated by the increase in rebar polarization resistance. The layer's protection against corrosion was studied by comparing rebar weight loss in presence and absence of this layer, and was validated by further investigations on the physical protection of mortar/concrete against corrosion. The physical protection of mortar/concrete was examined by comparing the chloride permeability of control and GT-based concrete, and the corrosion rate of steel reinforced control mortar and steel reinforced mortar which incorporated the residual solid of GT. The following describe the corrosion-inhibiting mechanisms of green tea:

- Visual inspections and microscopic examinations (optical microscope and scanning electron microscope) demonstrated the formation of protective layer on the surface of rebar extracted from GT-based mortar.
- Elemental analyses with energy-dispersive X-ray spectroscopy (EDX) indicated that the layer was enriched with calcium.
- Further analyses with X-ray diffractometry (XRD) and Fourier transform infrared spectroscopy (FTIR) revealed enrichment of the layer with calcium carbonate polymorphs (calcite, aragonite, and vaterite).
- The calcium carbonate enriched-layer inhibited rebar corrosion, as the presence of this layer reduced rebar weight loss.
- Corrosion reduction due to the presence of this layer was further validated by a similar chloride permeability between control and GT-based concrete, and a similar corrosion rate of steel reinforced control mortar and steel reinforced mortar incorporating the residual solid of GT.
- GT did not reduce corrosion rate by improving the physical protection of mortar against corrosion.
- Instead, GT induced formation of a protective layer enriched with calcium carbonate, and increased rebar polarization resistance.
- The increase in polarization resistance and decrease in corrosion rate were affected by the magnitude of GT's antioxidant activity.
- Liquid chromatography-mass spectrometry (LCMS) and liquid chromatography-tandem mass spectrometry (LCMS-MS) analyses suggested that catechin or (-)-epicatechin, (-)-epicatechin gallate, and (-)-epigallocatechin gallate were pluasibly accountable for the corrosion-inhibiting activity of GT.

In summary, the potential of natural antioxidants as green admixed corrosion inhibitors against chloride-induced rebar corrosion has been positively demonstrated by green tea throughout this study, both in SCPS and mortar. GT behaves as a mixed-type green corrosion inhibitor, which increases rebar polarization resistance by forming a protective layer enriched with calcium carbonate polymorphs (calcite, aragonite, and vaterite) on the surface of rebar embedded in mortar. The magnitude of antioxidant

activity affects the increase in polarization resistance. Nonetheless, GT outperforms CI in this study, particularly at the higher range of volume. Amongst GT's constituents, catechin or (-)-epicatechin, (-)-epicatechin gallate, and (-)-epigallocatechin gallate were the likely compounds being responsible for the corrosion inhibition by GT.

Given the demonstrated GT's inhibition on rebar corrosion, natural antioxidants are deemed to be suitable green corrosion inhibitors for steel rebar embedded in concrete, as alternatives or potential substitutes to existing commercial corrosion inhibitors. The natural antioxidants exhibit a higher corrosion inhibition efficiency at higher electron donation capacity. The higher electron donation capacity enhances the antioxidant's efficiency to increase rebar polarization resistance and subsequently impedes rebar corrosion as admixed, mixed-type corrosion inhibitors. The value of natural antioxidants as green corrosion inhibitors is further compounded by the scarcity of studies on natural organic corrosion inhibitors in alkaline pH of concrete. Hence, the next section covers the recommendations for future studies on natural antioxidant-based green corrosion inhibitors.

6.2 Recommendations for future studies

The following are the recommendations for future studies on natural antioxidant-based green corrosion inhibitors:

- Investigations on IE of more cost-effective sources of natural antioxidants. These materials can be derived from various agricultural by-products such as fruit peels, fruit seeds, and solid wastes from cereal grain processing (e.g. corncob, rice bran, and wheat husk) [180, 186, 256-260].
- Investigations on the IE of green corrosion inhibitors from the alternative sources of natural antioxidants with a longer-term natural corrosion test.
- Comparison on the IE derived by adopting natural corrosion test with the IE derived by adopting the accelerated corrosion procedures described in this study.

- Cost and service-life analyses of the green corrosion inhibitors, to evaluate the additional costs and the additional benefits (i.e. improved corrosion resistance and prolonged service life) of incorporating the inhibitors into a reinforced concrete structure.

REFERENCES

1. McCarter, W. et al. (2013). *Characterization of physio-chemical processes and hydration kinetics in concretes containing supplementary cementitious materials using electrical property measurements.* Cement and Concrete Research, 50: pp. 26-33.
2. Mala, K. et al. (2014). *Effect of relative levels of mineral admixtures on corrosion resistance of cracked ternary cement blend concrete.* Journal of Sustainable Cement-Based Materials, 3(1): pp. 24-46.
3. Shubina, V. et al. (2016). *Biomolecules as a sustainable protection against corrosion of reinforced carbon steel in concrete.* Journal of Cleaner Production, 112(1): 666-671.
4. Padilla, V. et al. (2013). *Effect of de-icing salts on the corrosion performance of galvanized steel in sulphate contaminated soil.* Construction and Building Materials, 40: pp. 908-918.
5. Goyal, A. et al. (2018). *A review of corrosion and protection of steel in concrete.* Arabian Journal for Science and Engineering: pp. 1-21.
6. Yang, Z. et al. (2013). *Modified hydrotalcites as a new emerging class of smart additive of reinforced concrete for anticorrosion applications: A literature review.* Materials and Corrosion, 64(12): pp. 1066-1074.
7. Baltazar-Zamora, M. et al. (2012). *Efficicency of galvanized steel embedded in concrete previously contaminated with 2, 3 and 4% of NaCl.* International Journal of Electrochemical Science, 7: pp. 2997-3007.
8. Feng, L. et al. (2011). *Experimental and theoretical studies for corrosion inhibition of carbon steel by imidazoline derivative in 5% NaCl saturated $Ca(OH)_2$ solution.* Electrochimica Acta, 58: pp. 427-436.
9. Vera, R. et al. (2012). *Performance of carbon steel and galvanized steel in reinforced concrete structures after accelerated carbonation.* International Journal of Electrochemical Science, 7(11): pp. 10722-10734.
10. Ormellese, M. et al. (2009). *A study of organic substances as inhibitors for chloride-induced corrosion in concrete.* Corrosion Science, 51(12): pp. 2959-2968.
11. Polder, R.B. et al. (2011). *Early stage beneficial effects of cathodic protection in concrete structures.* Materials and Corrosion, 62(2): pp. 105-110.

12. Criado, M. et al. (2011). *Corrosion behaviour of a new low-nickel stainless steel embedded in activated fly ash mortars.* Cement and Concrete Composites, 33(6): pp. 644-652.
13. Elsener, B. et al. (2011). *Stainless steel reinforcing bars – Reason for their high pitting corrosion resistance.* Materials and Corrosion, 62(2): pp. 111-119.
14. Wilson, K. et al. (2013). *The selection and use of cathodic protection systems for the repair of reinforced concrete structures.* Construction and Building Materials, 39: pp. 19-25.
15. Gerengi, H. and Sahin, H.I. (2011). *Schinopsis lorentzii extract as a green corrosion inhibitor for low carbon steel in 1 M HCl solution.* Industrial and Engineering Chemistry Research, 51(2): pp. 780-787.
16. Khadom, A.A. et al. (2015). *Evaluation of environmentally friendly inhibitor for galvanic corrosion of steel–copper couple in petroleum waste water.* Process Safety and Environmental Protection, 98: pp. 93-101.
17. Asipita, S.A. et al. (2014). *Green Bambusa arundinacea leaves extract as a sustainable corrosion inhibitor in steel reinforced concrete.* Journal of Cleaner Production, 67: pp. 139-146.
18. Söylev, T.A. and Richardson, M.G. (2008). *Corrosion inhibitors for steel in concrete: State-of-the-art report.* Construction and Building Materials, 22(4): pp. 609-622.
19. Lee, H.S. et al. (2018). *Corrosion inhibitors for reinforced concrete: A review.* in *Corrosion Inhibitors, Principles and Recent Applications*. InTech.
20. Bolzoni, F. et al. (2014). *Experiences on corrosion inhibitors for reinforced concrete.* International Journal of Corrosion Scale Inhibition, 3(4): pp. 254-278.
21. Saricimen, H. et al. (2002). *Effectiveness of concrete inhibitors in retarding rebar corrosion.* Cement and Concrete Composites, 24(1): pp. 89-100.
22. Hansson, C.M. et al. (1998). *Corrosion inhibitors in concrete − Part I: The principles.* Cement and Concrete Research, 28(12): pp. 1775-1781.
23. Reou, J.S. and Ann, K.Y. (2008). *The electrochemical assessment of corrosion inhibition effect of calcium nitrite in blended concretes.* Materials Chemistry and Physics, 109(2): pp. 526-533.
24. Aïtcin, P.C. (2016). *24 − Corrosion inhibition.* in *Science and Technology of Concrete Admixtures*, P.C. Aïtcin and R.J. Flatt (Editors). Woodhead Publishing, pp. 471-479.

25. Sideris, K.K. and Savva, A.E. (2005). *Durability of mixtures containing calcium nitrite based corrosion inhibitor.* Cement and Concrete Composites, 27(2): pp. 277-287.
26. Vaysburd, A.M. and Emmons, P.H. (2004). *Corrosion inhibitors and other protective systems in concrete repair: Concepts or misconcepts.* Cement and Concrete Composites, 26(3): pp. 255-263.
27. Ormellese, M. et al. (2006). *Corrosion inhibitors for chloride induced corrosion in reinforced concrete structures.* Cement and Concrete Research, 36(3): pp. 536-547.
28. Abd El Fattah, A. et al. (2018). *Field evaluation of corrosion mitigation on reinforced concrete in marine exposure conditions.* Construction and Building Materials, 165: pp. 663-674.
29. Montes, P. et al. (2004). *Influence of calcium nitrite inhibitor and crack width on corrosion of steel in high performance concrete subjected to a simulated marine environment.* Cement and Concrete Composites, 26(3): pp. 243-253.
30. Civjan, S.A. et al. (2005). *Effectiveness of corrosion inhibiting admixture combinations in structural concrete.* Cement and Concrete Composites, 27(6): pp. 688-703.
31. Ngala, V.T. et al. (2002). *Corrosion inhibitor systems for remedial treatment of reinforced concrete − Part 1: Calcium nitrite.* Corrosion Science, 44(9): pp. 2073-2087.
32. Królikowski, A. and Kuziak, J. (2011). *Impedance study on calcium nitrite as a penetrating corrosion inhibitor for steel in concrete.* Electrochimica Acta, 56(23): pp. 7845-7853.
33. Mammoliti, L. et al. (1999). *Corrosion inhibitors in concrete − Part II: Effect on chloride threshold values for corrosion of steel in synthetic pore solutions.* Cement and Concrete Research, 29(10): pp. 1583-1589.
34. Trépanier, S.M. et al. (2001). *Corrosion inhibitors in concrete − Part III: Effect on time to chloride-induced corrosion initiation and subsequent corrosion rates of steel in mortar.* Cement and Concrete Research, 31(5): pp. 713-718.
35. Kondratova, I. et al. (2003). *Natural marine exposure results for reinforced concrete slabs with corrosion inhibitors.* Cement and Concrete Composites, 25(4): pp. 483-490.
36. Benzina Mechmeche, L. et al. (2008). *Investigation of the early effectiveness of an amino-alcohol based corrosion inhibitor using simulated pore solutions and mortar specimens.* Cement and Concrete Composites, 30(3): pp. 167-173.

37. Wombacher, F. et al. (2004). *Aminoalcohol based mixed corrosion inhibitors.* Cement and Concrete Composites, 26(3): pp. 209-216.
38. Obot, I.B. et al. (2009). *Antifungal drugs as corrosion inhibitors for aluminium in 0.1 M HCl.* Corrosion Science, 51(8): pp. 1868-1875.
39. Urquiaga, I. and Leighton, F. (2000). *Plant polyphenol antioxidants and oxidative stress.* Biological Research, 33: pp. 55-64.
40. Stewart, A.J. et al. (2005). *On-line high-performance liquid chromatography analysis of the antioxidant activity of phenolic compounds in green and black tea.* Molecular Nutrition and Food Research, 49(1): pp. 52-60.
41. Atoui, A.K. et al. (2005). *Tea and herbal infusions: Their antioxidant activity and phenolic profile.* Food Chemistry, 89(1): pp. 27-36.
42. Henning, S.M. et al. (2004). *Bioavailability and antioxidant activity of tea flavanols after consumption of green tea, black tea, or a green tea extract supplement.* The American Journal of Clinical Nutrition, 80(6): pp. 1558-1564.
43. Lee, K.W. et al. (2003). *Cocoa has more phenolic phytochemicals and a higher antioxidant capacity than teas and red wine.* Journal of Agricultural and Food Chemistry, 51(25): pp. 7292-7295.
44. Borges, G. et al. (2009). *Identification of flavonoid and phenolic antioxidants in black currants, blueberries, raspberries, red currants, and cranberries.* Journal of Agricultural and Food Chemistry, 58(7): pp. 3901-3909.
45. Tanner, P. et al. (2013). *The role of corrosion inhibitors in maintaining concrete durability: 15 years experience in New Zealand and around the world.*
46. Wiktor, V. and Jonkers, H.M. (2011). *Quantification of crack-healing in novel bacteria-based self-healing concrete.* Cement and Concrete Composites, 33(7): pp. 763-770.
47. Achal, V. et al. (2013). *Biogenic treatment improves the durability and remediates the cracks of concrete structures.* Construction and Building Materials, 48: pp. 1-5.
48. Achal, V. et al. (2015). *Biomineralization for sustainable construction − A review of processes and applications.* Earth-Science Reviews, 148: pp. 1-17.
49. Chahal, N. et al. (2012). *Influence of bacteria on the compressive strength, water absorption and rapid chloride permeability of fly ash concrete.* Construction and Building Materials, 28(1): pp. 351-356.

50. Verma, R.K. and Chourasia, A. (2015). *Protection of bio-deteriorated reinforced concrete using concrete sealers.* International Journal of Materials Chemistry and Physics.
51. Wang, J. et al. (2012). *Diatomaceous earth as a protective vehicle for bacteria applied for self-healing concrete.* Journal of Industrial Microbiology and Biotechnology, 39(4): pp. 567-577.
52. Karahan, O. and Atiş, C.D. (2011). *The durability properties of polypropylene fiber reinforced fly ash concrete.* Materials and Design, 32(2): pp. 1044-1049.
53. Stuckrath, C. et al. (2014). *Quantification of chemical and biological calcium carbonate precipitation: Performance of self-healing in reinforced mortar containing chemical admixtures.* Cement and Concrete Composites, 50: pp. 10-15.
54. Pérez-Quiroz, J.T. et al. (2008). *Assessment of stainless steel reinforcement for concrete structures rehabilitation.* Journal of Constructional Steel Research, 64(11): pp. 1317-1324.
55. Knudsen, A. et al. (1998). *Cost-effective enhancement of durability of concrete structures by intelligent use of stainless steel reinforcement*. in *Conference on Corrosion and Rehabilitation of Reinforced Concrete Structures, Florida*.
56. Hansson, C.M. (2011). *The impact of corrosion on society.* Metallurgical and Materials Transactions A, 42(10): pp. 2952-2962.
57. Pacheco-Torgal, F. and Labrincha, J.A. (2013). *Biotech cementitious materials: Some aspects of an innovative approach for concrete with enhanced durability.* Construction and Building Materials, 40: pp. 1136-1141.
58. Aguirre-Guerrero, A.M. and Mejía de Gutiérrez, R. (2018). *13 − Assessment of corrosion protection methods for reinforced concrete.* in *Eco-efficient Repair and Rehabilitation of Concrete Infrastructures*, F. Pacheco-Torgal et al. (Editors). Woodhead Publishing, pp. 315-353.
59. Jiang, S. et al. (2017). *Deoxyribonucleic acid as an inhibitor for chloride-induced corrosion of reinforcing steel in simulated concrete pore solutions.* Construction and Building Materials, 150: pp. 238-247.
60. Chen, D. and Mahadevan, S. (2008). *Chloride-induced reinforcement corrosion and concrete cracking simulation.* Cement and Concrete Composites, 30(3): pp. 227-238.

61. Pour-Ali, S. et al. (2015). *Corrosion protection of the reinforcing steels in chloride-laden concrete environment through epoxy/polyaniline–camphorsulfonate nanocomposite coating.* Corrosion Science, 90: pp. 239-247.
62. Redaelli, E. and Bertolini, L. (2011). *Electrochemical repair techniques in carbonated concrete − Part I: Electrochemical realkalisation.* Journal of Applied Electrochemistry, 41(7): pp. 817-827.
63. Shi, X. et al. (2011). *Strength and corrosion properties of Portland cement mortar and concrete with mineral admixtures.* Construction and Building Materials, 25(8): pp. 3245-3256.
64. Negm, N.A. et al. (2012). *Gravimetric and electrochemical evaluation of environmentally friendly nonionic corrosion inhibitors for carbon steel in 1 M HCl.* Corrosion Science, 65: pp. 94-103.
65. Hornbostel, K. et al. (2013). *Relationship between concrete resistivity and corrosion rate − A literature review.* Cement and Concrete Composites, 39: pp. 60-72.
66. Okeniyi, J.O. et al. (2013). *Effect of ethylenediaminetetraacetic disodium dihydrate and sodium nitrite admixtures on steel-rebar corrosion in concrete.* European Journal of Environmental and Civil Engineering, 17(5): pp. 398-416.
67. Jeong, J.A. and Jin, C.K. (2013). *Three year performance of sacrificial anode cathodic protection system in the reinforced concrete bridge structures*. in *Advanced Materials Research*. Trans Tech Publishing.
68. Fajardo, S. et al. (2011). *Corrosion behaviour of a new low-nickel stainless steel in saturated calcium hydroxide solution.* Construction and Building Materials, 25(11): pp. 4190-4196.
69. García, S.J. et al. (2011). *A critical appraisal of the potential of self healing polymeric coatings.* Progress in Organic Coatings, 72(3): pp. 211-221.
70. Deshpande, P.P. et al. (2014). *Conducting polymers for corrosion protection: A review.* Journal of Coatings Technology Research, 11(4): pp. 473-494.
71. McCafferty, E. (2010). *Thermodynamics of corrosion: Pourbaix diagrams.* in *Introduction to Corrosion Science*. Springer, pp. 95-117.
72. Pourbaix, M. (1949). *Corrosion, passivity and passivation from the thermodynamic point of view.* Corrosion, 5(4): pp. 121-133.

73. Andrade, C. and Alonso, C. (2001). *On-site measurements of corrosion rate of reinforcements.* Construction and Building Materials, 15(2–3): pp. 141-145.
74. Schmuki, P. and Graham, M.J. (2001). *Corrosion.* in *Encyclopedia of Chemical Physics and Physical Chemistry − 3 Volume Set*. Taylor & Francis.
75. García, J. et al. (2012). *Effect of cathodic protection on steel–concrete bond strength using ion migration measurements.* Cement and Concrete Composites, 34(2): pp. 242-247.
76. Freire, L. et al. (2012). *Electrochemical and analytical investigation of passive films formed on stainless steels in alkaline media.* Cement and Concrete Composites, 34(9): pp. 1075-1081.
77. Cheung, M.M.S. and Cao, C. (2013). *Application of cathodic protection for controlling macrocell corrosion in chloride contaminated RC structures.* Construction and Building Materials, 45: pp. 199-207.
78. Zhou, Y. et al. (2014). *Carbonation-induced and chloride-induced corrosion in reinforced concrete structures.* Journal of Materials in Civil Engineering.
79. Nasser, A. et al. (2010). *Influence of steel–concrete interface condition on galvanic corrosion currents in carbonated concrete.* Corrosion Science, 52(9): pp. 2878-2890.
80. Boğa, A.R. and Topçu, İ.B. (2012). *Influence of fly ash on corrosion resistance and chloride ion permeability of concrete.* Construction and Building Materials, 31: pp. 258-264.
81. Szklarska-Smialowska, Z. (2002). *Mechanism of pit nucleation by electrical breakdown of the passive film.* Corrosion Science, 44(5): pp. 1143-1149.
82. Apostolopoulos, C.A. et al. (2013). *Chloride-induced corrosion of steel reinforcement − Mechanical performance and pit depth analysis.* Construction and Building Materials, 38: pp. 139-146.
83. Morris, W. et al. (2004). *Chloride induced corrosion of reinforcing steel evaluated by concrete resistivity measurements.* Electrochimica Acta, 49(25): pp. 4447-4453.
84. Page, C.L. and Sergi, G. (2000). *Developments in cathodic protection applied to reinforced concrete.* Journal of Materials in Civil Engineering, 12(1): pp. 8-15.
85. Gupta, R.K. and Birbilis, N. (2015). *The influence of nanocrystalline structure and processing route on corrosion of stainless steel: A review.* Corrosion Science, 92: pp. 1-15.

86. Gencel, O. et al. (2011). *Workability and mechanical performance of steel fiber-reinforced self-compacting concrete with fly ash.* Composite Interfaces, 18(2): pp. 169-184.
87. Berrocal, C.G. et al. (2013). *Influence of steel fibres on corrosion of reinforcement in concrete in chloride environments: A review*. in *7th International Conference Fibre Concrete 2013 Proceedings*.
88. Kakooei, S. et al. (2012). *The effects of polypropylene fibers on the properties of reinforced concrete structures.* Construction and Building Materials, 27(1): pp. 73-77.
89. Lee, C.L. et al. (2012). *Establishment of the durability indices for cement-based composite containing supplementary cementitious materials.* Materials and Design, 37: pp. 28-39.
90. Ramezanianpour, A.A. and Bahrami Jovein, H. (2012). *Influence of metakaolin as supplementary cementing material on strength and durability of concretes.* Construction and Building Materials, 30: pp. 470-479.
91. Thomas, M.D.A. et al. (2012). *The effect of supplementary cementitious materials on chloride binding in hardened cement paste.* Cement and Concrete Research, 42(1): pp. 1-7.
92. Juenger, M.C.G. and Siddique, R. (2015). *Recent advances in understanding the role of supplementary cementitious materials in concrete.* Cement and Concrete Research, 78, Part A: pp. 71-80.
93. Duan, P. et al. (2013). *Efficiency of mineral admixtures in concrete: Microstructure, compressive strength and stability of hydrate phases.* Applied Clay Science, 83–84: pp. 115-121.
94. Achal, V. et al. (2011). *Improved strength and durability of fly ash-amended concrete by microbial calcite precipitation.* Ecological Engineering, 37(4): pp. 554-559.
95. Christodoulou, C. et al. (2013). *Long-term performance of surface impregnation of reinforced concrete structures with silane.* Construction and Building Materials, 48: pp. 708-716.
96. Diamanti, M.V. et al. (2013). *Effect of polymer modified cementitious coatings on water and chloride permeability in concrete.* Construction and Building Materials, 49: pp. 720-728.

97. Khanzadeh Moradllo, M. et al. (2012). *Time-dependent performance of concrete surface coatings in tidal zone of marine environment.* Construction and Building Materials, 30: pp. 198-205.
98. Fouda, A.S. et al. (2015). *Alcamines as corrosion inhibitors for reinforced steel and their effect on cement based materials and mortar performance.* RSC Advances, 5(46): pp. 36957-36968.
99. Siddique, R. and Chahal, N.K. (2011). *Effect of ureolytic bacteria on concrete properties.* Construction and Building Materials, 25(10): pp. 3791-3801.
100. *Electrochemical techniques.* in *Corrosion of Steel in Concrete*.
101. Polder, R.B. et al. (2014). *Service life and life cycle cost modelling of cathodic protection systems for concrete structures.* Cement and Concrete Composites, 47: pp. 69-74.
102. Pedeferri, P. (1996). *Cathodic protection and cathodic prevention.* Construction and Building Materials, 10(5): pp. 391-402.
103. Redaelli, E. et al. (2014). *Cathodic protection with localised galvanic anodes in slender carbonated concrete elements.* Materials and Structures, 47(11): pp. 1839-1855.
104. Gurrappa, I. (2005). *Cathodic protection of cooling water systems and selection of appropriate materials.* Journal of Materials Processing Technology, 166(2): pp. 256-267.
105. Christodoulou, C. et al. (2011). *Corrosion risk of reinforced concrete structures following three years of interrupted cathodic protection.*
106. Christodoulou, C. and Kilgour, R. (2013). *The world's first hybrid corrosion protection systems for prestressed concrete bridges.*
107. Figueira, R.B. et al. (2015). *Hot-dip galvanized steel dip-coated with ureasilicate hybrid in simulated concrete pore solution: Assessment of coating morphology and corrosion protection efficiency.* Progress in Organic Coatings, 88: pp. 245-255.
108. Li, H.Y. et al. (2013). *Comparison on corrosion behaviour of arc sprayed and zinc-rich coatings.* Surface and Coatings Technology, 235: pp. 259-266.
109. Liu, S. et al. (2012). *Effects of pH and Cl^- concentration on corrosion behavior of the galvanized steel in simulated rust layer solution.* Corrosion Science, 65: pp. 520-527.
110. Fayala, I. et al. (2013). *Effect of inhibitors on the corrosion of galvanized steel and on mortar properties.* Cement and Concrete Composites, 35(1): pp. 181-189.

111. Lindström, D. and Odnevall Wallinder, I. (2011). *Long-term use of galvanized steel in external applications: Aspects of patina formation, zinc runoff, barrier properties of surface treatments, and coatings and environmental fate.* Environmental Monitoring and Assessment, 173(1-4): pp. 139-153.

112. Ebell, G. et al. (2012). *Electrochemical investigations on the corrosion behaviour of galvanized reinforcing steels in concrete with chromate-reduced cements.* Materials and Corrosion, 63(9): pp. 791-802.

113. Bellezze, T. et al. (2011). *Effect of concrete carbonation process on the passivating products of galvanized steel reinforcements.* Materials and Corrosion, 62(2): pp. 155-160.

114. Ismail, M. et al. (2012). *Corrosion behaviour of dual-phase and galvanized steels in concrete.* Anti-Corrosion Methods and Materials, 59(3): pp. 132-138.

115. Jiang, Q. et al. (2014). *Corrosion behavior of arc sprayed Al–Zn–Si–Re coatings on mild steel in 3.5 wt% NaCl solution.* Electrochimica Acta, 115: pp. 644-656.

116. Olsson, C.O.A. and Landolt, D. (2003). *Passive films on stainless steels − Chemistry, structure and growth.* Electrochimica Acta, 48(9): pp. 1093-1104.

117. Alvarez, S.M. et al. (2011). *Corrosion behaviour of corrugated lean duplex stainless steels in simulated concrete pore solutions.* Corrosion Science, 53(5): pp. 1748-1755.

118. Okeniyi, J.O. et al. (2014). *Electrochemical performance of Anthocleista djalonensis on steel-reinforcement corrosion in concrete immersed in saline/marine simulating-environment.* Transactions of the Indian Institute of Metals, 67(6): pp. 959-969.

119. Ameer, M.A. and Fekry, A.M. (2010). *Inhibition effect of newly synthesized heterocyclic organic molecules on corrosion of steel in alkaline medium containing chloride.* International Journal of Hydrogen Energy, 35(20): pp. 11387-11396.

120. Jiang, S. et al. (2018). *Effects of deoxyribonucleic acid on cement paste properties and chloride-induced corrosion of reinforcing steel in cement mortars.* Cement and Concrete Composites, 91: pp. 87-96.

121. Abdel-Gaber, A.M. et al. (2011). *Utilizing Arghel extract as corrosion inhibitor for reinforced steel in concrete.* Materials and Corrosion, 62(12): pp. 1159-1162.

122. Pan, T. and Wang, Z. (2013). *A polyaniline based intrinsically conducting coating for corrosion protection of structural steels.* Microscopy Research and Technique, 76(11): pp. 1186-1195.

123. Monticelli, C. et al. (2011). *Influence of two specific inhibitors on steel corrosion in a synthetic solution simulating a carbonated concrete with chlorides.* Materials and Corrosion, 62(2): pp. 178-186.

124. Michael, T.C. (2009). *Corrosion inhibitors and rust preventatives.* in *Lubricant Additives*. CRC Press, pp. 421-444.

125. Kohl, M. and Kalendová, A. (2015). *Effect of polyaniline salts on the mechanical and corrosion properties of organic protective coatings.* Progress in Organic Coatings, 86: pp. 96-107.

126. Rakanta, E. et al. (2013). *Corrosion protection of steel with DMEA-based organic inhibitor.* Construction and Building Materials, 44: pp. 507-513.

127. Ahmad, S. (2003). *Reinforcement corrosion in concrete structures, its monitoring and service life prediction − A review.* Cement and Concrete Composites, 25(4): pp. 459-471.

128. Funahashi, M. and Bushman, J. (1991). *Technical review of 100 mV polarization shift criterion for reinforcing steel in concrete.* Corrosion, 47(5): pp. 376-386.

129. Robert, G.K. (2002). *Passivity and localized corrosion.* in *Electrochemical Techniques in Corrosion Science and Engineering*. CRC Press.

130. Raja, P.B. et al. (2013). *Neolamarckia cadamba alkaloids as eco-friendly corrosion inhibitors for mild steel in 1 M HCl media.* Corrosion Science, 69: pp. 292-301.

131. Deng, S. and Li, X. (2012). *Inhibition by Ginkgo leaves extract of the corrosion of steel in HCl and H_2SO_4 solutions.* Corrosion Science, 55: pp. 407-415.

132. Kalendová, A. et al. (2008). *Anticorrosion efficiency of organic coatings depending on the pigment volume concentration of polyaniline phosphate.* Progress in Organic Coatings, 63(2): pp. 228-237.

133. Berke, N.S. and Rosenberg, A. (1989). *Technical review of calcium nitrite corrosion inhibitor in concrete.* Transportation Research Record (1211).

134. Ann, K.Y. et al. (2006). *Effect of calcium nitrite-based corrosion inhibitor in preventing corrosion of embedded steel in concrete.* Cement and Concrete Research, 36(3): pp. 530-535.

135. Raja, P.B. et al. (2015). *Natural corrosion inhibitors for steel reinforcement in concrete − A review.* Surface Review and Letters, 22(03): pp. 1550040.

136. Verbruggen, H. et al. (2016). *Inhibitor evaluation in different simulated concrete pore solution for the protection of steel rebars.* Construction and Building Materials, 124: pp. 887-896.
137. Chidiebere, M.A. et al. (2012). *Corrosion inhibition and adsorption behavior of Punica granatum extract on mild steel in acidic environments: Experimental and theoretical studies.* Industrial and Engineering Chemistry Research, 51(2): pp. 668-677.
138. Kamal, C. and Sethuraman, M.G. (2012). *Caulerpin—a bis-indole alkaloid as a green inhibitor for the corrosion of mild steel in 1 M HCl solution from the marine alga Caulerpa racemosa.* Industrial and Engineering Chemistry Research, 51(31): pp. 10399-10407.
139. Raja, P.B. et al. (2013). *Evaluation of green corrosion inhibition by alkaloid extracts of Ochrosia oppositifolia and isoreserpiline against mild steel in 1 M HCl medium.* Industrial and Engineering Chemistry Research, 52(31): pp. 10582-10593.
140. Moretti, G. et al. (2004). *Tryptamine as a green iron corrosion inhibitor in 0.5 M deaerated sulphuric acid.* Corrosion Science, 46(2): pp. 387-403.
141. de Souza, F.S. and Spinelli, A. (2009). *Caffeic acid as a green corrosion inhibitor for mild steel.* Corrosion Science, 51(3): pp. 642-649.
142. Ferreira, E.S. et al. (2004). *Evaluation of the inhibitor effect of L-ascorbic acid on the corrosion of mild steel.* Materials Chemistry and Physics, 83(1): pp. 129-134.
143. Satapathy, A.K. et al. (2009). *Corrosion inhibition by Justicia gendarussa plant extract in hydrochloric acid solution.* Corrosion Science, 51(12): pp. 2848-2856.
144. Verma, C. et al. (2018). *An overview on plant extracts as environmental sustainable and green corrosion inhibitors for metals and alloys in aggressive corrosive media.* Journal of Molecular Liquids.
145. Zaferani, S.H. et al. (2013). *Application of eco-friendly products as corrosion inhibitors for metals in acid pickling processes − A review.* Journal of Environmental Chemical Engineering, 1(4): pp. 652-657.
146. Verma, C. et al. (2018). *Substituents effect on corrosion inhibition performance of organic compounds in aggressive ionic solutions: A review.* Journal of Molecular Liquids, 251: pp. 100-118.

147. Etteyeb, N. and Nóvoa, X. (2016). *Inhibition effect of some trees cultivated in arid regions against the corrosion of steel reinforcement in alkaline chloride solution.* Corrosion Science, 112: pp. 471-482.

148. Asaad, M.A. et al. (2018). *Enhanced corrosion resistance of reinforced concrete: Role of emerging eco-friendly Elaeis guineensis/silver nanoparticles inhibitor.* Construction and Building Materials, 188: pp. 555-568.

149. Shanmugapriya, S. et al. (2018). *Corrosion resistance property of mild steel in simulated concrete pore solution prepared in well water by using an aqueous extract of turmeric.* Materials Today: Proceedings, 5(2): pp. 8789-8795.

150. Charles, D.J. (2013). *Antioxidant assays.* in *Antioxidant Properties of Spices, Herbs and Other sources*. New York: Springer, pp. 9-38.

151. Shahidi, F. (2015). *1 - Antioxidants: Principles and applications.* in *Handbook of Antioxidants for Food Preservation*. Woodhead Publishing, pp. 1-14.

152. Muzolf, M. et al. (2008). *pH-dependent radical scavenging capacity of green tea catechins.* Journal of Agricultural and Food Chemistry, 56(3): pp. 816-823.

153. Benzie, I.F. and Szeto, Y. (1999). *Total antioxidant capacity of teas by the ferric reducing/antioxidant power assay*. Journal of Agricultural and Food Chemistry, 47(2): pp. 633-636.

154. Andrade, C. and Martínez, I. (2010). *14 − Techniques for measuring the corrosion rate (polarization resistance) and the corrosion potential of reinforced concrete structures.* in *Non-destructive Evaluation of Reinforced Concrete Structures*. Woodhead Publishing, pp. 284-316.

155. González, J.A. et al. (1995). *Comparison of rates of general corrosion and maximum pitting penetration on concrete embedded steel reinforcement.* Cement and Concrete Research, 25(2): pp. 257-264.

156. Alonso, C. et al. (1998). *Factors controlling cracking of concrete affected by reinforcement corrosion.* Materials and Structures, 31(7): pp. 435-441.

157. Chan, E. et al. (2007). *Antioxidant activity of Camellia sinensis leaves and tea from a lowland plantation in Malaysia.* Food Chemistry, 102(4): pp. 1214-1222.

158. Andrade, C. and González, J.A. (1978). *Quantitative measurements of corrosion rate of reinforcing steels embedded in concrete using polarization resistance measurements.* Materials and Corrosion, 29(8): pp. 515-519.
159. Andrade, C. et al. (1986). *Some laboratory experiments on the inhibitor effect of sodium nitrite on reinforcement corrosion.* Cement, Concrete and Aggregates, 8(2): pp. 110-116.
160. Aiad, I. et al. (2003). *Rheological properties of cement pastes admixed with some alkanolamines.* Cement and Concrete Research, 33(1): pp. 9-13.
161. Bancirova, M. (2010). *Comparison of the antioxidant capacity and the antimicrobial activity of black and green tea.* Food Research International, 43(5): pp. 1379-1382.
162. Tsai, T.H. et al. (2008). *In vitro antimicrobial activities against cariogenic Streptococci and their antioxidant capacities: A comparative study of green tea versus different herbs.* Food Chemistry, 110(4): pp. 859-864.
163. Abosrra, L. et al. (2011). *Corrosion of steel reinforcement in concrete of different compressive strengths.* Construction and Building Materials, 25(10): pp. 3915-3925.
164. Abu-Dalo, M.A. et al. (2013). *Evaluating the performance of sulfonated kraft lignin agent as corrosion inhibitor for iron-based materials in water distribution systems.* Desalination, 313: pp. 105-114.
165. Ormellese, M. et al. (2011). *Organic substances as inhibitors for chloride-induced corrosion in reinforced concrete.* Materials and Corrosion, 62(2): pp. 170-177.
166. Mennucci, M.M. et al. (2009). *Evaluation of benzotriazole as corrosion inhibitor for carbon steel in simulated pore solution.* Cement and Concrete Composites, 31(6): pp. 418-424.
167. Suryavanshi, A.K. et al. (1996). *Mechanism of Friedel's salt formation in cements rich in tricalcium aluminate.* Cement and Concrete Research, 26(5): pp. 717-727.
168. Okeniyi, J.O. et al. (2013). *Analysis of inhibition of concrete steel-rebar corrosion by $Na_2Cr_2O_7$ concentrations: Implications for conflicting reports on inhibitor effectiveness.* Journal of Central South University, 20(12): pp. 3697-3714.
169. Chan, E. et al. (2009). *Effects of different drying methods on the antioxidant properties of leaves and tea of ginger species.* Food Chemistry, 113(1): pp. 166-172.
170. Papavinasam, S. (2008). *3 − Electrochemical polarization techniques for corrosion monitoring.* in *Techniques for Corrosion Monitoring*. Woodhead Publishing, pp. 49-85.

171. Alghamdi, S.A. and Ahmad, S. (2014). *Service life prediction of RC structures based on correlation between electrochemical and gravimetric reinforcement corrosion rates.* Cement and Concrete Composites, 47: pp. 64-68.
172. Silverman, D.C. (2011). *Practical corrosion prediction using electrochemical techniques.* Uhlig's Corrosion Handbook: pp. 1129-1166.
173. Aperador, W. et al. (2015). *Improved protection against corrosion of galvanized steel embedded in alkali-activated concrete.* International Journal of Electrochemical Science, 10: pp. 4585-4595.
174. Gu, G.P. et al. (2001). *12 − Techniques for corrosion investigation in reinforced concrete.* in *Handbook of Analytical Techniques in Concrete Science and Technology*. Norwich: William Andrew Publishing, pp. 441-504.
175. Mansfeld, F. (2005). *Tafel slopes and corrosion rates obtained in the pre-Tafel region of polarization curves.* Corrosion Science, 47(12): pp. 3178-3186.
176. Mansfeld, F. (2009). *Fundamental aspects of the polarization resistance technique − The early days.* Journal of Solid State Electrochemistry, 13(4): pp. 515-520.
177. Recio, F.J. et al. (2011). *Hydrogen embrittlement risk of high strength galvanized steel in contact with alkaline media.* Corrosion Science, 53(9): pp. 2853-2860.
178. Norušis, M.J. (2006). *SPSS 14.0 Guide to Data Analysis*. New Jersey: Prentice Hall.
179. du Toit, R. et al. (2001). *Comparison of the antioxidant content of fruits, vegetables and teas measured as vitamin C equivalents.* Toxicology, 166(1-2): pp. 63-69.
180. Guo, C. et al. (2003). *Antioxidant activities of peel, pulp and seed fractions of common fruits as determined by FRAP assay.* Nutrition Research, 23(12): pp. 1719-1726.
181. Mahattanatawee, K. et al. (2006). *Total antioxidant activity and fiber content of selected Florida-grown tropical fruits.* Journal of Agricultural and Food Chemistry, 54(19): pp. 7355-7363.
182. Lim, Y. et al. (2007). *Antioxidant properties of several tropical fruits: A comparative study.* Food Chemistry, 103(3): pp. 1003-1008.
183. Lim, Y.Y. et al. (2006). *Antioxidant properties of guava fruit: Comparison with some local fruits.* Sunway Academic Journal, 3: pp. 9-20.
184. Carlsen, M.H. et al. (2010). *The total antioxidant content of more than 3100 foods, beverages, spices, herbs and supplements used worldwide.* Nutrition Journal, 9(1): pp. 3.

185. Fu, L. et al. (2011). *Antioxidant capacities and total phenolic contents of 62 fruits.* Food Chemistry, 129(2): pp. 345-350.
186. Anwar, H. et al. (2018). *Antioxidants from natural sources.* in *Antioxidants in Foods and its Applications*. IntechOpen.
187. Xu, D.P. et al. (2017). *Natural antioxidants in foods and medicinal plants: Extraction, assessment and resources.* International Journal of Molecular Sciences, 18(1): pp. 96.
188. Leong, L. and Shui, G. (2002). *An investigation of antioxidant capacity of fruits in Singapore markets.* Food Chemistry, 76(1): pp. 69-75.
189. Daniel, D.G. and Lobo, C.L. (2005). *User's guide to ASTM specification C 94 on ready-mixed concrete*. ASTM International.
190. Ormellese, M. et al. (2011). *Corrosion inhibitors in reinforced concrete structures − Part 3:Migration of inhibitors into concrete.* Corrosion Engineering, Science and Technology, 46(4): pp. 334-339.
191. Sherif, E.M. and Park, S.M. (2006). *2-amino-5-ethyl-1,3,4-thiadiazole as a corrosion inhibitor for copper in 3.0% NaCl solutions.* Corrosion Science, 48(12): pp. 4065-4079.
192. Ashassi-Sorkhabi, H. et al. (2008). *EN, EIS and polarization studies to evaluate the inhibition effect of 3H-phenothiazin-3-one, 7-dimethylamine on mild steel corrosion in 1 M HCl solution.* Corrosion Science, 50(12): pp. 3363-3370.
193. Akbarzadeh, E. et al. (2011). *Corrosion inhibition of mild steel in near neutral solution by kraft and soda lignins extracted from oil palm empty fruit bunch.* International Journal Electrochemical Science, 6(11): pp. 5396-5416.
194. Chetouani, A. et al. (2005). *Inhibitive action of bipyrazolic type organic compounds towards corrosion of pure iron in acidic media.* Applied Surface Science, 249(1–4): pp. 375-385.
195. Elsener, B. et al. (2003). *Hall-cell potential measurements − Potential mapping on reinforced concrete structures.* Materials and Structures, 36(7): pp. 461-471.
196. Ahmad, S. (2009). *Techniques for inducing accelerated corrosion of steel in concrete.* Arabian Journal for Science and Engineering, 34(2): pp. 95.
197. Caré, S. et al. (2008). *Mechanical properties of the rust layer induced by impressed current method in reinforced mortar.* Cement and Concrete Research, 38(8): pp. 1079-1091.

198. Caré, S. and Raharinaivo, A. (2007). *Influence of impressed current on the initiation of damage in reinforced mortar due to corrosion of embedded steel.* Cement and Concrete Research, 37(12): pp. 1598-1612.
199. El Maaddawy, T.A. and Soudki, K.A. (2003). *Effectiveness of impressed current technique to simulate corrosion of steel reinforcement in concrete.* Journal of Materials in Civil Engineering, 15(1): pp. 41-47.
200. Otieno, M. et al. (2016). *Chloride-induced corrosion of steel in cracked concrete − Part I: Experimental studies under accelerated and natural marine environments.* Cement and Concrete Research, 79: pp. 373-385.
201. Altoubat, S. et al. (2016). *Laboratory simulation of corrosion damage in reinforced concrete.* International Journal of Concrete Structures and Materials, 10(3): pp. 383-391.
202. Rosenberg, A. et al. (1977). *A corrosion inhibitor formulated with calcium nitrite for use in reinforced concrete.* in *Chloride Corrosion of Steel in Concrete*. ASTM International.
203. Naqash, J. et al. (2014). *Effect of accelerating admixture on properties of concrete.* IOSR Journal of Engineering, 4(3): pp. 48-55.
204. Berke, N.S. and Hicks, M.C. (2004). *Predicting long-term durability of steel reinforced concrete with calcium nitrite corrosion inhibitor*. Cement and Concrete Composites, 26(3): pp. 191-198.
205. Okeniyi, J. et al. (2016). *Effects of Phyllanthus muellerianus leaf-extract on steel-reinforcement corrosion in 3.5% NaCl-immersed concrete.* Metals, 6(11): pp. 255.
206. Vera, R. et al. (2009). *Corrosion products of reinforcement in concrete in marine and industrial environments.* Materials Chemistry and Physics, 114(1): pp. 467-474.
207. Ha, T.H. et al. (2007). *Accelerated short-term techniques to evaluate the corrosion performance of steel in fly ash blended concrete*. Building and Environment, 42(1): pp. 78-85.
208. Malumbela, G. et al. (2010). *Interaction between corrosion crack width and steel loss in RC beams corroded under load.* Cement and Concrete Research, 40(9): pp. 1419-1428.
209. Koleva, D. et al. (2006). *Quantitative characterisation of steel/cement paste interface microstructure and corrosion phenomena in mortars suffering from chloride attack.* Corrosion Science, 48(12): pp. 4001-4019.

210. Blunt, J. et al. (2015). *Enhancing corrosion resistance of reinforced concrete structures with hybrid fiber reinforced concrete.* Corrosion Science, 92: pp. 182-191.
211. Güneyisi, E. and Gesoğlu, M. (2008). *A study on durability properties of high-performance concretes incorporating high replacement levels of slag.* Materials and Structures, 41(3): pp. 479-493.
212. Pech-Canul, M. and Castro, P. (2002). *Corrosion measurements of steel reinforcement in concrete exposed to a tropical marine atmosphere.* Cement and Concrete Research, 32(3): pp. 491-498.
213. Berke, N.S. et al. (1990). *Comparison of the polarization resistance technique to the macrocell corrosion technique.* in *Corrosion Rates of Steel in Concrete*. ASTM International.
214. Nmai, C.K. (2004). *Multi-functional organic corrosion inhibitor.* Cement and Concrete Composites, 26(3): pp. 199-207.
215. Mihashi, H. et al. (2011). *Corrosion of reinforcing steel in fiber reinforced cementitious composites.* Journal of Advanced Concrete Technology, 9(2): pp. 159-167.
216. Maalej, M. et al. (2003). *Corrosion durability and structural response of functionally-graded concrete beams.* Journal of Advanced Concrete Technology, 1(3): pp. 307-316.
217. Malumbela, G. et al. (2012). *A step towards standardising accelerated corrosion tests on laboratory reinforced concrete specimens.* Journal of the South African Institution of Civil Engineering, 54(2): pp. 78-85.
218. Berrocal, C.G. et al. (2017). *Corrosion-induced cracking and bond behaviour of corroded reinforcement bars in SFRC.* Composites Part B: Engineering, 113(Supplement C): pp. 123-137.
219. Tang, D. et al. (2011). *Influence of surface crack width on bond strength of reinforced concrete.* ACI Materials Journal, 108(1).
220. Zandi Hanjari, K. and Coronelli, D. (2010). *Anchorage capacity of corroded reinforcement*. Chalmers University of Technology.
221. Andrade, C. et al. (1990). *An initial effort to use the corrosion rate measurements for estimating rebar durability.* in *Corrosion Rates of Steel in Concrete*. ASTM International.
222. Hong, K. and Hooton, R. (1999). *Effects of cyclic chloride exposure on penetration of concrete cover.* Cement and Concrete Research, 29(9): pp. 1379-1386.

223. Torres-Acosta, A.A. and Martínez-Madrid, M. (2003). *Residual life of corroding reinforced concrete structures in marine environment.* Journal of Materials in Civil Engineering, 15(4): pp. 344-353.

224. Poupard, O. et al. (2006). *Corrosion damage diagnosis of a reinforced concrete beam after 40 years natural exposure in marine environment.* Cement and Concrete Research, 36(3): pp. 504-520.

225. Singh, J.K. and Singh, D.D.N. (2012). *The nature of rusts and corrosion characteristics of low alloy and plain carbon steels in three kinds of concrete pore solution with salinity and different pH.* Corrosion Science, 56: pp. 129-142.

226. Loftus, E. et al. (2015). *A simple method to establish calcite: aragonite ratios in archaeological mollusc shells.* Journal of Quaternary Science, 30(8): pp. 731-735.

227. Dauphin, Y. et al. (2008). *Soluble organic matrices of aragonitic skeletons of Merulinidae (Cnidaria, Anthozoa).* Comparative Biochemistry and Physiology Part B: Biochemistry and Molecular Biology, 150(1): pp. 10-22.

228. Horie, H. and Kohata, K. (2000). *Analysis of tea components by high-performance liquid chromatography and high-performance capillary electrophoresis.* Journal of Chromatography A, 881(1-2): pp. 425-438.

229. Nanjo, F. et al. (1996). *Scavenging effects of tea catechins and their derivatives on 1, 1-diphenyl-2-picrylhydrazyl radical.* Free Radical Biology and Medicine, 21(6): pp. 895-902.

230. Janeiro, P. and Brett, A.M.O. (2004). *Catechin electrochemical oxidation mechanisms.* Analytica Chimica Acta, 518(1-2): pp. 109-115.

231. Miketova, P. et al. (2000). *Tandem mass spectrometry studies of green tea catechins − Identification of three minor components in the polyphenolic extract of green tea.* Journal of Mass Spectrometry, 35(7): pp. 860-869.

232. Bastos, D. et al. (2007). *Phenolic antioxidants identified by ESI-MS from yerba mate (Ilex paraguariensis) and green tea (Camelia sinensis) extracts.* Molecules, 12(3): pp. 423-432.

233. Tao, W. et al. (2016). *Simultaneous determination of eight catechins and four theaflavins in green, black and oolong tea using new HPLC–MS–MS method.* Journal of Pharmaceutical and Biomedical Analysis, 131: pp. 140-145.

234. Saleem, H. et al. (2019). *Biological, chemical and toxicological perspectives on aerial and roots of Filago germanica (L.) huds: Functional approaches for novel phyto-pharmaceuticals.* Food and Chemical Toxicology, 123: pp. 363-373.

235. Del Rio, D. et al. (2004). *HPLC-MS^n analysis of phenolic compounds and purine alkaloids in green and black tea.* Journal of Agricultural and Food Chemistry, 52(10): pp. 2807-2815.

236. Poon, G. (1998). *Analysis of catechins in tea extracts by liquid chromatography–electrospray ionization mass spectrometry.* Journal of Chromatography A, 794(1-2): pp. 63-74.

237. Tyrakowska, B. et al. (1999). *TEAC antioxidant activity of 4-hydroxybenzoates.* Free Radical Biology and Medicine, 27(11-12): pp. 1427-1436.

238. Zhang, Y. et al. (2015). *Role of calcium sources in the strength and microstructure of microbial mortar*. Construction and Building Materials, 77: pp. 160-167.

239. Dhami, N.K. et al. (2012). *Improvement in strength properties of ash bricks by bacterial calcite.* Ecological Engineering, 39: pp. 31-35.

240. Kontoyannis, C.G. and Vagenas, N.V. (2000). *Calcium carbonate phase analysis using XRD and FT-Raman spectroscopy.* Analyst, 125(2): pp. 251-255.

241. Stepkowska, E.T. et al. (2003). *Calcite, vaterite and aragonite forming on cement hydration from liquid and gaseous phase.* Journal of Thermal Analysis and Calorimetry, 73(1): pp. 247-269.

242. Loste, E. et al. (2003). *The role of magnesium in stabilising amorphous calcium carbonate and controlling calcite morphologies.* Journal of Crystal Growth, 254(1-2): pp. 206-218.

243. De Muynck, W. et al. (2008). *Bacterial carbonate precipitation as an alternative surface treatment for concrete*. Construction and Building Materials, 22(5): pp. 875-885.

244. Wang, C. et al. (2006). *Synthesis of nanosized calcium carbonate (aragonite) via a polyacrylamide inducing process.* Powder Technology, 163(3): pp. 134-138.

245. Liu, A. et al. (2014). *Formation of lepidocrocite (γ-FeOOH) from oxidation of nanoscale zero-valent iron (nZVI) in oxygenated water.* RSC Advances, 4(101): pp. 57377-57382.

246. Walker, J.D. and Tannenbaum, R. (2006). *Characterization of the sol−gel formation of iron(III) oxide/hydroxide nanonetworks from weak base molecules.* Chemistry of Materials, 18(20): pp. 4793-4801.

247. Sheydaei, M. and Aber, S. (2013). *Preparation of nano-lepidocrocite and an investigation of its ability to remove a metal complex dye.* CLEAN–Soil, Air, Water, 41(9): pp. 890-898.
248. Rodriguez-Blanco, J.D. et al. (2011). *The kinetics and mechanisms of amorphous calcium carbonate (ACC) crystallization to calcite, via vaterite.* Nanoscale, 3(1): pp. 265-271.
249. Wang, L. et al. (1999). *Preparation of uniform needle-like aragonite particles by homogeneous precipitation.* Journal of Colloid and Interface Science, 218(2): pp. 545-553.
250. Chakrabarty, D. and Mahapatra, S. (1999). *Aragonite crystals with unconventional morphologies.* Journal of Materials Chemistry, 9(11): pp. 2953-2957.
251. Plav, B. et al. (1999). *Identification of crystallization forms of $CaCO_3$ with FTIR spectroscopy.* Kovine Zlitine Tehnology, 33: pp. 6.
252. Nakayama, N. (2000). *Inhibitory effects of nitrilotris(methylenephosphonic acid) on cathodic reactions of steels in saturated $Ca(OH)_2$ solutions.* Corrosion Science, 42(11): pp. 1897-1920.
253. De Angelis Curtis, S. et al. (2010). *Crystal structure and thermoanalytical study of a cadmium (II) complex with 1-allylimidazole.* Journal of Analytical and Applied Pyrolysis, 87(1): pp. 175-179.
254. Susanti, E. et al. (2015). *Qualitative analysis of catechins from green tea GMB-4 clone using HPLC and LC-MS/MS.* Asian Pacific Journal of Tropical Biomedicine, 5(12): pp. 1046-1050.
255. Reto, M. et al. (2007). *Chemical composition of green tea (Camellia sinensis) infusions commercialized in Portugal.* Plant Foods for Human Nutrition, 62(4): pp. 139.
256. Makris, D.P. et al. (2007). *Polyphenolic content and in vitro antioxidant characteristics of wine industry and other agri-food solid waste extracts.* Journal of Food Composition and Analysis, 20(2): pp. 125-132.
257. Sultana, B. et al. (2008). *Antioxidant potential of extracts from different agro wastes: Stabilization of corn oil.* Grasas y Aceites, 59(3): pp. 205-217.
258. Khiari, Z. et al. (2009). *An investigation on the recovery of antioxidant phenolics from onion solid wastes employing water/ethanol-based solvent systems.* Food and Bioprocess Technology, 2(4): pp. 337.

259. Ku, C.S. and Mun, S.P. (2008). *Antioxidant activities of ethanol extracts from seeds in fresh Bokbunja (Rubus coreanus Miq.) and wine processing waste.* Bioresource Technology, 99(10): pp. 4503-4509.

260. Okonogi, S. et al. (2007). *Comparison of antioxidant capacities and cytotoxicities of certain fruit peels.* Food Chemistry, 103(3): pp. 839-846.